On the interaction of myo-Inositol hexakisphosphate with human Hemoglobin

a ^{31}P NMR and pH-stat study

E.R.P. Zuiderweg

ON THE INTERACTION OF MYO-INOSITOL HEXAKISPHOSPHATE WITH HUMAN HEMOGLOBIN

a ^{31}P NMR and pH-stat study

promotor:

PROF. DR. C.W. HILBERS

co-referent:

DR. S.H. DE BRUIN

ON THE INTERACTION OF MYO-INOSITOL HEXAKISPHOSPHATE WITH HUMAN HEMOGLOBIN

a ^{31}P NMR and pH-stat study

PROEFSCHRIFT

TER VERKRIJGING VAN DE GRAAD VAN DOCTOR IN DE WISKUNDE EN NATUURWETENSCHAPPEN AAN DE KATHOLIEKE UNIVERSITEIT TE NIJMEGEN, OP GEZAG VAN DE RECTOR MAGNIFICUS PROF. DR. P. G. A. B. WIJDEVELD, VOLGENS BESLUIT VAN HET COLLEGE VAN DECANEN IN HET OPENBAAR TE VERDEDIGEN OP WOENSDAG 25 JUNI 1980, DES NAMIDDAGS TE 2 UUR PRECIES

DOOR

ERIK ROEL PETER ZUIDERWEG

GEBOREN TE AMSTERDAM

krips repro meppel

The investigations reported in this thesis were supported by the Netherlands Foundation for Chemical Research (S.O.N.) with financial aid from the Netherlands Organization for the Advancement of Pure Research (Z.W.O.).

Aan mijn ouders
Aan Lineke, Mieke en Adriaan

Gaarne wil ik allen bedanken, die hebben bijgedragen aan de totstandkoming van dit proefschrift. Ik denk hierbij in de eerste plaats aan mijn vrienden en ex-collega's Bob van Beek, Maarten Geerdes en Harry Rollema, die altijd tijd wisten te vinden, om met mij over de interpretatie van meetgegevens te discussieren. Mijn dank gaat verder uit naar Rens Hamers, Peter Hekman en Bert van de Laar, die in het kader van hun hoofd- en bijvakstages hebben bijgedragen aan het experimentele werk. Tevens ben ik Carla Prinse, Jos Joordens, Jan van Kessel, John Roef en de heer Schreurs erkentelijk voor hun technische bijstand. De medewerkers van de afdeling fotografie wil ik danken voor de correcte en snelle wijze, waarop zij de vele figuren hebben bewerkt.
Zeker niet onvermeld wil ik laten, degenen, die hebben bijgedragen aan andere onderzoeksprojecten tijdens mijn promotietijd. I would like to thank Mrs. Dr. J. Brygier (Dept. of Protein Chemistry, University of Bruxelles) for teaching me the isolation procedure of chicken hemoglobin. Ik denk met genoegen terug aan de samenwerking met Dr. R. Kaptein en de heer K. Dijkstra (Afd. Fysische Chemie, Rijksuniversiteit te Groningen) betreffende de ontwikkeling van flash-fotolyse/NMR experimenten. Veel waardering heb ik voor Frank van der Ven en Willy Frambach, die in kader van hun hoofdvak- resp. bijvakstage zeer veel werk aan valentie hybrides van hemoglobine hebben verricht.

CONTENTS

a) Zuiderweg, E.R.P., van Beek, G.G.M. & de Bruin, S.H. (1979) Eur. J. Biochem. 94, 297-306

b) Zuiderweg, E.R.P., Hamers, L.F., de Bruin, S.H. & Hilbers,C.W. (1980) Eur. J. Biochem. submitted for publication

c) Zuiderweg, E.R.P., Hamers, L.F., Rollema, H.S., de Bruin, S.H. & Hilbers, C.W. (1980) Eur. J. Biochem. submitted for publication

CHAPTER I

GENERAL INTRODUCTION

Hemoglobin which is present in the erythrocytes of vertebrates, serves to transport oxygen from the lungs to the tissues. The molecule possesses a number of remarkable properties which make its biological functioning very effective. Hemoglobin binds oxygen cooperatively, a process which turns out to be influenced by a number of so-called effectors. These are molecules which bind to hemoglobin at sites spatially removed from the oxygen binding sites. Because of these properties, which characterize hemoglobin as an allosteric protein, the molecule has been extensively studied.

X-ray diffraction studies of human and horse hemoglobin performed by Perutz and collaborators (1-6) have provided us with a detailed knowledge of the three dimensional structure of the protein. Together with the relatively simple procedure by which this highly abundant protein can be isolated, this knowledge makes the molecule particularly attractive for the study of structure-function relationships. In fact hemoglobin has served as a model for protein function for many years.

myo- Inositol hexakisphosphate, IHP, resembles in its effect the in-vivo effectors of the oxygen binding by human hemoglobin. With the aim of extending our insight into the structure-function relationships of protein-effector complexes, the interaction of IHP with human hemoglobin is investigated in this thesis.

In this introductory chapter a number of hemoglobin properties relevant to the results presented in the following chapters is briefly discussed. For general reviews on the subject of structure-function relationships the reader is referred to a number of excellent papers and textbooks (7-11).

Structure of Human Hemoglobin

Hemoglobin has a molecular weight of 64,500. It consists of four subunits which are pairwise identical (see Fig. 1). The two different chains are called α- and β-chains which contain 141 and 146 amino acid residues respectively. Each chain carries an iron-protoporphyrin IX complex, called heme group, to which reversible ligand binding may take place. Depending on the oxydation state of the heme iron several ligands can be bound. In this thesis we are primarily concerned with human ferrous hemoglobin either unligated or ligated with O_2 or CO, abbreviated as Hb, HbO_2 and HbCO respectively.

The overall appearance of the molecule is that of a sphere having a radius of approximately 3 nm (see Fig. 1). The four subunits are arranged tetrahedrically resulting in a molecule with a two-fold axis of symmetry. This dyad axis runs through a central cavity which extends from the N-termini of the α-chains to the N-termini of the β-chains.

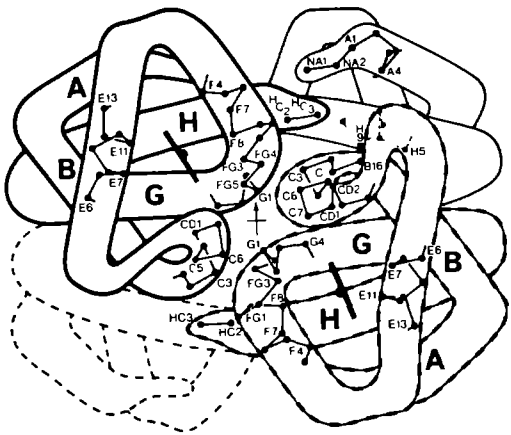

Fig. 1. Schematic drawing of the deoxyhemoglobin tetramer. The course of the α-chains is shown in solid outline, that of the β-chains in broken outline. The heme groups are shown edge-on. The molecular dyad is vertical. Capitals identify helices. (Reproduced with permission from Fermi, G. (1975) J. Mol. Biol. 97, 237-256. Copyright by Academic Press inc. (London) Ltd.).

Hemoglobin crystalizes in two distinct conformations depending on the ligation state of the heme groups. These conformations have been named the T state (tensed) for unligated and the R state (relaxed) for ligated hemoglobin. The major difference between these conformations is found in the orientation of the subunits with respect to each other, leading to a difference in interfacial contacts between the chains. Furthermore pronounced differences at the N- and C-terminal groups were observed. In the T state the N-terminal group of one α-chain forms an interchain saltbridge with the C-terminal group of the partner α-chain while these groups are free to move in the R state. A similar observation was made for the C-terminal group of the β-chains which form an intrachain saltbridge with Asp 94 β of the same chain in the T state only. The N-terminal groups of the β-chains, which are of importance for effector binding (see below), are separated by 1 nm in the T state and by 1.6 nm in the R state.

Relatively small changes were observed in the tertiary structure of the hemoglobin subunits upon the T to R transition. However, such changes in tertiary structure are expected to be the trigger for the large quaternary change occurring upon oxygenation. In this respect the displacement of the ferrous-ion relative to the plane of the porphyrin group which takes place upon ligation has received much attention (6).

X-ray diffraction studies provide an accurate though static picture of the structure of proteins. Information on the fluctuations in structure in solution, expected to be of importance for the function of these molecules, can however not be obtained from such studies. That these fluctuations indeed occur was recently demonstrated in a number of studies on other proteins. In this respect we mention computer calculations on the molecular dynamics of bovine pancreatic trypsine inhibitor (13), dynamic fluorescence decay studies of the accessebility for molecular oxygen to tryptophane residues in the interior of a number of proteins (14) and ^{13}C NMR relaxation measurements of the ^{13}C signals of various proteins at different magnetic fields yielding information on the correlation time of fluctuations in amino acid conformations (15). All studies point to the presence of structural fluctuations with frequencies

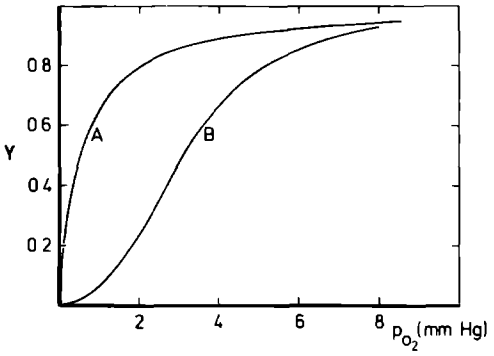

Fig. 2. Oxygen saturation (Y) of isolated α-chains (curve A) and hemoglobin (curve B) as a function of the oxygen pressure P_{O2}.

covering the pico- and nano-second time domain. The root mean-square amplitude of these fluctuations was estimated to be 0.2 nm (13).

From these observations it is expected that the hemoglobin molecule undergoes extensive fluctuations in structure as well. In light of the relevance of conformational equilibria for the biological functioning of the molecule (see below) it is therefore particularly unfortunate that no studies on this aspect of the hemoglobin structure have been published as yet.

Functional Properties of Hemoglobin

Fig. 2 shows an oxygen saturation curve of hemoglobin and of the monomeric α-chains. In contrast to the hyperbolic binding curve obtained for these chains the curve obtained for hemoglobin shows the oxygen affinity to increase as saturation proceeds. This behaviour, referred to as cooperative binding, is essential to the physiological function of the protein; upon a decrease in oxygen pressure the oxygen release is facilitated as compared to non-cooperative binding (see Fig. 2). Physically the phenomenon of cooperative ligand binding implies that the oxygen affinity of unligated heme groups increases upon ligation of other heme groups in the same molecule. This heme-heme interaction must be caused by ligand induced conformational changes since the distance between the hemes is too large to permit a direct coupling.

Several models have been proposed to explain the oxygen binding properties of hemoglobin. The two most cited are that of Monod, Wyman and Changeux (MWC (16)) and that of Koshland, Némethy and Filmer (KNF (17)).

The MWC model is in fact a two-state model. It is assumed that hemoglobin is capable the adopt two different quaternary structures at any state of ligation. One structure, having low oxygen affinity, is predominant at low levels of saturation. When oxygen saturation proceeds, the dynamic conformational equilibrium is shifted to the other structure having high oxygen affinity. This shift from one conformation to the other accounts for the cooperativity. The two structures determined in X-ray cristallography are commonly identified with the two structures of the MWC model.

In the KNF model it is assumed that upon oxygen binding the conformation of hemoglobin changes sequentially. After each oxygen binding step the structure of the molecule is altered. The change in inter-subunit contact energy accounts for the cooperativity in this case.

Although both models are able to explain the phenomenon of positive cooperativity, they are not capable to fit quantitatively very accurate measurements of the oxygen binding (18, 19). Moreover, experiments on solutions containing partly ligated hemoglobin were interpreted to show two distinct conformations favouring the MWC model at one hand (see for instance, flash photolysis experiments (20) and experiments on spin-state hybrids (21-23)) while other experiments were interpreted to reflect intermediate conformations favouring the KNF model on the other hand (see for instance, NMR studies on partly saturated hemoglobin solutions (24, 25)). This dualism has led to the formulation of a number of modified models bearing the characteristics of both the KNF and MWC models. A good representative is the model of Weber (26,27).

Irrespective of the molecular mechanism of conformational changes it is however beyond any doubt that ligated and unligated hemoglobin possess different quaternary structures, each having characteristic binding properties for heme ligands and for effectors.

That protons are effectors of the oxygen binding was established

as early as in 1904 (28) as it appeared that the oxygen affinity of hemoglobin increases upon an increase in pH. This effect, referred to as the Bohr-effect, is readily explained by a larger affinity of protons towards unligated hemoglobin than towards ligated hemoglobin.

Perutz (6) has proposed a stereochemical explanation for this difference in affinity. Due to saltbridge formation (see above), the N-terminal groups of the α-chains and the C-terminal groups of the β-chains are supposed to have a larger proton affinity in unligated hemoglobin as compared to ligated hemoglobin. In our laboratory it was recently shown (29-32) that the Bohr-effect consists of a chloride independent and a chloride dependent contribution. Strong evidence was provided that in deoxyhemoglobin chloride ions form a complex with the α-NH_2 group of Val 1α of one α-chain and with the guanidino group of Arg 141α of the partner chain. As a result the proton affinity of these residues increases upon an increase in chloride activity, accounting for the chloride ion dependent Bohr-effect. The salt independent Bohr-effect could be attributed to His 146β which forms a saltbridge with Asp 94β in unligated hemoglobin. Chloride binding by the α-chain termini was also observed in X-ray diffraction studies (33, 34).

A class of compounds exerting a very strong influence on the oxygen binding by hemoglobin is formed by polyphosphates such as 2,3-diphosphoglycerate, adenosine triphosphate and *myo*- inositol hexakis- and pentakis-phosphate. These polyphosphates are commonly referred to as allosteric effectors. Because of the central part these polyphosphates play in the studies described in this thesis, their influence on the oxygen binding and on the structure of hemoglobin is described into some detail below.

Interaction of Polyphosphates with Hemoglobin

Although the presence of organic phosphates in the erythrocytes of mammals was discovered as early as in 1925 by Greenwald (35), the function of those molecules in relation with hemoglobin was not recognized until 1967. In that year Benesch and Benesch (36) and Chanutin and Curnish (37) showed that 2,3-diphosphoglycerate (DPG) present in human erythrocytes in equimolar amount with hemo-

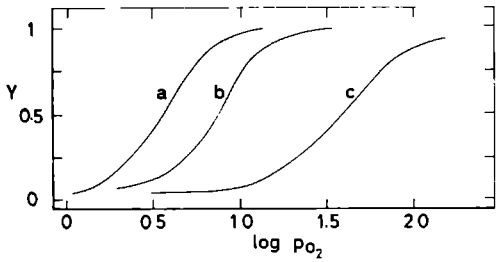

Fig. 3. Effect of DPG and IHP on the oxygenation curve of human hemoglobin. (a), stripped hemoglobin; (b), hemoglobin + DPG; (c), hemoglobin + IHP. Bistris buffer, pH 7.3.

globin, suppresses strongly the oxygen affinity of the protein. These findings promoted a number of studies examining the effect of DPG analogues on the oxygen binding by hemoglobin. Amongst these molecules, *myo*- inositol hexakisphosphate (IHP) has received most attention.

IHP is an analogue of *myo*- inositol pentakisphosphate present in the erythrocytes of avians and turtoise (38). It was shown to be an even more powerfull effector than DPG (39,40). Fig. 3 illustrates the effect of DPG and IHP on the oxygen binding by human hemoglobin. Upon adding saturating amounts of polyphosphate, the oxygen binding isotherm is shifted to lower affinity. This effect is more pronounced for IHP than for DPG. The shape of the binding isotherm is hardly dependent on the presence or absence of polyphosphate molecules. This implies that the hemoglobin cooperativety is almost unaffected by these effectors.

At 37°C, the oxygen pressure for half saturating (p_{50}) in the presence of DPG is about equal to the mean oxygen pressure in venous blood. Under these conditions stripped hemoglobin remains completely saturated with oxygen showing the physiological importance of DPG.

The decrease in oxygen affinity upon adding effectors is explained by a preferential binding of the polyphosphate molecules to unligated hemoglobin and is quantitatively expressed by the following relation (41)

$$\log p_m - \log p_m^o = 1/4 \log \frac{K_D}{K_O} \quad (1)$$

where p_m^o and p_m are the median oxygen pressure in the absence and presence of effector respectively and K_D and K_O the association constants for the binding of the effector molecule to unligated and fully ligated hemoglobin. In most cases p_m^o and p_m may be replaced by p_{50}^o and p_{50} being the oxygen pressure at half saturation. The use of eqn. (1) tacitly assumes that under the conditions of the experiments both Hb and HbO_2 are fully saturated with polyphosphate.

Analysis of the data in Fig. 3 based on eqn. (1) demonstrates that the ratio K_D / K_O is larger for IHP than for DPG.

At physiological salt conditions (circa 0.16 M) both DPG and IHP bind to Hb and HbO_2 in equimolar amounts, in other words, the stoichiometry of binding is unity (42-45). At low ionic strength additional binding sites of low affinity were observed on ligated hemoglobin (46-48).

The binding site for IHP and DPG on deoxyhemoglobin was identified by means of X-ray diffraction studies (49,50) and was demonstrated to be formed by a cluster of eight positively charged amino acid residues located at the β-chain side of the central cavity. The residues involved are Val 1β, His 2β, Lys 82β and His 143β of both β-chains. From experiments on IHP binding to mutant hemoglobins in which one or more of these groups have been replaced, it was shown that in solution IHP binds to the same residues as well (51-53). Furthermore, evidence for this location of the polyphosphate binding site has been provided by a number of studies on the binding of different polyelectrolytes to deoxyhemoglobin. In this respect we mention the binding of pyridoxal compounds (54,55) and the binding of benzene hexacarboxylate (56). Experiments in which the affinities of IHP for human and chicken carboxyhemoglobin are compared very strongly suggest that the allosteric binding site for polyphosphates in ligated hemoglobin consists of the same cluster of positively charged residues as in deoxyhemoglobin (45). Recently additional evidence for this

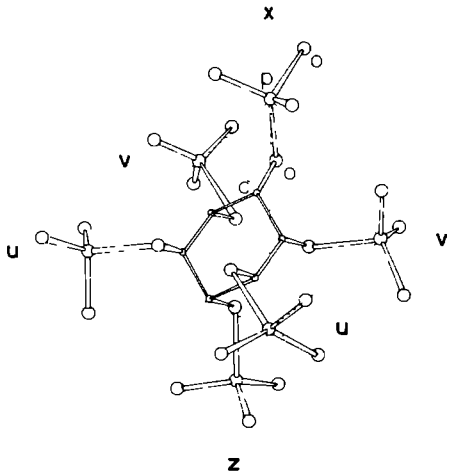

Fig. 4. The structure of IHP. The phosphate group labeled X is disposed equatorially, the other groups axially. The hydrogen atoms bound to the carbon atoms are omitted.

location of the binding site was provided by ^{31}P NMR relaxation measurements; it was shown that the spin-lattice relaxation times of the phosphorous resonances of DPG bound to spin-labeled Hb and HbO_2 are equal (57). The identification of the binding site in ligated hemoglobin is furthermore consistent with thermodynamic data on the binding of DPG to Hb and HbCO at low pH (58).

Further Aspects of IHP Binding to Hemoglobin

Fig. 4 shows the structure of IHP according to the X-ray analysis of Blank at al. (59). The molecule consists of a cyclohexane backbone bearing six phosphate groups. An axial position is found for five phosphate groups while one group is disposed equatorially. As a result the molecule possesses mirror symmetry, i.e. the groups labeled U in Fig. 4 are equivalent; the same is true for the groups labeled V. The overall appearance of the molecule is that of a sphere with a radius of 0.5 nm. This is close to the dimensions of the central cavity of hemoglobin in which the IHP binding site is located (see above). The IHP molecule bears a six-fold negative charge at pH 4 and a twelve-fold negative charge

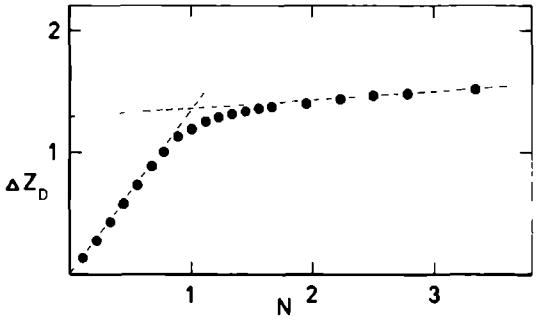

Fig. 5. Number of protons absorbed (ΔZ_D) upon binding of IHP to deoxyhemoglobin at pH 8.0. N is the molar ratio of IHP over Hb.

above pH 11 (44).

At neutral pH the reversible binding of IHP to deoxyhemoglobin is associated with proton uptake (44,45,60) due to a pK shift of the basic groups making up the binding site (56). This pK shift results from the electrostatic interaction of the highly charged IHP molecule with the basic groups. In a pH-stat experiment this proton uptake is used as a monitor of the degree of binding of IHP to hemoglobin as a function of the polyphosphate / protein molar ratio (see Fig. 5). Using this approach an association constant of 1.6×10^7 M^{-1} was obtained for the binding of IHP to deoxyhemoglobin at physiological pH (44).

In the absence of IHP both the α- and β-chains of hemoglobin bind CO at the same rate. In the presence of IHP however pronounced heterogenity in the CO-binding kinetics was observed. This was interpreted to reflect an IHP induced inequivalence of the hemes on the α- and β-chains (47). IHP was further shown to decrease the oxygen affinity of unligated hemoglobin (61). Both effects point to the occurence of IHP induced conformational changes in deoxyhemoglobin. Indeed X-ray diffraction studies showed changes in the relative orientations of the helices in the β-chains upon polyphosphate binding (49,50).

At neutral pH, the binding of IHP to ligated hemoglobin is too weak to be quantified by direct binding studies. The extent of

binding can however be estimated from the shift of the oxygenation curve (see Fig. 3 and eqn. (1)). In this way a value of 10^3 M^{-1} for K_0 could be estimated.
Strong evidence have been presented that conformational changes occur in ligated hemoglobin upon IHP binding as well. For example, upon IHP binding i) ligand dissociation is enhanced (62), ii) the optical spectra of HbCO and HbO_2 change (63), iii) EPR measurements of HbCO and HbO_2 spin-labeled at the Cys 93β position reveal distinct changes in the magnetic environment of this label (64). In this respect it is interesting to note that according to the early X-ray studies of Perutz and collaborators (1-6) the central cavity in ligated hemoglobin is too small to accommodate organic phosphates. However recently evidence have been presented showing unambigiously that these molecules do bind to this site (see above); hence a change in protein structure is very likely to occur upon IHP binding to ligated hemoglobin.

SURVEY OF THIS THESIS

As has been pointed out above, IHP has a strong effect on the functional properties of human hemoglobin. To provide a better understanding of these phenomena, the nature of IHP binding to both ligated and unligated is investigated in this thesis.
These investigations were started by studying the proton binding behaviour of IHP free in solution using ^{31}P NMR and potentiometric titration techniques (Chapter II). An anomalous buffer capacity was observed for this molecule. This could be explained by introducing a model taking into account the large electrostatic interaction within the IHP molecule. From this model computer simulations of the pH dependence of the ^{31}P NMR spectra were carried out.
Chapter III presents a similar study on IHP bound to Hb or HbCO. A modified version of the model presented in Chapter II appears to be capable to grossly account for the pH dependence of the ^{31}P NMR spectra of IHP bound. In this Chapter a mechanism is discussed explaining the large difference in affinity of IHP for Hb and HbCO at neutral pH.

Chapter IV describes a ^{31}P NMR study on the kinetics of IHP binding. It appears that IHP rapidly exchanges between the solution and the central cavity of hemoglobin. This observation is quite unexpected in view of the high affinity of IHP towards the protein. Furthermore evidence is provided for an additional IHP binding site of low affinity on both Hb and HbCO. In this Chapter a kinetic model is proposed which accounts for the observation of fast exchange. In this model the additional site serves as a entry or leaving site for IHP binding to the central cavity.

REFERENCES

1. Perutz, M.F., Muirhead, H., Cox, J.M., Goaman, L.C.G., Matthews, F.S., McGandy, E.L. & Webb, L.E. (1968) Nature (London) 219, 29-32
2. Perutz, M.F., Muirhead, H., Cox, J.M. & Goaman, L.C.G. (1968) Nature (London) 219, 131-139
3. Perutz, M.F. (1969) Proc. Roy. Soc. B173, 113-140
4. Muirhead, H. & Greer, J. (1970) Nature (London) 228, 516-519
5. Bolton, W. & Perutz, M.F. (1970) Nature (London) 228, 551-552
6. Perutz, M.F. (1970) Nature (London) 228, 726-739
7. Antonini, E. & Brunori, M. (1971) Hemoglobin and Myoglobin in their Reactions with Ligands, North-Holland Publishing Company, Amsterdam
8. Weissbluth, M. (1974) Hemoglobin, Cooperativity and Electronic Properties, Springer-Verlag, Berlin, New York
9. Shulman, R.G., Hopfield, J.J. & Ogawa, S. (1974) Quart. Rev. Biophys. 8, 325-420
10. Edelstein, S.J. (1975) Ann. Rev. Biochem. 44, 209-232
11. Perutz, M.F. (1978) Sci. Am. 239 (6), 68-87
12. Fermi, G. (1975) J. Mol. Biol. 97, 237-256
13. McCammon, J.A., Gelin, B.R. & Karplus, M. (1977) Nature (London) 267, 585-590
14. Lackowicz, J. & Weber, G. (1973) Biochemistry 12, 4171-4179
15. Howarth, O.W. (1978) Faraday Trans. II 1978, 1031-1041
16. Monod, J., Wyman, J. & Changeux, J.P. (1965) J. Mol. Biol. 12, 88-118

17. Koshland, D.E., Némethy, G. & Filmer, D. (1966) Biochemistry 5, 365-385
18. Imai, K. & Yonetani, T. (1975) J. Biol. Chem. 250, 7093-7098
19. Otsaka, J. & Kunisawa, T. (1977) Arch. Biochem. and Biophys. 179, 706-714
20. Ferrone, F.A. & Hopfield, J.J. (1976) Proc. Natl. Acad. Sci. U.S.A. 73, 4497-4501
21. Cassoly, R. & Gibson, Q.H. (1972) J. Biol. Chem. 247, 7332-7341
22. Ogawa, S. & Shulman, R.G. (1972) J. Biol. Chem. 70, 315-336
23. Rollema, H.S., Raap, A. & de Bruin, S.H. (1978) Eur. J. Biochem. 83, 313-317
24. Huestis, W.H. & Raftery, M.A. (1975) Biochemistry 14, 1886-1892
25. Viggiano, G. & Ho, C. (1979) Proc. Natl. Acad. Sci. U.S.A. 76, 3673-3677
26. Weber, G. (1972) Biochemistry 11, 864-878
27. Weber, G. (1975) Adv. Protein Chem. 29, 1-84
28. Bohr, C., Hasselbach, K. & Drought, A. (1904) Skand. Arch. Physicol. 16, 402-412
29. de Bruin, S.H., Rollema, H.S., Janssen, L.H.M. & van Os, G.A.J. (1974) Biochem. Biophys. Res. Commun. 58, 210-215
30. Rollema, H.S., de Bruin, S.H., Janssen, L.H.M. & van Os, G.A.J. (1975) J. Biol. Chem. 250, 1333-1339
31. van Beek, G.G.M., Zuiderweg, E.R.P. & de Bruin, S.H. (1979) Eur. J. Biochem. 99, 379-383
32. van Beek, G.G.M. & de Bruin, S.H. (1980) Eur. J. Biochem., in the press
33. Arnone, A., Benesch, R.E. & Benesch, R. (1977) J. Mol. Biol. 115, 627-642
34. O'Donnel, S., Mandaro, R., Schuster, T.M. & Arnone, A. (1979) J. Biol. Chem. 254, 12204-12208
35. Greenwald, I.J. (1925) J. Biol. Chem. 63, 339-349
36. Benesch, R. & Benesch, R.E. (1967) Biochem. Biophys. Res. Commun. 26, 162-167
37. Chanutin, A. & Curnish, R.R. (1967) Arch. Biochem. Biophys. 121, 96-102

38. Johnson, L.F. & Tate, M.E. (1969) Can. J. Chem. 47, 63-73
39. Benesch, R., Benesch, R.E. & Yu, C.I. (1968) Proc. Natl. Acad. Sci. U.S.A. 59, 526-632
40. Bunn, H.F. & Guidotti, G. (1971) J. Biol. Chem. 247, 2345-2350
41. Szabo, A. & Karplus, M. (1976) Biochemistry 15, 2869-2877
42. de Bruin, S.H., Rollema, H.S., Janssen, L.H.M. & van Os, G.A.J. (1974) Biochem. Biophys. Res. Commun. 58, 204-209
43. Nelson, D.P., Miller, W.D. & Kiesow, L.A. (1973) J. Biol. Chem. 249, 4770-4775
44. Edalji, R., Benesch, R.E. & Benesch, R. (1976) J. Biol. Chem. 251, 7720-7721
45. Brygier, J., de Bruin, S.H., van Hoof, P.K.M.B. & Rollema, H.S. (1975) Eur. J. Biochem. 60, 379-383
46. Garby, L., Gerber, G. & de Verdier, C.H. (1969) Eur. J. Biochem. 10, 110-115
47. Gray, R.D. & Gibson, Q.H. (1971) J. Biol. Chem. 246, 7168-7174
48. Desbois, A. & Banerjee, R. (1975) J. Mol. Biol. 92, 479-493
49. Arnone, A. (1972) Nature (London) 237, 146-149
50. Arnone, A. & Perutz, M.F. (1974) Nature (London) 249, 34-36
51. Bare, G.H., Alben, J.O., Bromberg, P.A., Jones, T.J., Brimhall, B. & Padilla, F. (1973) J. Biol. Chem. 249, 773-779
52. Bonaventura, J., Bonaventura, C., Sullivan, B. & Godette, G. (1975) J. Biol. Chem. 250, 9250-9255
53. Bonaventura, J., Bonaventura, C., Sullivan, B. & Ferruzi, G. (1976) J. Biol. Chem. 251, 7563-7571
54. Benesch, R.E., Benesch, R., Renthal, R.D. & Maeda, N. (1972) Biochemistry 11, 3576-3582
55. Benesch, R.E., Yung, S., Suzuki, T., Bauer, C. & Benesch, R. (1973) Proc. Natl. Acad. Sci. U.S.A. 70, 2595-2599
56. Bucci, E., Salahuddin, A., Bonaventura, J. & Bonaventura, C. (1978) J. Biol. Chem. 253, 821-827
57. Gupta, R.K., Benovic, J.L. & Rose, Z.B.(1979) J. Biol. Chem. 254, 8250-8255
58. van Beek, G.G.M. & de Bruin, S.H. (1979) Eur. J. Biochem 100, 497-502

59. Blank, G.E., Pletcher, J. & Sax, M. (1971) Biochem. Biophys. Res. Commun. 44, 319-325
60. Benesch, R.E., Edalji, R. & Benesch, R. (1977) Biochemistry 16, 2594-2597
61. Minton, A.P. & Imai, K. (1974) Proc. Natl. Acad. Sci. U.S.A. 71, 1418-1421
62. Gibson, Q.H. & Gray, R.D. (1970) Biochem. Biophys. Res. Commun. 41, 415-420
63. Perutz, M.F., Kilmartin, J.V., Nagai, K. & Szabo, A. (1976) Biochemistry 15, 378-387
64. Johnson, M.E., Scholler, D.M., Hoffman, B.M. & Ho, C. (1978) Biochim. Biophys. Acta 535, 193-205

CHAPTER II

THE INFLUENCE OF ELECTROSTATIC INTERACTION ON THE PROTON-BINDING BEHAVIOUR OF *myo*-INOSITOL HEXAKISPHOSPHATE

The hexakisorthophosphate ester of *myo*-inositol, *myo*-inositol hexakisphosphate (IHP), is found in the seeds of several plants (1). In hemoglobin research IHP is known as allosteric effector of the oxygen binding process (2,3) and its influence on the functional behaviour of human hemoglobin is analogous to the effect which 2,3-diphosphoglycerate and *myo*-inositol pentakisphosphate have in vivo on human and avian hemoglobin respectively (4,5).

In both unligated and fully ligated hemoglobin, IHP binds to a cluster of positively charged amino acid residues located at the entrance of the central cavity (6-8). The geometry of this binding site has been shown to be different for fully ligated and unligated hemoglobin (9). This is reflected in the ^{31}P NMR spectrum of IHP bound to the protein (Chapter III). In case the binding site of IHP on partially ligated hemoglobin differs in geometry from the site on fully ligated and unligated hemoglobin, information about intermediate structures can be obtained by using ^{31}P NMR techniques.

In this Chapter we present a study of the pH dependence of the ^{31}P NMR spectra of IHP free in solution which is complemented by an investigation of the proton binding behaviour of IHP using potentiometric methods. This study is a prerequisite for the interpretation of the ^{31}P NMR spectra of the hemoglobin IHP system.

The structure of IHP is depicted in Fig. 1 which is a projection of the three-dimensional structure as determined by X-ray analysis (10). An axial position is found for five phosphate groups, while one group is disposed equatorially. This places the phosphate groups on the angular points of a distorted octahedron.

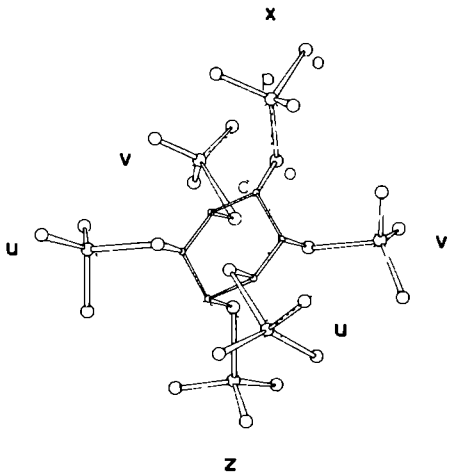

Fig. 1. The structure of IHP. The phosphate group labeled X is disposed equatorially, the other groups axially. The hydrogen atoms bound to the carbon atoms are omitted.

The overall appearance of the molecule is that of a sphere with a radius of 0.5 nm. Each phosphate group bears a twofold negative charge at a pH value higher than 11 and is fully protonated at a pH value lower than - 1. As will be shown in this chapter, the high charge density on the molecule produces several anomalous effects on the potentiometric titration curve, the pH dependence of the ^{31}P NMR spectrum and the linewidths of the phosphorous resonances of IHP. These effects are analysed in terms of electrostatic interactions between the different phosphate groups on the molecule.

myo- Inositol pentakisphosphate (IPP), having a structure closely resembling that of IHP (5), was isolated from chicken blood. The proton binding behaviour of this organic phosphate was studied by potentiometric and ^{31}P NMR methods as well.

Potentiometric Titration of IHP

A solution of 0.1 M IHP, sodium salt (BDH Chemicals Ltd) in H_2O was freed from inorganic impurities by gel filtration over Sephadex G-15; subsequently it was converted to the free acid by recycling for 1 h through Amberlite IR-120 (BDH). Samples of this solution, to which KCl was added up to a concentration of 0.1 M, were used to measure the proton binding at 25°C by automatic titration with NaOH (11). The concentration of IHP was calculated from the 1:1 stoichiometry in the binding of IHP to deoxyhemoglobin at pH 6.5 (8), as monitored by a pH-stat apparatus (12). Independently, the concentration was determined spectrophotometrically as the phosphomolybdate complex according to the method of Fiske and Subbarow (13). The potentiometric titration curves were corrected for the buffer capacity of water. To this end the titration curve of a solution of 0.2 M KCl was used as a blank.

pH Dependence of the ^{31}P Chemical Shifts of IHP

A solution of 0.01 M IHP, free acid, in 50% (v/v) ^2H_2O (0.10 M KCl, 0.001 M EDTA) was titrated with 0.10 M KOH in 50% (v/v) ^2H_2O. Nitrogen gas was continuously flushed through the titration vessel. At different pH values (pH meter reading) samples were taken and transferred into 5-mm NMR tubes (Wilmad) which were flushed with N_2 just before. EDTA was added to bind paramagnetic metal ions. The ^{31}P NMR spectra were recorded on a Varian XL-100 NMR spectrometer operating in the Fourier Transform mode. The spectra consist of up to 100 accumulations each, having digital resolution of 0.25 Hz/point and being proton-decoupled. Field stabilization was achieved by locking to the ^2H NMR signal of the ^2HOH present in the samples. The temperature of the samples was kept at 25 ± 1°C. Chemical shifts δ are reported as parts per million (ppm) from 20% H_3PO_4 in ^2H_2O. Downfield shifts are defined positive. Trimethyl phosphate was used as internal or external reference.

Isolation of myo-Inositol Pentakisphosphate

IPP was isolated from washed chicken erythrocytes which were ultrasonically lysed. The hemolysate was dialyzed against distilled water; KCl was added up to a concentration of 0.1 M. The solution was freed from adenosine phosphates by passage over Sephadex G-50 equilibrated with 0.1 M KCl. Subsequently the pH of the solution was adjusted to pH 10 with ammonium buffer (0.1 M NH_4Cl/NH_4OH, 0.1 M in KCl). At this high pH IPP dissociates from the chicken hemoglobin. IPP and hemoglobin were separated on a Sephadex G-50 column by elution with the same ammonium buffer. IPP was desalted by gel filtration over Sephadex G-10. The solutions were concentrated by lyophilization. Potentiometric titration curves and NMR spectra were obtained as for IHP.

Miscellaneous

^2H_2O (99.75%) was purchased from Merck; all reagents were of analytical grade.

Curve simulations were carried out on an IBM 370/158 computer.

RESULTS

Potentiometric Titration of IHP

The results of the titration of IHP with NaOH are presented in Fig. 2 where pH is plotted versus Z, the mean charge of the molecule (Fig. 2, lower panel). In Fig. 2, upper panel, $\Delta pH/\Delta Z$ is plotted versus Z. The titration curves (pH vs Z) are only partly shown: data in the low and high pH regions, which only reflect titration of water, are not included. To be able to compare the potentiometric results with the NMR data a solution of IHP in 50% (v/v) ^2H_2O was titrated as well. The curve obtained does not deviate significantly from the titration curve of IHP in H_2O (Fig.2). The differential titrations curve ($\Delta pH/\Delta Z$ vs Z) displays maxima at Z = -12, -8 and -6. The maxima at Z = -12 and Z = -6 can be considered as equivalence points for the double and single deprotonated state of each of the six phosphate groups on the IHP molecule. This interpretation is based on the assumption that deprotonation of IHP occurs in two well separated steps. The validity of this assumption will be discussed in connection with the ^{31}P

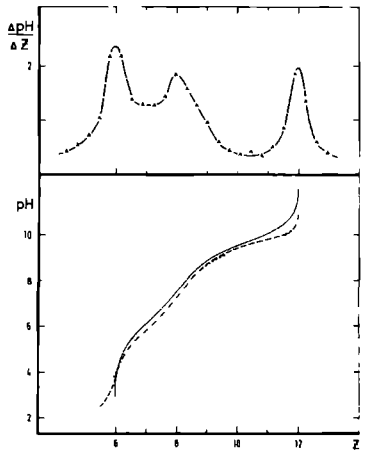

Fig. 2. Potentiometric titration of IHP. Lower panel, titration curves in H_2O (— — —) and 50% (v/v) ^2H_2O (- - -). The solid line (——) represents the titration curve calculated from the NMR data shown in Fig. 5. Upper panel, differential titration curve of IHP in 50% (v/v) ^2H_2O. Experimental conditions: 5 - 10 mM IHP, 0.10 M KCl, 25°C.

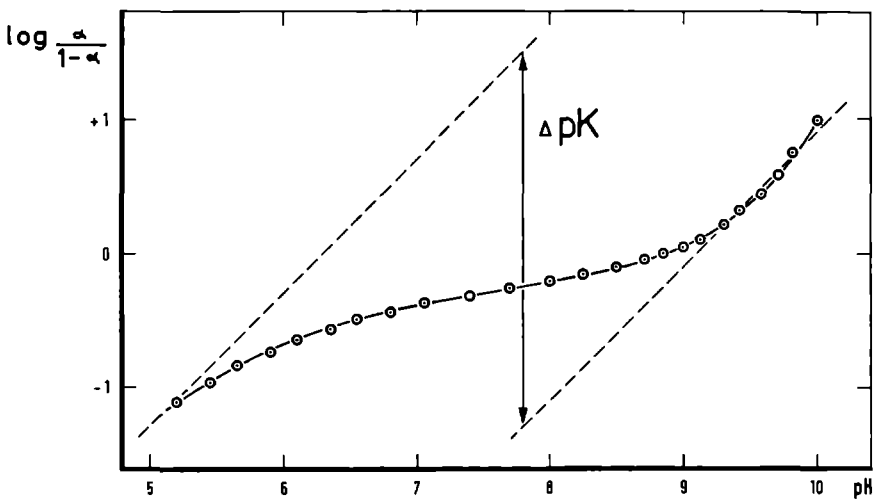

Fig. 3. Hill plot calculated from the titration data of IHP in 50% (v/v) ^2H_2O.

NMR data. The maximum at Z = -8 cannot be assigned to any specific IHP structure; it indicates an anomalous buffer capacity which will be extensively discussed below.

In this chapter we will concentrate on the proton binding behaviour of IHP above pH 3.5; the protons titrated are referred to as the second protons. In Fig. 3 a Hill plot, log (α/1 -α) vs pH, is shown which was calculated from the titration data of IHP in 50% (v/v) ^2H_2O assuming that α, the overall degree of dissociation of the second protons, is zero at pH 3.5 and unity at pH 11. The difference between the intercepts of the two asymptotes, ΔpK, is equal to the increase in pK in going to high pH (14); from this value the interaction free energy ΔF_{int} between the phosphate groups was calculated to be 15.5 kJ/mol according to the relation $\Delta F_{int} = 2.3\ RT\ \Delta pK$ (15).

pH Dependence of the ^{31}P NMR Spectra of IHP

As it is known (16) that the chemical shift of phosphorous esters is dependent on the concentration and the nature of counter ions, care was taken to keep the potassium-ion concentration constant in all NMR experiments. This counter ion effect was apparent in spectra of IHP titrated with NaOH which differed significantly from those titrated with KOH as presented in this chapter.

Fig. 4 shows some examples of ^1H-decoupled ^{31}P NMR spectra relevant to our discussion. Spectrum A (pH 3.70) shows four rather broad resonances with intensity ratio 1:2:2:1. This ratio is a result of the magnetic equivalence of the nuclei in the groups u,u and v,v due to the presence of a mirror plane in the molecule (cf. Fig. 1). Spectrum B (pH 5.67) shows the presence of a J-coupling between three ^{31}P nuclei observed in the pH region from 4 to 8. Spectrum C (pH 10.41) shows the effect of chemical exchange; all resonances are broadened to a different extent. At pH 12.75 (spectrum D) all resonances have small linewidths; five phosphate group nuclei resonate at approximately the same frequency, while one resonance is found further down field.

Fig. 5 presents the pH dependence of the ^{31}P chemical shifts of the phosphate group resonances of IHP. At pH 12 the IHP molecule is fully deprotonated (Fig. 2), therefore we attribute the resonances above pH 12 to the doubly charged phosphate groups.

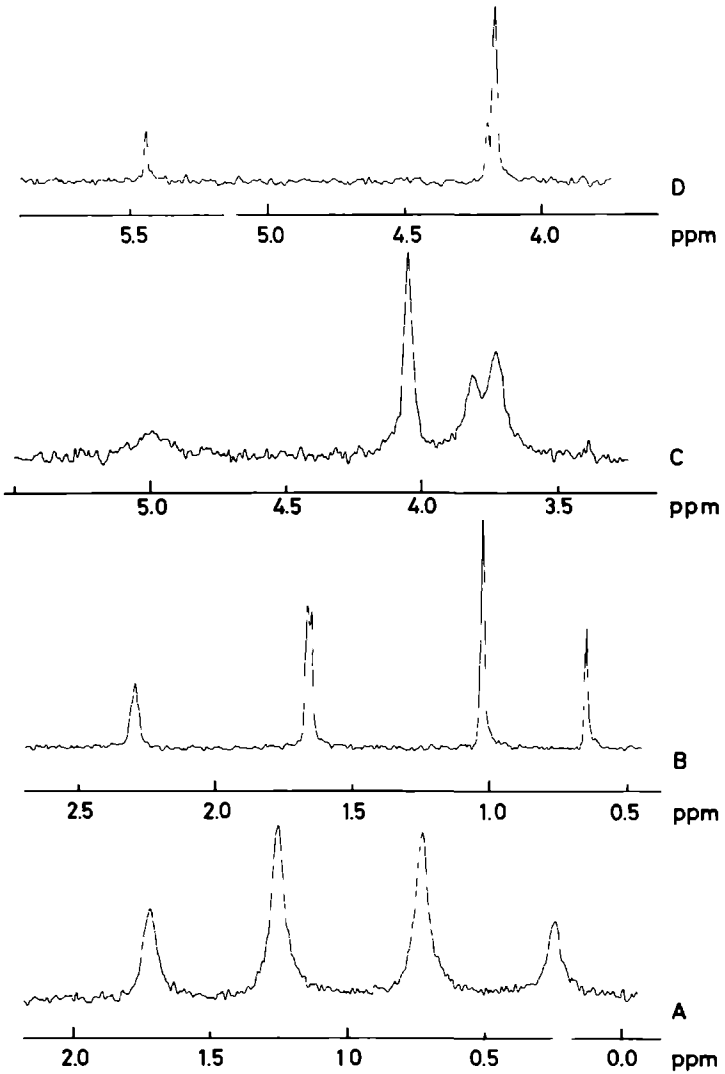

Fig. 4. Proton-decoupled ^{31}P NMR spectra of 10 mM IHP in 50% (v/v) $^{2}H_2O$, 1 mM EDTA, .10 M in K^+, 25 °C. The solutions were freed from oxygen. Spectrum A was recorded at pH 3.70, B at pH 5.67, C at pH 10.41 and D at pH 12.75. Chemical shifts δ are reported downfield from 20% H_3PO_4 in $^{2}H_2O$.
Note the shift of scale for the different spectra.

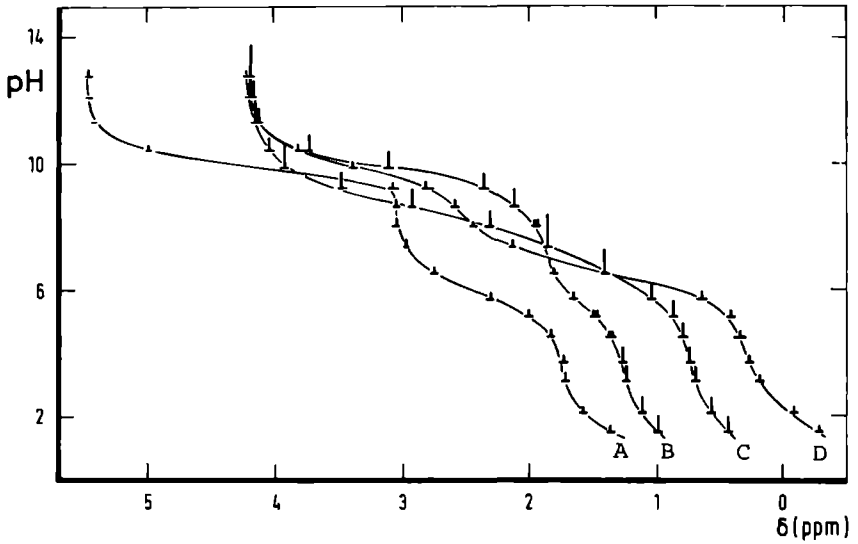

Fig. 5. pH dependence of the ^{31}P chemical shifts of IHP. Experimental conditions as in Fig. 4. The length of the vertical bar of the symbols is proportional to the resonance intensity. Doublet splitting is shown schematically. Chemical shifts are reported as in Fig. 4. A,B,C,D refer to the broadening pattern shown in Fig 11.

Upon lowering the pH, the resonances shift monotonously upfield, most resonances go through pseudo-equivalence points at different pH values, until a real equivalence point is reached at pH 3.5 for all resonances. At this pH the mean charge of the molecule is -6. The shift difference between the resonance positions at pH 12 and pH 3.5 is 3 - 4 ppm in magnitude. This value corresponds to the shift difference usually observed between the resonance positions of phosphate groups differing by one charge unit (17,18). At pH values lower than 3.5 the resonance positions are still function of pH. From these results we conclude that the resonances at pH 3.5 arise from phosphate groups with one single proton bound.

Assuming that the shift of each resonance k is solely determined by fast exchange of the phosphorous nucleus between the sites $-OPO_3^{2-}H^+$ (P) and $-OPO_3^{2-}$ (D), α_k , the degree of dissociation of the

second proton of group can be calculated from the relation (19)

$$\alpha_k = \frac{\omega_k - \omega_{Pk}}{\omega_{Dk} - \omega_{Pk}}$$

where ω_k is the pH-dependent resonance frequency of group k, ω_{Pk} and ω_{Dk} the resonance frequency of the singly protonated and deprotonated state of group k respectively.
With the values obtained for α_k, the contribution of each group to the mean charge Z was calculated as a function of pH according to the relation

$$Z = Z_{ref} - \sum_k \alpha_k$$

with a value of -6 taken for Z_{ref}.
The overall titration curve obtained in this way is included in Fig. 2. The curve almost coincides with the potentiometric titration curves. This result supports very strongly the validity of our assumption that the resonance positions are determined by fast exchange between two sites only. In other words, the chemical shift of the phosphorous resonance of one group is determined by the degree of deprotonation of that group only. This implies that the observed pseudo-equivalence points (Fig. 5) are a result of a pH-independence of α around pH 8. We can safely exclude shifts arising from any direct influence of the deprotonation state of one group on the electron orbitals of neighbouring groups, as was observed in pH-dependent ^{31}P NMR studies of adenosine triphosphate (20).

pH dependence of the Linewidths of the ^{31}P Resonances

In Fig. 11, left-hand panel, (see below) the linewidths of the ^{31}P resonances of IHP are plotted versus pH. The linewidths of the resonances in the multiplets were not determined; the total width of the multiplets is included in this figure. The observed minimum linewidth of 0.6 Hz for all resonances is due to inhomogenity of the magnetic field. The resonances broaden to a different extent as a function of pH; one resonance disappears completely around pH 10. A maximum linewidths of 10 Hz was estimated for this resonance. The pH-dependent linebroadening is interpreted in

terms of chemical exchange. A broadening pattern calculated as described in Discussion, is presented in Fig. 11, right-hand panel. The broadening is superimposed on a linewidth of 0.6 Hz.

pH Dependence of the ^{31}P NMR Spectra of IPP

Except for the equatorial hydroxyl function, which is not esterified in IPP, the structure of this molecule is identical to that of IHP (5). Two pairs of phosphate groups are magnetically equivalent due to the presence of a mirror plane in the molecule. Therefore, the proton-decoupled ^{31}P NMR spectra consist of three resonances with intensity ratio 1:2:2. The pH dependence of the resonance positions of IPP, presented in Fig. 6, is even more anomalous than that observed for IHP. For one phosphate group a decrease in α is observed upon an increase in pH. Broadening and J-coupling effects as observed for IHP are found for IPP as well. The overall NMR titration curve, calculated as described above, corresponds satisfactorily with the potentiometric data (results not shown).

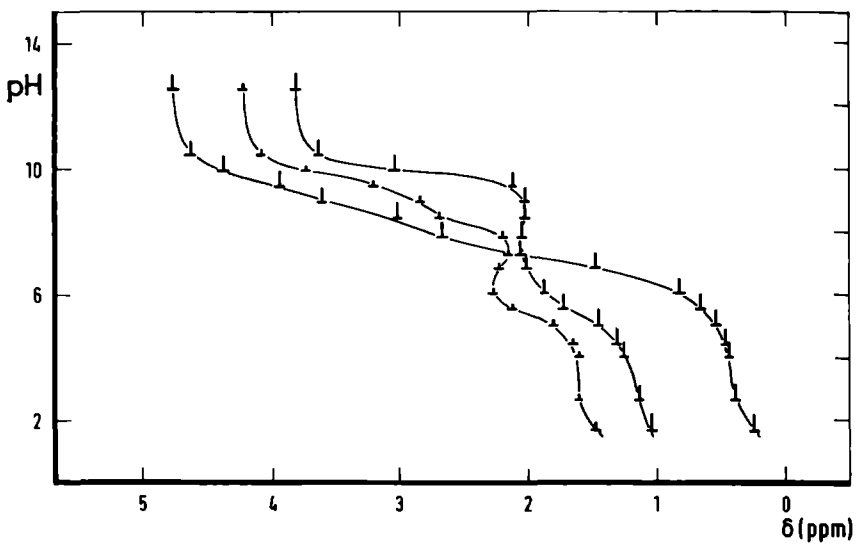

Fig. 6. pH dependence of the ^{31}P chemical shifts of IPP. Experimental conditions: 1.5 mM IPP, 50% (v/v) $^{2}H_2O$, 1mM EDTA, 0.10 M K^+, 25°C. The solutions were freed from oxygen. The length of the vertical bar of the symbols is proportional to the resonance intensity. Chemical shifts are reported as in Fig. 4.

The potentiometric and ^{31}P NMR studies on the proton binding behaviour of IHP and of IPP reveal three interesting physico-chemical properties of these molecules: first, dissociation of the second protons of the phosphate groups covers a large pH range; secondly, pseudo-equivalence points are present in the titration curves of both the whole molecules and the individual phosphate groups; thirdly, broadening of the ^{31}P magnetic resonances is strongly dependent on pH. These phenomena will be discussed in this order.

Range of Titration

Fig. 2 shows that the agreement between the potentiometric titration curves and the curve obtained from the ^{31}P NMR results is quite satisfactory. From this it is concluded that in both experiments the same quantity, namely the degree of dissociation for the second protons of the phosphate groups, is measured. Inspection of Fig. 2 reveals that the second deprotonation of the phosphate groups covers a pH range of 6.5 and exhibits a pseudo-equivalence point at Z = -8. These features cannot be explained by the mere presence of phosphate groups with substantially different pK values, as all δ/pH curves start at pH 3.5 and are completed at pH 12 (Fig. 5). This broad titration region is obviously a result of anticooperativity in proton release. The free energy of interaction, ΔF_{int}, has a value of 15.5 kJ/mol as calculated from a Hill plot (Fig. 3). This energy is electrostatic in nature as is shown by the following argument.

Assuming that ΔF_I, the free energy change of the reaction

$IHP^{11-} \rightarrow IHP^{12-} + H^+$ (predominant at pH 10)

and ΔF_{II}, the free energy change of the reaction

$IHP^{6-} \rightarrow IHP^{7-} + H^+$ (predominant at pH 5)

consists of an intrinsic contribution, ΔF_i, and an electrostatic contribution, $\Delta F_{el,I}$ and $\Delta F_{el,II}$ respectively, we can write:

$$\Delta F_I = \Delta F_i + \Delta F_{el,I} = \Delta F_i + (W^{12} - W^{11})$$

$$\Delta F_{II} = \Delta F_i + \Delta F_{el,II} = \Delta F_i + (W^{7} - W^{6})$$

with W^Z the work of charging the molecule to charge -Z.
For the free energy of interaction, ΔF_{int}, which is equal to $\Delta F_I - \Delta F_{II}$, we can write accordingly

$$\Delta F_{int} = (W^{12} - W^{11}) - (W^7 - W^6)$$

Applying the Debye-Hückel model, in which the charges on IHP are assumed to be smeared out over an impenetrable sphere (21), we estimate ΔF_{int} to be 8.8 kJ/mol at an ionic strength of 0.2. The calculation was carried out using a value of 80 for the dielectric constant of the solvent, a value of 0.5 nm for the distance of closest approach of mobile ions to the sphere. The result shows that the charge-dependent electrostatic contribution to the free energy of deprotonation can grossly account for the observed anti-cooperativity in proton release.

The Pseudo-equivalence Points

The Debye-Hückel model cannot explain the occurrence of pseudo-equivalence points in the titration curves of both the whole molecule and the individual phosphate groups. To account for these phenomena we developed the following model, which is basically analogous to the model of Koshland et al. (22) describing the cooperativity in oxygen binding to hemoglobin.
At any pH the ensemble of IHP ions in solution consists of species with all possible proton distributions, hereafter referred to as configurations.
In the pH region of interest (pH = 3.5 - 12) configurations with more than one proton bound per phosphate group will be present in negligable amount. Taking the symmetry of IHP into account, 40 different configurations need to be considered in this pH region; 14 of them are presented in Fig. 7. The main object of our model is to evaluate the concentrations of all configurations. Z, the quantity measured in the potentiometric titration experiment, obeys the relation

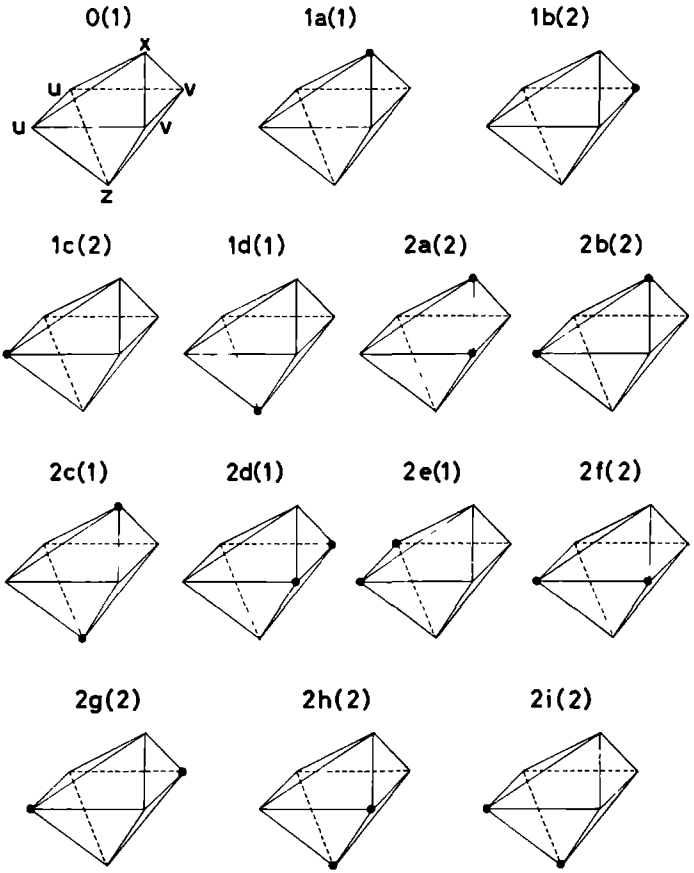

Fig. 7. Configurations of IHP with 0, 1 and 2 protons bound. Closed circles represent the protons bound. The labeling is arbitrary. Figures within brackets indicate the number of identical configurations.

$$Z = -12 + \frac{\sum_{\nu=0}^{6} \sum_{J} \nu(I_{\nu J})}{\sum_{\nu=0}^{6} \sum_{J} (I_{\nu J})}$$

where the right-hand term is equal to the mean value of the number of protons bound to IHP (23). $(I_{\nu J})$ represent the concentration of configurations with ν protons bound in distribution J. For instance, (I_{2a}) is the concentration of configuration 2a shown in Fig. 7. In order to calculate Z as a function of pH, it is sufficient to obtain values for the relative concentrations of the configurations as a function of pH (23). These relative concentrations are determined by the equilibrium constants linking the different configurations and by the proton concentration. For instance, the deprotonation of configuration 2d into 1b is governed by the equilibrium

$$I_{2d} \rightleftarrows I_{1b} + H^{+}$$

with dissociation constant $K_{2d,1b}$. The concentration ratio of the two configurations is given by:

$$\frac{(I_{1b})}{(I_{2d})} = K_{2d,1b}\ (H^{+})^{-1}$$

The procedure we developed to obtain values for all equilibrium constants $K_{\nu J,\nu' J'}$, will be illustrated for $K_{2d,1b}$.
$\Delta F_{2d,1b}$, the difference in free energy contents between 2d and 1b, will be equal to the free energy change of dissociation of the second proton from group v of configuration 2d (see Fig. 7).
$\Delta F_{2d,1b}$ consists of three contributions. The first is the intrinsic change in free energy, ΔF_{i}, which is equal to the deprotonation free energy of group v with uncharged neighbours. The second contribution, ΔF_{e}, corresponds to the work needed to remove the proton out of the potential well effective at group v as a result of the negative charge on each phosphate group due to the first

proton dissociation. The third contribution to $\Delta F_{2d,1b}$ equals the work needed to withdraw the proton out of the potential well due to a second negative charge on the adjacent groups x and z and on both groups u, of which one is opposing, while the other is adjacent to group v. This contribution consists therefore of terms describing the electrostatic interaction between adjacent groups, denoted as ΔF_{adj} and terms describing the interaction between opposing groups, denoted by ΔF_{opp}.
We define ΔF_v as the sum of the first two contributions ($\Delta F_v = \Delta F_i + \Delta F_e$); ΔF_v will be constant in the pH region considered. In first approximation the values for ΔF_{adj} and ΔF_{opp} are taken to be independent of the groups concerned. For $\Delta F_{2d,1b}$ we obtain

$$\Delta F_{2d,1b} = \Delta F_v + 3\Delta F_{adj} + \Delta F_{opp}$$

Introducing the equilibrium constants K_v, K_{adj} and K_{opp} using the general equation $\Delta F = - RT \ln K$ we can write:

$$K_{2d,1b} = K_v K_{adj}^3 K_{opp}$$

Proceeding in a similar way, all constants needed to calculate Z can be written as a function of K, K_{opp} and K_{adj} where $K = K_u = K_v = K_x = K_z$. It can easily be shown that under these conditions the electrostatic constants K_{opp} and K_{adj} obey the relation:

$$K_{adj}^4 K_{opp} = 10^{-\Delta pK}$$

where ΔpK can be estimated from the Hill plot (Fig. 3). From this relation values for K_{opp} and K_{adj} can simply be obtained by choosing the ratio $\Delta F_{opp}/\Delta F_{adj}$. Taking this ratio to be unity, the model describes the electrostatic interaction between equivalent groups, and becomes identical to the Linderstrøm-Lang model (24), based on the approximation of smeared-out charges. Accordingly an extended titration curve without a pseudo-equivalence point was calculated (result not shown). However, a ratio larger than unity

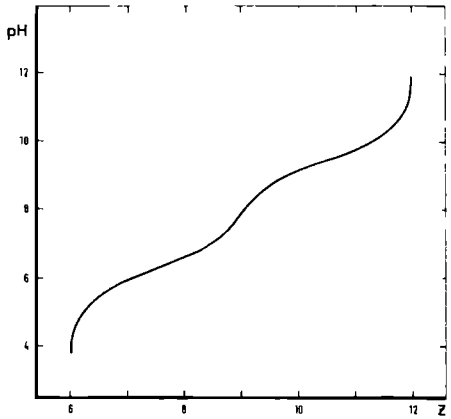

Fig. 8. Model calculation of the titration curve of IHP.
$\Delta F_{opp}/\Delta F_{adj}$ = 25; pK = 6.5. For further details see text.

is more plausible as is shown by the following argument.
Since the phosphate groups are rather polar, hydratation of these groups will occur. As a result, electrostatic interaction between adjacent groups will be drastically reduced due to the presence of a medium of high polarizability. On the other hand, due to the absence of water in the centre of the molecule, the medium between the opposing groups will be of low polarizability. We therefore choose ΔF_{opp} much larger than ΔF_{adj}, despite the greater distance between the opposing groups.
With $\Delta F_{opp}/\Delta F_{adj}$ = 25 and pK = 6.5, we calculated the titration curve shown in Fig. 8. The curve shows a very clear pseudo-equivalence point at Z = -9. In terms of our model, this titration behaviour can easily be understood. For values of Z smaller than -9, the configurations with adjacent groups deprotonated are predominant, giving rise to a small increase in free energy change per proton dissociation. For values of Z larger than -9, deprotonation will mostly occur at groups with doubly charged opposing groups. As a result a large increase in free energy change will occur per deprotonation step. These two effects give rise to the pseudo-equivalence point.

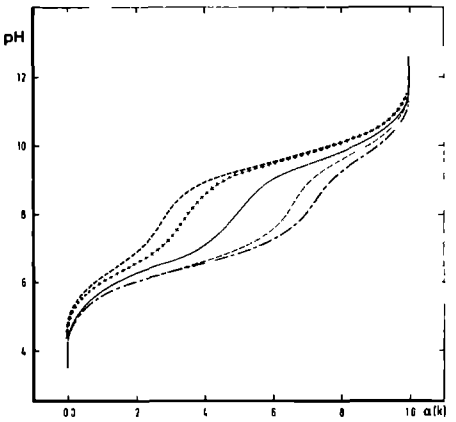

Fig. 9. Model calculation of the overall titration curve (——) and of the titration curves of the phosphate groups of IHP.
(++++) x; (----) z; (-·-·-) u; (— —) v, see also Fig. 1.
Parameters used:

$\Delta F^{ux}_{adj} = 0.79\Delta F^{og}_{adj}$, $\Delta F^{uv}_{opp} = 26\Delta F^{og}_{adj}$, $\Delta F^{xz}_{opp} = 28\Delta F^{og}_{adj}$,

$pK_x = 6.8$, $pK_z = pK_u = 6.5$, $pK_v = 6.9$.

og is an abbreviation for other groups. For further details see text.

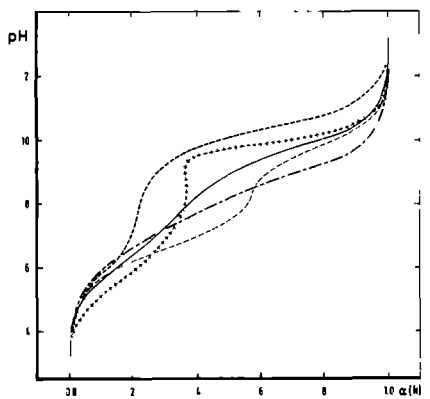

Fig. 10. Experimental titration curve (Fig. 2) and NMR curves (Fig.5) calibrated to the scale of Fig. 9. Symbols were chosen as in Fig. 9. The assignment of resonances with equal intensity to specific phosphate groups is arbitrary.

From an extended version of the model, where K, K_{adj} and K_{opp} are allowed to vary for different groups, the titration curves of individual phosphate groupswere calculated as well. The best resultsobtained for IHP, by varying the parameters by hand, are presented in Fig. 9, where pH is plotted versus α_k, the degree of dissociation for the second proton of the individual phosphate groups k. In order to calculate the overall titration curve, included in the figure, α was taken to be zero at Z = -6 and equal to unity at Z = -12. All curves exhibit additional equivalence points and titrate over the entire pH region; this is in qualitative agreement with the experimental data. For reasons of comparison Fig. 10 is presented where the potentiometric titration curve (Fig. 2) and the δ/pH curves (Fig. 5) are calibrated to the same scale. A fit of the model calculations to the experimental data by computer minimalisation (Minuit program, from CERN, Genève) was attempted but did not work out. This failure is probably due to the limitations of the model proposed, i.e. the model does not allow the geometry of IHP to vary with the proton distribution. For the IPP system, a decrease in proton dissociation is observed for one group upon an increase in pH (Fig. 6). As the structure of IPP resembles that of IHP, it is justified to use our model for a qualitative explanation of this behaviour. The degree of proton dissociation for each group is only determined by the difference in free energy of those configurations in which this group is protonated or deprotonated respectively. Configurations with this group deprotonated are predominant at some pH values, while at higher pH configurations with this group protonated are predominant, giving rise to the observed phenomenon. This effect could also be simulated for the titration curve of group z of IHP, using a parameter set $pK_x = pK_v = 6.3$, $pK_u = pK_z = 6.0$, $\Delta F^{xz}_{opp} = 7\Delta F^{og}_{adj}$, $\Delta F^{uv}_{opp} = 3\Delta F^{og}_{adj}$, $\Delta F^{xu}_{adj} = \Delta F^{xv}_{adj} = 0.5\Delta F^{og}_{adj}$, where the superscripts stand for the participating groups, and og is an abbriviation for other groups.

In conclusion we can say that the model proposed is able to descibe qualitatively all titration effects observed.

Broadening of the ^{31}P Resonances of IHP

In the pH range 4.5 to 8 a multiplet splitting with J = 2 Hz is observed for two of the ^{31}P resonances of IHP (cf. Fig. 4). One of the resonances of double intensity has doubled shape, while one of the resonances of single intensity has triplet shape. This splitting is caused by a scalar interaction between three phosphorous nuclei, two of them being equivalent. Two resonances with doubled and triplet shape are also observed in the ^{31}P NMR spectrum of IPP. A quantitative explanation for these effects in terms of orbital overlap between the phosphate groups cannot be given as yet.

A value of 1.3×10^{-10} s for the rotational correlation time of IHP was calculated from the Stokes-Einstein relation. This yields the relaxation parameters $T_1 = T_2 = 6$ s for the dipolar relaxation of the phosphorous nucleus by the decoupled vicinal proton (25). At pH 10.4 we observed a value of 4.5 s for T_1 in the IHP system. The correspondence between the calculated and observed values shows that dipolar relaxation is the predominant relaxation mechanism in this molecule.

This mechanism, however, cannot account for the linewidths up to 10 Hz as observed between pH 8 and pH 12 (Fig. 11, left-hand panel). This broadening is due to exchange phenomena. The phosphorous nuclei experience fluctuations in shielding as a result of proton exchange between water and the phosphate groups. This can be considered to be equivalent to exchange of the phosphorous nucleus between the sites $-OPO_3^{2-}H^+$ and $-OPO_3^{2-}$. Denoting these sites by P and D respectively, we obtain the broadening $\Delta\nu$ in the limit of fast exchange for each resonance from (19)

$$\Delta\nu = \frac{f_D f_P (\omega_P - \omega_D)^2}{(\tau_D^{-1} + \tau_P^{-1})\pi}$$

where f, ω and τ^{-1} are the fraction, the resonance frequency and the reciprocal lifetime of the site denoted by the subscript. The broadening pattern shown in Fig. 11, right-hand panel, was calculated from this relation. The fractions and resonance frequencies of the sites of each ^{31}P nucleus were obtained from the chemical shift data (Fig. 5). The lifetimes of the sites are

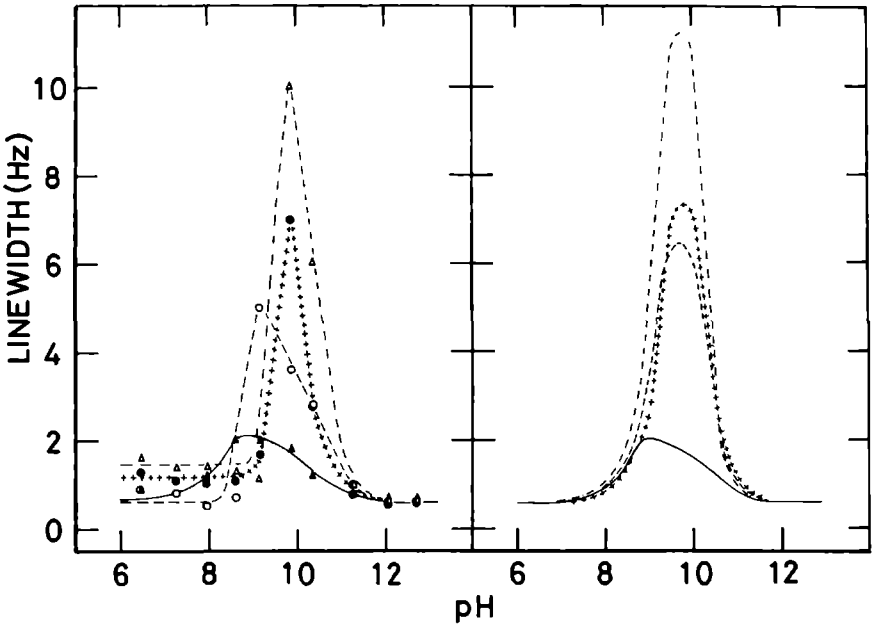

Fig. 11. pH dependence of the linewidths of the ^{31}P resonances of IHP. Left-hand panel, experimental values, conditions as in Fig. 4. The experimental points (△, ●, ▲, ○) correspond to the resonances A, B, C, D shown in Fig. 5 in this sequence. Right-hand panel, calculated broadening. Line symbols of both panels refer to the same resonances. For further details see text

determined by the kinetics of protolysis of the phosphate groups according to the following reaction scheme:

$$-OPO_3^{2-} + H_3O^+ \underset{k_1}{\overset{k_H}{\rightleftarrows}} -OPO_3^{2-} - H_3O^+ \underset{k_3}{\overset{k_2}{\rightleftarrows}} -OPO_3^{2-}H^+ + H_2O \qquad (1)$$

$$-OPO_3^{2-} + H_2O \underset{k_5}{\overset{k_6}{\rightleftarrows}} -OPO_3^{2-}H^+ - OH^- \underset{k_{OH}}{\overset{k_4}{\rightleftarrows}} -OPO_3^{2-}H^+ + OH^- \qquad (2)$$

At low pH, proton dissociation and uptake is governed by mechanism (1), at high pH by mechanism (2). In the neutral pH range both are relevant. For IHP, the conditions $k_2 >> k_1$ and $k_5 >> k_4$ are fullfilled (26) yielding a proton-diffusion-controlled proton-on

rate in (1) and a hydroxyl-ion-diffusion-controlled proton-off rate in (2). According to this scheme τ_D^{-1} and τ_P^{-1} were obtained from the relations

$$\tau_D^{-1} = k_H(H^+) + k_{OH}10^{-(14-pK_D)}$$

$$\tau_P^{-1} = k_H 10^{-pK_D} + k_{OH}(OH^-)$$

where (H^+) and (OH^-) represent the proton and hydroxyl-ion concentration respectively, K_D the dissociation constant of the equilibrium $-OPO_3^{2-}H^+ \rightleftarrows -OPO_3^{2-} + H^+$.
The parameters needed to calculate τ_D^{-1} and τ_P^{-1} were obtained in the following way: the pH-dependent value for pK_D, which differs for the phosphate groups, was calculated from the fractions of the species involved (Fig.5); the proton and hydroxyl-ion concentration were obtained from the pH meter reading without correction. A value of 10^{13} $M^{-1}s^{-1}$ for k_H and $2x10^7$ $M^{-1}s^{-1}$ for k_{OH} was used. τ_P^{-1} and τ_D^{-1} were calculated for all phosphate groups at several pH values and substituted in the equation for $\Delta\nu$ given above. Inspection of Fig.11 reveals that the calculated and observed broadening correspond very well. Calculations carried out with different values for k_H and k_{OH} showed that the shape of the curves and the position of the maxima are strongly dependent on those values. The magnitude of the second-order proton-diffusion and hydroxyl-ion-diffusion rate constants can be compared with the usually (26) observed values after introducing a correction for the electrostatic attraction and repulsion between IHP and protons and between IHP and hydroxyl ions respectively (27).
The charge-independent rate constants (k^o) are related to the observed rate constants (k_{obs}) by (28)

$$k_{obs} = k^o \frac{V/\beta}{e^{V/\beta} - 1}$$

with

$$V = \frac{Z_A Z_B e^2}{D\, r_{AB}}$$

where Z_A and Z_B are the charges of the reacting species, e the elementary charge and D the dielectric constant of the medium, r_{AB} is the sum of the effective radii of A and B, V the electrostatic interaction energy of A and B and the Boltzmann energy. Using a value of 0.7 nm for r_{AB}, -9 for the charge of the IHP molecule and 80 for the dielectric constant, we calculate for the charge-independent rate constants the values of 10^{12} $M^{-1}s^{-1}$ for k_H^o and of 2 x 10^{10} $M^{-1}s^{-1}$ for k_{OH}^o, which compare favourably with the values cited in the literature (26).

At pH values lower than 4 an equal broadening for all resonances is observed (cf. Fig. 4). We cannot present a mechanism for this effect as yet but merely note than this phenomenon is also observed in the ^{31}P NMR spectra of oligonucleotides at low pH (H.A.M. Geerdes, personal communication).

REFERENCES

1. Jennings, A.C. & Morton, R.K. (1963) Aust. J. Biol. Sci. 16, 332-341
2. Benesch, R., Benesch, R.E. & Yu, C. (1968) Proc. Natl. Acad. Sci. U.S.A. 59, 526-532
3. Benesch, R.E., Edalji, R. & Benesch, R. (1977) Biochemistry 16, 2594-2597
4. Benesch, R. & Benesch, R.E. (1967) Biochem. Biophys. Res. Commun. 26, 162-167
5. Johnson, L.F. & Tate, M.E. (1969) Can. J. Chem. 47, 63-73
6. Arnone, A. & Perutz, M.F. (1974) Nature (Lond.) 249, 34-36
7. Edalji, R., Benesch, R.E. & Benesch, R. (1976) J. Biol. Chem. 251, 7720-7721
8. Brygier, J., de Bruin, S.H., van Hoof, P.M.K.B. & Rollema, H.S. (1975) Eur. J. Biochem. 60, 379-383
9. Perutz, M.F. (1970) Nature (Lond.) 228, 734-739
10. Blank, G.E., Pletcher, J. & Sax, M. (1971) Biochem. Biophys. Res. Commun. 44, 319-325
11. Janssen, L.H.M., de Bruin, S.H. & van Os, G.A.J. (1970) Biochim. Biophys. Acta 221, 214-227
12. de Bruin, S.H., Janssen, L.H.M. & van Os, G.A.J. (1973) Biochem. Biophys. Res. Commun. 55, 193-199

13. Fiske, C.H. & Subbarow, Y. (1925) J. Biol. Chem. 66, 375-386
14. Cornish-Bowden, A. & Koshland, D.E.,Jr (1975) J. Mol. Biol. 95, 201-212
15. Wyman, J. (1964) Adv. Protein. Chem. 19, 223-286
16. Costello, A.J.R., Glonek, T. & van Wazer, J.R. (1976) Inorg. Chem. 15, 972-974
17. Glonek, T. & van Wazer, J.R. (1976) J. Phys. Chem. 80, 639-643
18. Morgan, W.E. & van Wazer, J.R. (1975) J. Am. Chem. Soc. 97, 6347-6352
19. Carrington, A. & McLachlan, A.D. (1969) Introduction to Magnetic Resonance, 1st edn, p. 208, Harper & Row, New York
20. Moon, R.B. & Richards, J.H. (1973) J. Biol. Chem. 248, 7276-7278
21. Debye, P. & Hückel, E. (1923) Phys. Z. 24, 185-206
22. Koshland, D.E., Némethy, G. & Filmer, D. (1966) Biochemistry 5, 365-385
23. Tanford, C. (1965) Physical Chemistry of Macromolecules, 1st edn, pp. 526-532, John Wiley, New York, London, Sydney
24. Linderstrøm - Lang, K. (1924) Compt. Rend. Lab. Carlsberg, Sér. Chim. 15, no. 7
25. Solomon, I. (1955) Phys. Rev. 99, 559-565
26. Eigen, M. (1963) Angew. Chem. 75, 489-508
27. Wilting, J., Nauta, H. & Braams, R. (1971) FEBS Lett. 16, 147-151
28. Debye, P. (1942) Trans. Electrchem. Soc. 82, 265-272

CHAPTER III

EQUILIBRIUM PROPERTIES OF THE BINDING OF *myo*-INOSITOL HEXAKISPHOSPHATE TO HUMAN HEMOGLOBIN

The proton-binding behaviour of *myo*-inositol hexakisphosphate (IHP) free in solution was studied in detail in the preceding chapter. It was shown that IHP bears a twelve-fold negative charge above pH 11 while all phosphate groups display an anomalous proton-binding behaviour below that pH. As was demonstrated this anomaly is mainly the result of a strong electrostatic interaction between opposing phosphate groups within the IHP molecule.

In the present chapter these studies are extended to the investigation of the proton binding by IHP in the presence of deoxy- or carboxyhemoglobin.

Arnone and Perutz (1) showed that in deoxyhemoglobin IHP binds to a cluster of eight positively charged residues located at the β-chain side of the central cavity. Their analysis was confirmed by studies on IHP binding to mutant hemoglobins. It was shown that the strength of binding depends on replacements of these residues (2-4). At moderate ionic strength IHP forms a tight 1:1 complex with deoxyhemoglobin. The association constant was found to be $1.6 \times 10^7\ M^{-1}$ at pH 7.3 in 0.1 M KCl (5).

Recent experiments showed that the binding site for polyphosphate molecules in ligated hemoglobin is also located at the entrance of the central cavity (6-8). The stoichiometry of the binding was found to be unity (6). From oxygenation experiments (9) the affinity of IHP towardsligated hemoglobin is known to be very low at neutral pH.

Due to the difference in affinity of IHP for deoxyhemoglobin (Hb) and oxyhemoglobin (HbO_2) the molecule lowers the oxygen affinity of human hemoglobin. The molecule is therefore in its function related to the in-vivo effector 2,3-diphosphoglycerate (10-12).

In this chapter pH-stat experiments are described from which the association constants characterizing the binding of IHP to Hb and carboxyhemoglobin (HbCO) were obtained as a function of pH. The results show that the large difference in affinity of IHP for Hb and HbCO mentioned above exists at neutral pH only. It is suggested that this is caused by a conformational change induced in HbCO upon binding of IHP. Furthermore the pH-stat experiments provide the number of protons taken up upon the binding of IHP to Hb and HbCO. In order to evaluate which groups contribute to the proton uptake, the data were compared with the proton binding of IHP bound to the protein as studied by ^{31}P NMR techniques.
The latter results were explained semi-quantitatively using a modified version of the model describing the proton-binding behaviour of IHP free in solution (see Chapter II).

MATERIALS AND METHODS

pH-Stat Experiments

Human blood was obtained from local hospitals. Hemoglobin was isolated according to the toluene method of Drabkin (13). The lysate, saturated with CO, was dialyzed and then deionized by passage over a mixture of Amberlite IR-120 and IRA-400 (BDH Chemicals Ltd.). Hemoglobin concentrations were determined spectrophotometrically as carboxyhemoglobin using a heme absorption coefficient of 14,000 $M^{-1}cm^{-1}$ at 537.5 nm.
pH-stat experiments were carried out as described elsewhere (14). The procedure can briefly be summarized as follows: to study the binding of IHP to deoxyhemoglobin, a HbCO solution containing 0.1 M KCl was first converted to HbO_2 in a rotating tonometer by a stream of oxygen under constant illumination at 0°C. The solution was then deoxygenated by a stream of pure N_2 at 20°C. This solution (typical hemoglobin concentration, 0.2 mM in tetramer) was anaerobically transferred into a thermostated titration vessel and was adjusted to a desired pH value. A solution containing IHP (BDH Chemicals Ltd.), prepared as described in Chapter IV, was carefully deaerated and adjusted to the same pH value. This solution was added in small increments to the hemoglobin solution.

After each IHP addition the original pH of the hemoglobin solution was restored by automatic titration with an appropriate amount of acid or base. The proton uptake or release is considered to be proportional to the degree of IHP saturation. Apparent proton uptake, caused by the dilution of IHP in this procedure, was corrected for by carrying out blanks in which IHP was added to a protein free solution. In this way IHP binding isotherms were obtained from which the affinity of IHP for the protein was calculated.
To determine the binding of IHP to HbCO similar experiments were carried out.

NMR Experiments

All NMR experiments were carried out with hemoglobin A_1 prepared as described in Chapter IV. Throughout this chapter we refer to hemoglobin A_1 as hemoglobin.
A solution of HbCO (0.1 M in KCl and approximately 0.5 mM in tetramer) was adjusted to a particular pH value. The solution obtained was concentrated by ultrafiltration up to a concentration of approximately 4 mM in tetramer. Subsequently, a solution of ^2H_2O (99.75% ^2H_2O (Merck), 0.1 M in KCl, 1 mM in EDTA), was added up to a concentration of 75% v/v ^2H_2O followed by ultrafiltration. After measuring the protein concentration IHP was added to a molar ratio of 2.0 (Hb/IHP) at alkaline pH (pH > 8) and to a ratio of 1.33 at neutral and acid pH. The solution was deoxygenated as described above and transferred into an oxygen free titration vessel. After determining the pH (uncorrected meter reading) an aliquot of this Hb.IHP solution was injected into a 5 mm NMR tube (Wilmad) which was flushed with N_2 prior to use and sealed with a serum cap. HbCO.IHP solutions were obtained by equilibrating the deoxygenated solutions with CO. Subsequently the pH was measured.
The protein concentration in all samples was typically 3.5 mM in tetramer. The samples were free of methemoglobin at all pH values except for pH 5.2. At this pH the samples contained up to 30% of oxydized material.
The proton-decoupled ^{31}P NMR spectra were recorded at 40.5 MHz. Chemical shifts (δ) are reported as parts per million (ppm)

relative to the resonance of 20% H_3PO_4 in ^2H_2O. Downfield shifts are defined positive.
For an exact description of the procedure followed for the recording of the NMR spectra the reader is referred to Chapter IV.

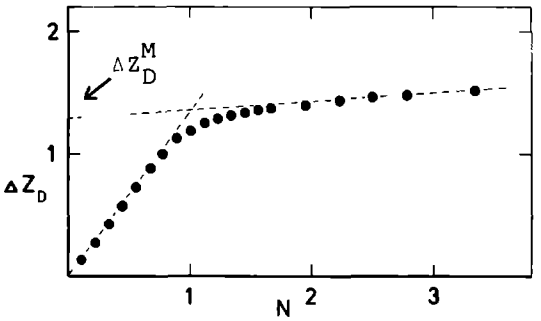

Fig. 1. Number of protons absorbed (ΔZ_D) upon binding of IHP to deoxyhemoglobin at pH 8.0. N is the molar ratio of IHP over Hb. ΔZ_D^M represents the maximum number of protons absorbed per tetramer. The data were not corrected for dilution effects. Hb concentration, 0.2 mM in tetramer, 0.1 M KCl, 25°C.

RESULTS

^{31}P NMR and pH-stat methods were employed to probe the binding of IHP to deoxy- and carboxyhemoglobin. The results obtained from the pH-stat experiments characterize the proton-binding behaviour of the Hb.IHP and HbCO.IHP complexes, thereby yielding information on the affinity and stoichiometry of the binding of IHP to the protein. Complementary to this the results obtained from ^{31}P NMR experiments characterize the proton binding by IHP when bound to hemoglobin.

pH-Stat Experiments

Fig. 1 shows the results of a pH-stat titration experiment of deoxyhemoglobin with IHP at pH 8.0. The curve, representing the number of protons taken up per hemoglobin molecule as a function of the molar ratio of IHP over Hb (N), shows an equivalence point at N = 1. Below this value (N < 1) the proton uptake is propor-

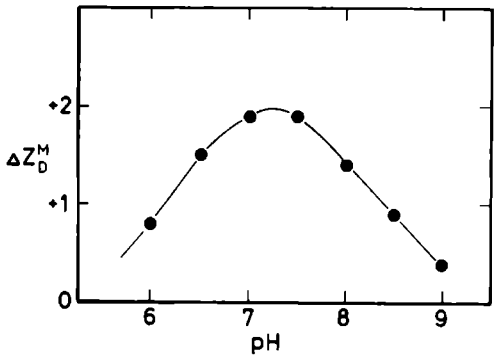

Fig. 2. Maximum number of protons absorbed (ΔZ_D^M) upon binding of IHP to deoxyhemoglobin as a function of pH. Experimental conditions as in Fig. 1.

tional to the fraction of hemoglobin molecules to which IHP is bound. The apparent proton uptake observed for N larger than unity is due to the dilution of IHP (see Materials and Methods). From the proton absorption curve the binding constant for IHP deoxyhemoglobin complex formation was calculated to be 8×10^5 M^{-1} at pH 8. At lower pH this constant is too large to be determined from titration experiments.

Fig. 2 shows the pH dependence of the maximum proton uptake by the Hb.IHP complex, ΔZ_D^M. It is seen that proton absorption occurs in the entire pH range studied. This indicates that IHP binds to groups titrating in the neutral pH range.

As derived by Wyman (15), the pH dependence of the apparent binding constant (K_D) is given by

$$\frac{d \log K_D}{d\ pH} = -\Delta Z_D^M \qquad (1)$$

Upon integration this relation becomes

$$\log K_D\ (pH_1) - \log K_D\ (pH_2) = \int_{pH_1}^{pH_2} \Delta Z_D^M\ dpH \qquad (2)$$

pH	K_D (M^{-1})	K_{CO} (M^{-1})
5.5	> 1.6×10^9	2×10^7
6.0	1.6×10^9	5×10^6
6.5	4.0×10^8	4×10^5
7.0	5.0×10^7	2×10^4
7.3	1.6×10^7	4×10^3
8.0	8.0×10^5	6×10^3
9.0	1.0×10^5	> 2×10^4

Table I. Values of the association constants for IHP binding to deoxyhemoglobin (K_D) and to carboxyhemoglobin (K_{CO}) obtained by graphical integration of the data shown in Figs. 2 and 4 respectively. K_D was determined by pH-stat titration at pH 8.0 and pH 8.5, K_{CO} at pH 6.5.

We used eqn. (2) to calculate K_D at low and high pH by graphical integration of the curve shown in Fig. 2. The results of the calculations are listed in Table I. At pH 7.3 K_D amounts to 1.6×10^7 M^{-1} which is in excellent agreement with the value obtained from pH-stat experiments carried out with Hb solutions of extremely low concentrations (5). At pH 9 K_D was found to be equal to 10^5 M^{-1} showing that binding takes place to at least two groups with high pK values. This is consistent with X-ray diffraction data from which it was derived that two lysyl residues are part of the IHP binding site in deoxyhemoglobin (1). At low pH K_D exceeds 10^9 M^{-1}.

Fig. 3 shows a plot of the IHP-induced Haldane effect as a function of pH. The curve represents the difference in number of protons

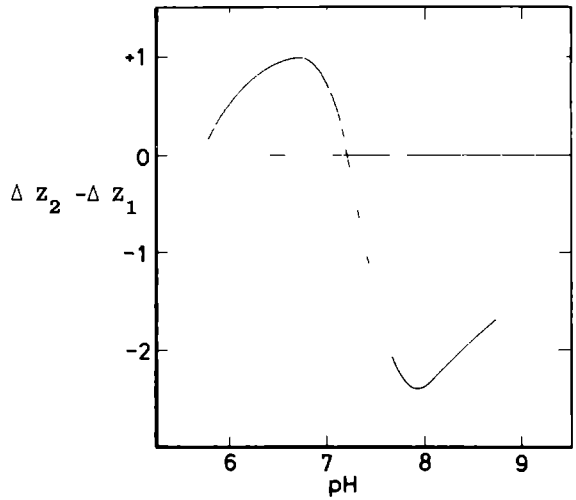

Fig. 3. IHP-induced Haldane effect, i.e. the Haldane effect with IHP (ΔZ_2) minus the Haldane effect without IHP (ΔZ_1). The curve was calculated from data obtained by Rollema et al. (16). Hemoglobin concentration, 0.17 mM in tetramer; IHP concentration, 1.0 mM, 0.1 M KCl; 25°C.

released upon the ligation of deoxyhemoglobin with CO in the presence and absence of IHP. The experiments in the presence of IHP were carried out with a five-fold excess of IHP. Under the conditions of the experiments, this excess is sufficient to fully saturate deoxyhemoglobin in the entire pH region of interest (see Table I). Below pH 7 also HbCO is fully saturated; above this pH it is estimated to be saturated up to 80% (see below).
The proton uptake associated with the conversion of Hb into HbCO, Hb.IHP and HbCO.IHP is summarized in the following scheme:

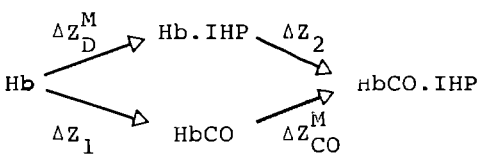

ΔZ_1 and ΔZ_2 represent the number of protons upon binding of CO to Hb in the absence and presence of IHP respectively, while ΔZ_{CO}^M and ΔZ_D^M represent the number of protons absorbed upon saturating HbCO and Hb with IHP respectively.

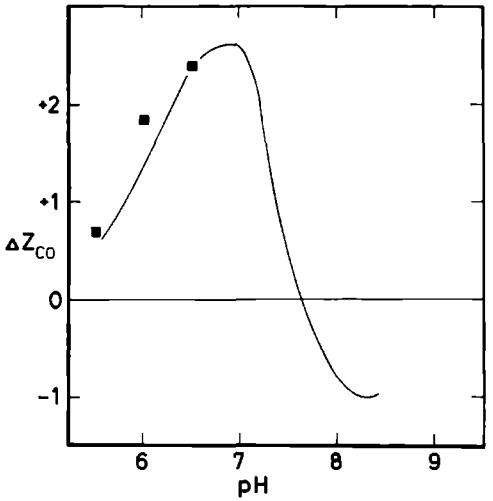

Fig. 4. Number of protons absorbed (ΔZ_{CO}) upon binding of IHP to HbCO. The curve obtained is equal to the sum of the curves shown in Figs. 2 and 3. The squares, representing the maximum number of protons absorbed per tetramer, were obtained from pH-stat titration experiments; hemoglobin concentration, 0.05 - 0.2 mM in tetramer; 0.1 M KCl; 25°C.

From the scheme it follows that the IHP-induced Haldane effect ($\Delta Z_2 - \Delta Z_1$) is equal to $\Delta Z^M_{CO} - \Delta Z^M_D$. Therefore, addition of the curves shown in Figs. 2 and 3 yields a curve representing the pH dependence of ΔZ^M_{CO} (see Fig. 4).

The squares in this figure represent data obtained by pH-stat experiments (cf. Fig. 1). They agree quite well with the calculated curve. It is noted that above pH 7 the curve in Fig. 4 gives only minimum values for ΔZ^M_{CO} because above this pH under the conditions of the experiments shown in Fig. 3 the binding of IHP to HbCO is not complete. Using an average value of K_{CO} = 5×10^3 M^{-1} a degree of saturation of about 80% can be calculated (see below).

Association constants for the binding of IHP to HbCO can now be calculated according to the procedure outlined above for the binding of IHP to Hb.

At pH 6.5 pH-stat experiments yield a value of 4×10^5 M^{-1} for K_{CO}. The association constants at different pH values were then calculated from the data shown in Fig. 4 using eqn. (2). The results are listed in Table I.

At pH 5.5, where all basic groups present in the central cavity are expected to be fully protonated, K_{CO} is significantly smaller than K_D. This result suggests either that in HbCO IHP binds to a smaller number of ionizable groups than in Hb or that it binds to the same number of groups but with a lower affinity. At pH 7.3 we calculated for K_{CO} a value of 4×10^3 M^{-1}. As mentioned above this leads to about 80% saturation of HbCO with IHP, which in turn leads to a small overestimation of K_{CO}.

A shape of the curve in Fig. 4 deserves some further comment. ΔZ_{CO} drops from a value of 2.5 to zero within one pH unit. This is in contrast to the well known bell-shaped curves resulting from a simple pK shift of the groups on the protein involved in binding. Such a pK shift results from the electrostatic field of the anion bound to a positively charged base (17).

The curve shown becomes strongly negative above pH 7.5. Proton release upon IHP binding by HbCO was also observed in pH-stat titration experiments at pH 8.0. However, due to the low affinity of IHP for HbCO, ΔZ^M_{CO} could not be evaluated quantitatively. Application of eqn. (2) to the data in Fig. 4 shows that K_{CO} has a minimum value at that pH where ΔZ^M_{CO} intersects the abscissa. In other words, K_{CO} increases upon an increase in pH above the pH of intersection. K_{CO} is estimated to have a value of 10^4 to 10^5 M^{-1} at high pH. This is about as large as K_D at this pH from which is inferred that IHP binds similarly to Hb and HbCO at high pH.

^{31}P NMR Experiments

Fig. 5 shows some examples of proton-decoupled ^{31}P NMR spectra of IHP in the presence of excess deoxyhemoglobin relevant to our discussion. The spectra represent the bound state since in the pH range studied K_D is larger than 10^5 M^{-1}. It is seen that the shape and position of the resonances strongly depends on pH and that the linewidths of the resonances are significantly larger than the widths observed for IHP free in solution (see Chapter II). Taking a value of 4 Hz to be representative for the linewidths of IHP bound, we calculate a rotational correlation time τ of 4×10^{-8}s for this molecule assuming that the dipolar interaction of the phosphorous nuclei with the decoupled vicinal protons of IHP is

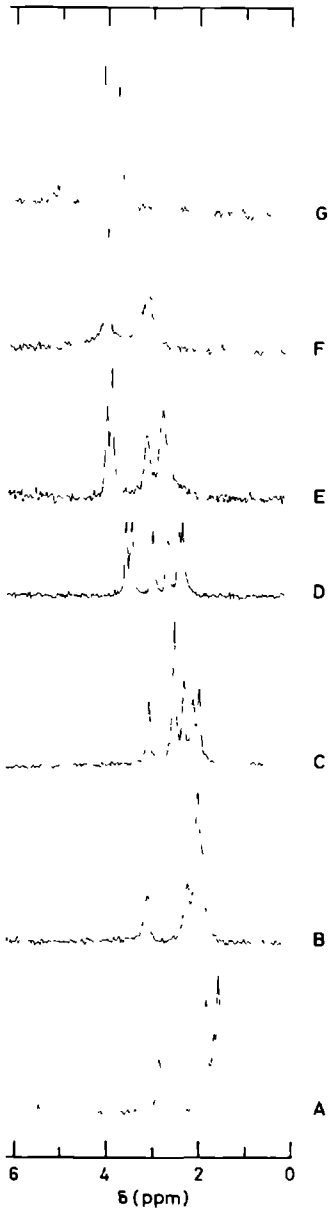

Fig. 5. Proton-decoupled ^{31}P NMR spectra of IHP bound to deoxyhemoglobin. Spectrum A, pH 5.2; B, pH 6.3; C, pH 7.3; D, pH 8.4; E, pH 9.0; F, pH 9.2; G, pH 9.5. The molar ratio of Hb over IHP was 1.33 below and 2.0 above pH 8. Hb concentration, 3-4 mM in tetramer; 0.1 M KCl; 1 mM EDTA; 75% v/v ^2H_2O; 25 ± 2 °C.

the only relaxation mechanism. This value for τ is equal to the rotational correlation time of Hb at 298 K calculated from the Stokes-Einstein relation.
This provides additional evidence that the spectra reflect the bound state of IHP.
Spectrum A, recorded at pH 5.2, shows four resonances from which two have single intensity and two have double intensity. This type of spectrum is also observed for IHP free in solution and shows that at this pH the mirror symmetry present in the IHP molecule (see Chapter II) is not affected upon binding.
Spectrum B, recorded at pH 6.3, shows an 1 : 1 : 4 intensity distribution. The high field resonance is the result of coalescence of two resonances of double intensity. Also at this pH the spectrum shows that the symmetry of IHP is unaffected upon binding to the protein.
In contrast, spectrum C which was recorded at pH 7.3, shows five resolved resonances reflecting a breakdown of the mirror symmetry of IHP. At pH 8.4 (spectrum D), this breakdown of symmetry is even more manifest; a spectrum with six distinct resonances is recorded.
Spectra E and F, recorded at pH 9.0 and pH 9.2 respectively, show significant line broadening while the resonances in spectrum G, recorded at pH 9.5 are narrow again. Note that the intensity distributions in spectra F and G show that the IHP symmetry is unaffected by binding at this pH, just as is observed at low pH.
Fig. 6 shows some examples of proton-decoupled ^{31}P NMR spectra of IHP in the presence of excess HbCO relevant to our discussion. Below pH 7 the spectra reflect the bound state of IHP to HbCO. In the pH range 7.0 to 8.5 the association constant K_{CO} has a value of about 5×10^3 M^{-1} (Table I). As a result approximately 30% of the IHP will be free in solution. The spectra in this pH range are therefore expected to reflect the weighted average of the spectra corresponding to the bound and to the free state (see Chapter IV). Above pH 9 K_{CO} increases to a value larger than 10^4 M^{-1}. Therefore the spectra recorded at high pH reflect the bound state.
In most spectra obtained for the HbCO.IHP system the high field

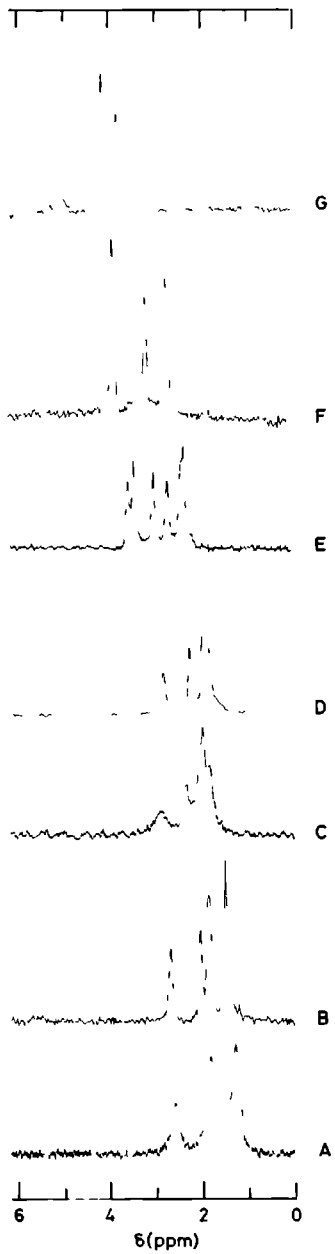

Fig. 6. Proton-decoupled ^{31}P NMR spectra of IHP in the presence of excess carboxyhemoglobin. Spectrum A, pH 5.2; B, pH 6.2; C, pH 6.3; D, pH 7.0; E, pH 8.6; F, pH 9.0; G, pH 9.5. Experimental conditions as in Fig. 5.

resonance of double intensity does not show a resolved splitting. This is in contrast with the spectra obtained for the Hb.IHP system (Fig. 5). Nevertheless the breakdown of IHP symmetry when bound to HbCO is observed in the five line spectra recorded in the pH range 7.5 to 8.6 from which an example is given in spectrum E (pH 8.6).

Spectrum A, recorded at pH 5.2, shows the same intensity distribution as that observed for the Hb.IHP system at the same pH (Fig. 5A). The chemical shift differences between both spectra are less than 0.2 ppm indicating a similar binding mode for IHP to both Hb and HbCO at low pH.

Spectrum B and D, recorded at pH 6.2 and 7.0 respectively, show small linewidths for all resonances. Significant line broadening is observed in spectrum C, recorded at pH 6.3 and in the spectrum obtained at pH 6.7 (not shown). This line broadening, which is confined to a small pH interval, is not observed in the spectra of IHP bound to Hb (Fig. 5B). On the other hand, spectrum F which was recorded at pH 9.0, does not show line broadening as observed in the Hb.IHP system at the same pH (Fig. 5F).

Spectrum G,recorded at pH 9.5, closely resembles that obtained for the Hb.IHP system (Fig. 5G), indicating a similar mode of binding at high pH.

Fig. 7 presents the ^{31}P NMR chemical shift of the resonances of IHP bound to Hb as a function of pH. Each resonance is labeled by one symbol; the splitting of a resonance of double intensity into two resonances of single intensity is indicated by the same two smaller symbols. The resonances of IHP bound were identified with those of IHP free by monitoring the resonance positions as a function of the IHP/Hb molar ratio (see Chapter IV).

It is seen that just as IHP free in solution (Chapter II) IHP bound shows an extended titration behaviour characterized by pseudo-equivalence points. Furthermore it is noted that the resonance positions of IHP bound are shifted by approximately 0.5 ppm down field with respect to those of IHP free. The origin of this shift will be discussed below. Fig. 7 very clearly shows the pH dependence of the apparent symmetry of IHP bound; the high field resonance of double intensity is splitted in the pH region 6.8 to 8.6 while the low field resonance of double intensity is

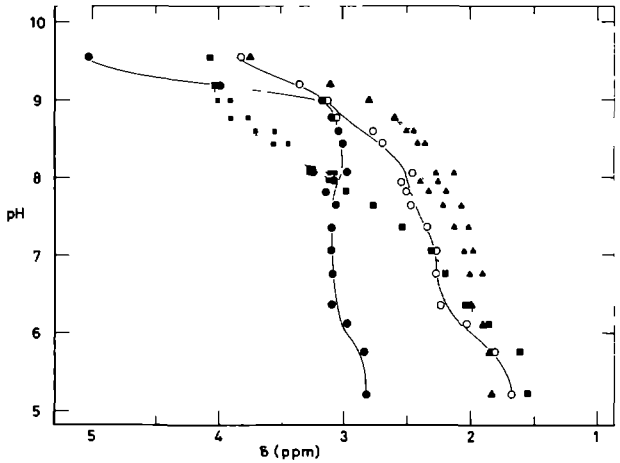

Fig. 7. ^{31}P *NMR chemical shift of the resonances of IHP bound to deoxyhemoglobin as a function of pH. The symbols correspond to those used in the* δ *vs* $1/l$ *plots presented in Chapter IV. (○), (●), resonances of single intensity; (▲), (■), resonances of double intensity. Experimental conditions as in Fig. 5.*

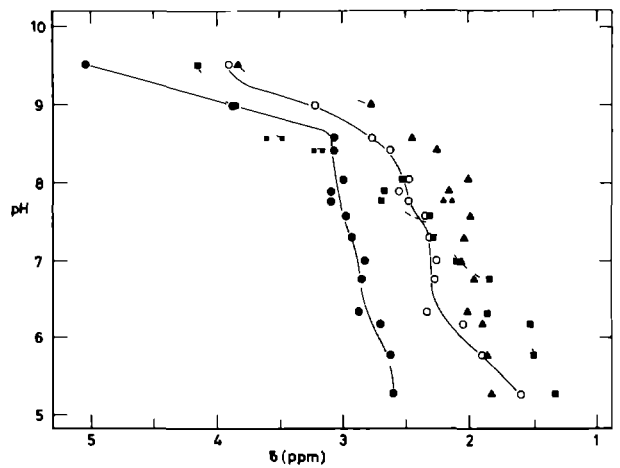

Fig. 8. ^{31}P *NMR chemical shift of the resonances of IHP in the presence of excess carboxyhemoglobin. The symbols have the same meaning as in Fig. 7. Experimental conditions as in Fig. 5.*

splitted in the pH range 8 to 9.
Fig. 8 shows the ^{31}P NMR chemical shifts of the resonances of IHP in the presence of excess HbCO as a function of pH. The symbols in this figure were chosen as in Fig. 7 and the identification of the resonances was carried out as described above. As a cross-check for this identification the resonances observed for the Hb.IHP and HbCO.IHP systems were correlated in a series of experiments in which Hb.IHP was stepwise saturated with CO at pH 6.8. The considerable scattering observed in Fig. 8 is explained by the fact that the protein concentration could not be kept exactly constant in the different samples leading to different fractions of IHP bound in that pH region where the value for the dissociation constant is about equal to the protein concentration.
Comparison of Figs. 7 and 8 reveals that the δ versus pH curves are very much alike in both systems. This result is surprising in view of the difference in affinity of IHP for Hb and HbCO which is usually attributed to a difference in central cavity geometry in these hemoglobin derivatives. Comparison of these figures furthermore shows that the splitting of the low field resonance with double intensity occurs in the same pH interval in both systems. Resolved splitting of the high field resonance is absent in the HbCO.IHP system except in one spectrum recorded at pH 7.75.

Analysis of the Chemical Shift Data

The chemical shift versus pH profile obtained from the spectra of IHP free in solution was analysed in terms of fast exchange of the ^{31}P nuclei between two sites corresponding with the singly protonated and unprotonated phosphates (see Chapter II).
The observed resonance frequency of phosphate i, δ_i, is given by

$$\delta_i = Y_i \, \delta_{Pi} + (1 - Y_i) \, \delta_{Di}$$

where δ_{Pi} is the resonance position when phosphate i is singly protonated and δ_{Di} the resonance position when this group is unprotonated. Y_i is the fraction of protonated phosphate groups i

at the pH value considered.
Using this equation Y_1 was determined for all phosphate groups at different pH values. The pH dependence of ΣY_1 was shown to coincide with the potentiometric titration curve of IHP. From this it was inferred that the chemical shifts of the resonances of IHP free in solution provide a reliable monitor for the degree of protonation of the phosphate groups.
This observation forms the basis of the analysis of the chemical shift data obtained for IHP bound to deoxy- and carboxyhemoglobin. It is assumed that the positions of the IHP phosphate resonances are determined by the protonation state of the phosphate groups only and that the resonance positions δ_{P1} and δ_{D1} are not affected by the amino acid side chains in the central cavity of the protein. Of course these side chains may influence the state of protonation of the phosphate groups in IHP and in this way indirectly determine their resonance positions. The validity of the assumption that δ_{P1} and δ_{D1} are unaffected by the protein is supported by the observation that the ^{31}P NMR resonance positions of ATP do not shift upon the binding of this molecule to Hb (18).
On this basis the protonated fraction Y of each phosphate group of IHP bound was calculated at several pH values; the results are presented in Fig. 9. The figure shows profiles for IHP bound to Hb (dashed lines), for IHP in the presence of excess HbCO (dotted lines) and for IHP free in solution (solid lines). The symbols refer to the data shown in Figs. 7 and 8.
At most pH values all phosphate groups of IHP bound to the protein are deprotonated to a greater extent than those of IHP free in solution (Fig. 9). This enhanced deprotonation is expected since binding of negatively charged phosphate groups to positively charged basic groups on the protein will induce a decrease in pK of the former groups giving rise to the observed phenomenon. It is noteworthy that at high pH only the two lysyl residues in the central cavity are expected to interact with IHP (19). If these groups were to bind specifically with two phosphate groups of IHP, only two groups would have shown enhanced deprotonation at high pH. As this is not observed aspecific binding of IHP to the central cavity is inferred from our data (see Discussion).

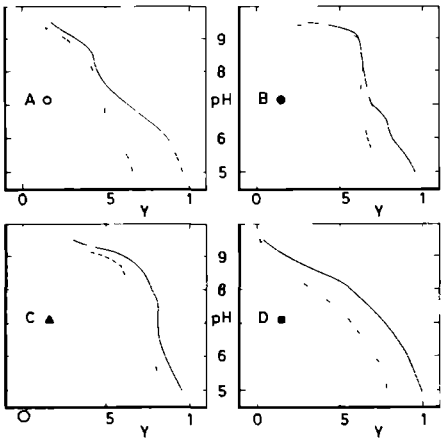

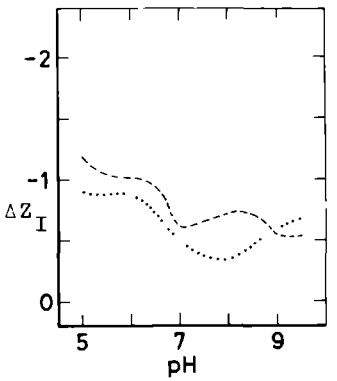

Fig. 9. (left) Degree of proton saturation (Y) for the 4 different phosphate groups of IHP as a function of pH. Y is equal to 1 when 1 proton is bound. Solid curves were calculated from NMR data obtained for IHP free in solution (Chapter II), dashed curves from the data on Hb.IHP (Fig.5), dotted curves from the data on HbCO.IHP (Fig.6). The symbols within brackets refer to the resonances in Figs. 7 and 8.

Fig.10. (right) Number of protons absorbed per IHP molecule (ΔZ_I) upon binding to Hb (dashed curve) and to HbCO (dotted curve), calculated from the curves shown in Fig. 9.

Further inspection of Fig. 9 reveals that the proton binding behaviour of IHP bound to Hb and HbCO is rather similar. This is most outspoken for the results shown in panel A where the curves coincide and in panel C where they differ between pH 7 and 8.5 only. This difference is supposedly due to the fact that in this pH range HbCO is not fully saturated with IHP (see above).
The difference between the curves for IHP bound and IHP free yields the number of protons released for each phosphate group upon binding as a function of pH. The total number of protons released by the IHP molecule upon binding as calculated from Fig.9 ($-\Delta Z_I$) is shown in Fig. 10. It is seen that upon binding to deoxy- and carboxyhemoglobin the proton release $-\Delta Z_I$ does not strongly depend on pH. The dip observed in the curve for the HbCO.IHP system around pH 8 is at least partly due to the incomplete binding mentioned above.

Proton Binding Behaviour of IHP Bound to Hemoglobin

Proton binding by IHP free in solution is characterized by a high anti-cooperativity, giving rise to an extended titration range and the appearance of pseudo-equivalence points in potentiometric titration experiments and in the pH dependence of the ^{31}P NMR chemical shift. These observations were explained by assuming that large electrostatic interaction exists between opposing phosphate groups due to the presence of a medium of low polarizability in the centre of the IHP molecule. Therefore the titration of a particular pnosphate group is most affected by the degree of protonation of its opposing group (see Chapter II).

So in a simplified model the titration behaviour of the entire IHP molecule can be represented by the proton binding characteristics of three pairs of opposing groups P and Q (see Fig. 11, left-hand panel). Each group is located at the end of a bar which represents a medium of low polarizability. K_P and K_Q are the dissociation constants for the deprotonation of the groups P and Q ($-PO_4^{2-}H^+ \rightarrow -PO_4^{2-}$) and K_I is the constant describing the electrostatic interaction between those groups. In this model, this interaction is effective only wnen both groups are fully deprotonated.

The relative concentrations of the four different species occurring are easily expressed in terms of the parameters K_P, K_Q, K_I and the proton activity (H^+) (see Fig. 11, left-hand panel). As a point of reference we take the concentration of the species in which both phosphate groups bear one proton (i.e. these groups have a single negative charge).

The proton saturation Y of group P is given by

$$Y_P = \frac{1 + K_Q(H^+)^{-1}}{1 + (K_P + K_Q)(H^+)^{-1} + K_P K_Q K_I (H^+)^{-2}} \qquad (1)$$

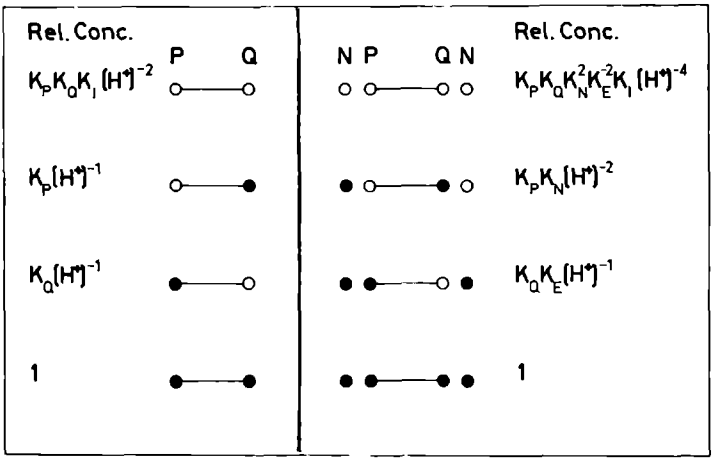

Fig. 11. Left-hand panel, model representation of IHP free in solution. Closed circles represent phosphate groups having a proton bound (i.e. they bear a single negative charge); open circles represent deprotonated phosphate groups with a double negative charge. The concentrations of the species, defined relative to the fully protonated form, are indicated in the figure (left).
Right-hand panel, model representation of IHP bound to ionizable groups N in the central cavity of hemoglobin. In contrast to the groups P and Q, the groups N bear a single positive charge when protonated (closed circles). Only four out of the total of 16 possible structures are given. The concentrations are defined relative to the fully protonated species. K_N, K_Q, K_P, K_I and K_E are defined in the text.

By varying K_P, K_Q and K_I, Y_P was calculated as a function of pH as to obtain a fit to the experimental proton-binding curves for the different phosphate groups of IHP free in solution (Fig. 9). The input parameters used are listed in Table II.
Two examples of these calculated curves are presented in Fig. 12. The capitals and symbols used for labeling the panels were chosen as in Fig. 9. The solid lines in panels B and B' (Fig. 12), which both represent a titration of the group labeled (●) of free IHP, display a clear pseudo-equivalence point at high pH at Y = 0.6. The solid lines in panels D and D' (Fig. 12) however show a titration behaviour without a pseudo-equivalence point. Comparison with the experimentally observed proton-binding behaviour of these groups in free IHP (Fig. 9, panels B and D, solid lines) shows that

Resonance symbol	K_P (M)	K_Q (M)	K_I
▲	1.0×10^{-7}	3.0×10^{-7}	3×10^{-3}
■	1.0×10^{-7}	3.0×10^{-7}	3×10^{-2}
o	1.5×10^{-7}	1.0×10^{-7}	1×10^{-2}
●	3.0×10^{-7}	4.5×10^{-7}	1×10^{-4}

Table II. Parameters used for fitting the proton-binding behaviour of group P (model, see Fig. 11) to the experimental data of the groups labeled by the resonance symbols. Note the difference in the constant for electrostatic interaction (K_I) required to obtain the fits. This constant largely determines the proton release of IHP upon binding to the protein.

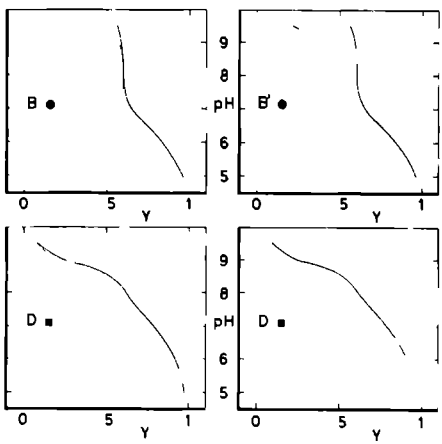

Fig. 12. Model calculation of the degree of proton saturation (Y) for two different phosphate groups. Solid lines indicate free IHP, dashed lines, IHP bound to groups N with a pK value of 5.6 (panels B and D) and to groups N with a pK value of 10 (panels B' and D'). Symbols were chosen as in Fig. 9. For further details, see text.

on the basis of this simple model reasonable fits can be obtained. After determining the parameters relevant to the proton binding of IHP free in solution, the change in proton-binding behaviour of group P resulting from the binding of IHP to positively charged groups of the central cavity was calculated.

To this end the simple scheme for free IHP was extended to 16 different structures occurring when a pair of opposing groups interacts with two ionizable groups N. Four of these structures are depicted in Fig. 11, right-hand panel. In order to obtain expressions for the concentrations of the different structures occurring, five parameters are needed. K_P, K_Q and K_I are defined as above, K_N is the proton dissociation constant for the groups N. K_E accounts for the electrostatic interaction between a single negatively charged phosphate group (i.e. a phosphate group bearing one proton) and a protonated group N. We assume that the free energy of interaction between a doubly charged phosphate group and a protonated group N is twice that between a singly charged phosphate group and a protonated group N. Furthermore, no interaction between an unprotonated group N and the phosphate groups is assumed.

As a point of reference for the calculation of the relative concentrations of the different species (e.g. Fig. 11, right-hand panel) we take the concentration of the fully protonated structure. In this way the partition function was obtained from which the proton saturation of group P, Y_P, was calculated analogously to eqn. (1) using the K_P, K_Q and K_I values listed in Table II. For K_E we used a value of 30 corresponding to the strength of binding of mono-valent ions to fully protonated bases (17). This leads to an association constant for hemoglobin IHP complex formation of $30^6 = 7.3 \times 10^8\ M^{-1}$ at low pH. This agrees quite well with the constant observed (Table I).

To study the influence of the N groups on the proton-binding behaviour of IHP we considered to extreme pK values. A pK of 5.6 was assumed to simulate the situation that all groups involved in binding are histidyl residues (19), while a pK of 10 was taken to represent the situation that all groups are lysyl residues. Since the IHP binding site is formed by six groups titrating in the neutral pH range namely Val 1β, His 2β and His 143β of both

β-chains and by only two lysyl residues, Lys 82β (1), we expect a priory that a pK value of 5.6 is more realistic than a pK value of 10.

The degree of proton binding by group P following from these calculations are shown in Fig. 12 as a function of pH together with the results obtained for IHP free in solution. Comparison of the dashed curves in panel B (binding to histidyl residues) and the dashed curves in panel B' (binding to lysyl residues) with the curves for IHP free (solid lines) shows that at low pH the difference in protonation between IHP free and IHP bound does not depend in the identity of the groups N. This is expected since at low pH both lysyl and histidyl residues are fully protonated. At high pH however, a large difference between the dashed curves in Fig. 12B and B' is observed. Obviously this is due to the fact that histidyl residues are deprotonated to a large extent at this pH while the lysyl residues are still positively charged.

Upon comparing the various curves characterizing the proton binding to the group labeled (■) (panels D and D') the same conclusions can be reached.

We will now compare the calculated curves for binding to histidyl residues (panels B and D of Fig. 12) with the experimental data (panels B and D of Fig. 9). In view of the assumptions made in the calculations, that is i) the parameters K_P, K_Q and K_I are taken equal to those obtained for IHP free, ii) the pK value of the N groups is 5.6 and iii) K_E is equal to 30, the agreement between the experimental and calculated curves for IHP bound is surprisingly well.

On the basis of the model the number of protons released by IHP upon binding to lysyl and histidyl residues has been calculated (see Fig. 13). When compared with the experimental values (Fig. 10) it is seen, that when N is taken to represent histidyl residues, a satisfactory agreement with the experimental data is obtained below pH 7. The calculated proton release is however too small at high pH. On the other hand, binding to only lysyl residues results in a large proton release at high pH. It is therefore suggested that the experimentally observed proton release (Fig. 10) is mainly the result of binding of IHP to histidyl residues while at high pH the effect of the two lysines 82β becomes

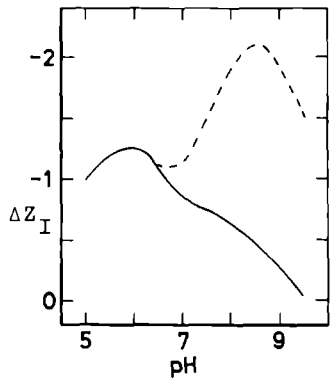

Fig. 13. The overall number of protons absorbed (ΔZ_I) calculated per IHP molecule upon binding to groups with a pK value of 5.6 (solid line) and to groups with a pK value of 10 (point-dashed line, coinciding with the drawn line at low pH). The curves were obtained from model calculations of the proton-binding behaviour of the four different phosphate groups of IHP.

significant.

In conclusion we can say i) that IHP binding to hemoglobin is purely electrostatic in nature, i.e. the complex is best described by ion-pair formation and ii) that the shape of the individual proton-binding curves (Figs. 9 and 12) of IHP bound is largely determined by the electrostatic interaction K_I between the opposing phosphate groups within the IHP molecule. It is noted that the first conclusion is at variance with that reached by Matthies and Zündel (20) who interpreted their IR-spectral data on solid state polyhistidin phosphate complexes to reflect proton transfer to the phosphate moiety.

The model calculations describe equally well the proton release by IHP upon binding to Hb and HbCO. This suggests that in carboxyhemoglobin the groups N located in the central cavity are protonated to roughly the same extent as in deoxyhemoglobin at any pH value.

Proton Absorption by the Hb.IHP and HbCO.IHP Complexes

The overall proton absorption taking place after the binding of IHP to the protein may be the result of three contributions.

i) Proton release by the phosphate groups of IHP as described in detail above. This release varies between 1.0 and 0.5 protons per complex in both HbCO and Hb.
ii) Proton absorption by groups in the central cavity as a result of electrostatic interaction with IHP. It is noted that the change in pK of these groups after IHP binding does depend on the concentration of chloride ions since IHP and chloride compete for the same groups. At low chloride concentration the change in pK for these groups will be larger that at high chloride concentration. As a consequence proton uptake upon IHP binding is largest at low ionic strength (see Chapter IV).
iii) IHP induced conformational changes of the protein can change the pK of titratable groups elsewhere in the molecule, thereby giving rise to proton release or absorption.
Considering all these effects, it becomes clear that the curves shown for ΔZ_D^M (Fig. 2) and ΔZ_{CO} (Fig. 4) are too complex to be quantitatively analysed as yet. However, from the large difference in shape observed for the curves it is obvious that different proton binding and release processes are involved in IHP binding to deoxy- and carboxyhemoglobin.
From the model described in the preceding section the proton saturation curves of the groups N were obtained as well. The results show that when these groups represent histidyl residues, proton uptake is considerable upto pH 8.5. This is indeed observed in the nett proton absorption upon IHP binding to deoxyhemoglobin (Fig. 2). Together with the observation, that the curve ΔZ_D^M has a bell-shaped form this provides evidence that only the processes i) and ii) are involved in IHP binding to deoxyhemoglobin. In contrast, proton release is observed around pH 8.5 upon binding of IHP to carboxyhemoglobin (Fig. 4). As was pointed out in the previous section, the groups in the central cavity of HbCO are protonated to roughly the same extent as in Hb at any pH value. Since the pK values for these groups do not differ in Hb and HbCO (17) proton uptake by the histidyl residues should occur in HbCO upon IHP binding as well. So we are led to the conclusion that around pH 8 the proton uptake by the central cavity groups in HbCO is compensated for by a proton release of groups elsewhere in the molecule (contribution iii)). To account for this

third contribution we propose the following mechanism.
First we assume that HbCO is capable of adopting two conformations R and R'. In the absence of IHP, R is predominant. Upon IHP binding the conformational equilibrium is shifted in favour of R', i.e. the affinity of IHP for R' is larger than for R. Furthermore it is assumed that in R' a number of ionizable groups M, have a lower pK value than in R.
As a result, proton release of groups M will occur upon IHP binding to HbCO. Due to the difference in proton affinity of the groups M in R and R', the relative concentrations of these conformations is function of pH both in the presence or absence of IHP.
The mechanism proposed is capable of describing the proton-binding data of the HbCO.IHP complex when the switchover-point between R and R' in the presence of IHP occurs below pH 7 and when the groups M titrate in the neutral pH range in conformation R.
The line broadening observed in the ^{31}P NMR spectra of the HbCO.IHP system around pH 6.5 (Fig. 6) suggests that the switchover point between the R and R' conformations takes place around this pH. The broadening possibly reflects the kinetics of the conformational change.
In this respect, it is interesting to compare our results with those obtained by Olson (21) on IHP binding to aquo-methemoglobin (Hb^+). Upon rapid mixing an IHP and a Hb^+ solution he observed a very fast change in the optical spectrum attributed to the binding of IHP followed by a slow spectral transition with a half-time of about 4 seconds. Furthermore he observed that the amplitude of this slow transition is function of pH. Olson attributed the slow transition to the formation of a deoxyhemoglobin-like conformation upon IHP binding. Evidence for conformational changes in HbCO upon IHP binding is also provided by the observation of a change in the magnetic environment of a nitroxyde spinlabel attached to Cys 93β in HbCO upon binding the polyphosphate (22). Conformational changes in HbCO and CO-ligated β-chain tetramers were suggested before from the observation of unusually steep ΔZ versus pH curves obtained for the binding of benzene hexacarboxylate to ligated hemoglobin (19,23). Moreover, Perutz and collaborators (24) concluded from their X-ray data on ligated

and unligated hemoglobin that the central cavity, being large enough to accommodate organic phosphates in deoxyhemoglobin, reduces in size upon ligation of the protein. They suggested that the polyphosphates are squeezed out upon heme ligation. Combining Perutz' X-ray analysis with recent experiments showing that polyphosphates do bind to the central cavity in ligated hemoglobin (6-8), it is inferred that a change in the dimensions of the central cavity should occur upon IHP binding to HbCO. This local conformational change may give rise to more wide-spread changes in the protein structure.

Characteristics of the NMR Spectra

The ^{31}P NMR spectra recorded for IHP bound to Hb and HbCO retain the appearance of the spectra of IHP free at low and high pH (Figs. 5-8). At neutral pH five to six resolved resonances are observed indicating a specific way of binding of IHP to the residues in the central cavity in both Hb and HbCO, thereby cancelling the mirror symmetry of IHP. The charge distribution in the central cavity is axially symmetric in this pH region as a result of the difference in pK of the residues involved in IHP binding. This influences the protonation state of equivalent groups in IHP in a different way, leading to the observed splitting.

In this respect it is interesting to note that in X-ray diffraction studies of IHP containing crystals of deoxyhemoglobin grown at pH 7.5 (1) a non-uniform electron density for IHP bound is observed. From this it was concluded that IHP binds in a specific way.

The spectra of IHP bound to hemoglobin indicate that the binding is aspecific at low pH. This can be explained by the homogeneous charge distribution in the cavity since all ionizable groups are expected to be fully protonated at low pH. At high pH, the two lysyl residues β82 are the only charged groups in the central cavity. This results in a charge distribution with mirror symmetry. Since IHP has mirror symmetry as well, specific binding if present will not necessarily show up in the symmetry of the NMR spectra. However, when specific binding were to take place, only two phosphate resonances with single intensity or only one resonance of double intensity would be shifted down field leaving

the others unaffected. Since shifts are observed for all resonances (Fig. 9) we conclude that IHP rotates in the central cavity at high pH.

Line broadening is observed for IHP bound to deoxyhemoglobin in a small range around pH 9 (Fig. 5). Similar broadening was found for IHP free in solution around pH 10 (see Chapter II). This phenomenon was explained by a proton and hydroxyl-ion exchange process. The rates of these processes are enhanced and reduced respectively due to the high charge density of the IHP molecule, resulting in line broadening at high pH. As a consequence of binding of IHP to hemoglobin, considerable masking of the high charge of IHP is to be expected. This will result in smaller electrostatic attraction and repulsion effects on the small ions as compared to free IHP. Therefore line broadening occurs at lower pH (Fig. 5).

REFERENCES

1. Arnone, A. & Perutz, M.F. (1974) Nature (London) 249, 34-36
2. Bonaventura, J., Bonaventura, C., Sullivan, B. & Godette, G. (1975) J. Biol. Chem. 250, 9250-9255
3. Bonaventura, J., Bonaventura, C., Sullivan, B. & Ferruzi, G. (1976) J. Biol. Chem. 251, 7563-7571
4. Bare, G.H., Alben, J.O., Bromberg, P.A., Jones, T.J., Brimhall, B. & Padilla, F. (1973) J. Biol. Chem. 249, 773-779
5. Edalji, R., Benesch, R.E. & Benesch, R. (1976) J. Biol. Chem. 251, 7720-7721
6. Brygier, J., de Bruin, S.H., van Hoof, P.K.M.B. & Rollema, H.S. (1975) Eur. J. Biochem. 60, 379-383
7. Gupta, R.K., Benovic, J.L. & Rose, Z.B. (1979) J. Biol. Chem. 254, 8250-8255
8. van Beek, G.G.M. & de Bruin, S.H. (1979) Eur. J. Biochem. 100, 497-502
9. Benesch, R., Edalji, R. & Benesch, R.E. (1976) Biochemistry 15, 3396-3398
10. Benesch, R. & Benesch, R.E. (1967) Biochem. Biophys. Res. Commun. 26, 162-167
11. Chanutin, A. & Curnish, R.R. (1967) Arch. Biochem. Biophys. 121, 96-102

12. Benesch, R., Benesch, R.E. & Yu, C.I. (1968) Proc. Natl. Acad. Sci. U.S.A. 59, 526-532
13. Drabkin, D.L. (1946) J. Biol. Chem. 164, 703-723
14. de Bruin, S.H., Janssen, L.H.M. & van Os, G.A.J. (1973) Biochem. Biophys. Res. Commun. 55, 193-199
15. Wyman, J. (1964) Advan. Protein Chem. 19, 223-286
16. Rollema, H.S., de Bruin,S.H. & van Os, G.A.J. (1976) FEBS Lett. 61, 148-150
17. van Beek, G.G.M., Zuiderweg,E.R.P. & de Bruin, S.H. (1979) Eur. J. Biochem. 99, 379- 383
18. Gupta, R.K., Benovic, J.L. & Rose, Z.B. (1978) J. Biol. Chem. 253, 6165-6171
19. Bucci, E., Salahuddin, A., Bonaventura, J. & Bonaventura, C. (1978) J. Biol. Chem. 253, 821-827
20. Matthies, M. & Zündel, G. (1977) Biochem. Biophys. Res. Commun. 74, 831-837
21. Olson, J.S. (1976) J. Biol. Chem. 251, 447-458
22. Johnson, M.E., Scholler, D.M., Hoffman, B.M. & Ho, C. (1978) Biochim. Biophys. Acta 535, 193-205
23. Salahuddin, A. & Bucci, E. (1976) Biochemistry 15, 3399-3405
24. Perutz, M.F. (1970) Nature (London) 228, 726-739

CHAPTER IV

^{31}P NMR STUDY OF THE KINETICS OF BINDING OF *myo*-INOSITOL HEXAKISPHOSPHATE TO HUMAN HEMOGLOBIN

OBSERVATION OF FAST EXCHANGE KINETICS IN HIGH AFFINITY SYSTEMS

myo-Inositol hexakisphosphate (IHP) is an analogue of 2,3-diphosphoglycerate present in human erythrocytes (1) and of *myo*-inositol pentakisphosphate present in the erythrocytes of avians and turtoise (2). These organic phosphates have in common that they reduce the oxygen affinity of hemoglobin by preferential binding to the unligated state of the protein (3,4,5).
At moderate ionic strength and neutral pH, IHP forms a tight complex with deoxyhemoglobin (Hb). It binds with high affinity to a cluster of positively charged residues located at the β-chain side of the central cavity (6-10); the binding stoichiometry is one IHP molecule per hemoglobin tetramer.
Binding of organic phosphates to ligated hemoglobin was shown to occur at the same cluster of positively charged residues as in deoxyhemoglobin, though with lower affinity (11-13). The binding ratio was demonstrated to be 1 : 1 at moderate ionic strength. However, at low ionic strength evidence was presented for the presence of additional binding sites (14-16).
In the preceding chapter the equilibrium properties of IHP binding to carboxyhemoglobin (HbCO) and Hb have been described. The binding energy was shown to be electrostatic in nature. The affinity of the polyphosphate towards the protein is strongly pH dependent. In particular, at pH 5.6 the association constant for IHP binding to Hb and HbCO amounts to 2×10^9 M^{-1} and 10^7 M^{-1} respectively while at neutral pH the affinity towards both species is much lower.
In this chapter we study the kinetics of the binding of IHP to Hb and HbCO in the pH range 5.5 to 6.35 employing ^{31}P NMR spectroscopy. At constant pH spectra were recorded as a function of the molar ratio of IHP over hemoglobin. The results show that IHP

rapidly exchanges between the solution and the central cavity of hemoglobin. This phenomenon is quite unexpected in view of the large association constants obtained for IHP binding (see above). Furthermore the experiments reveal the existence of additional binding sites for IHP on Hb and HbCO.
We present a kinetic model which accounts for the observation of fast IHP exchange. In this model the additional site serves as a entry or leaving site for binding to the central cavity.

MATERIALS AND METHODS

Preparation of the Hemoglobin Solutions
Human blood was obtained from local hospitals. Hemoglobin was isolated according to the toluene method of Drabkin (17). The lysate, saturated with CO, was dialyzed and then deionized by passage over a mixture of Amberlite IR-120 and IRA-400 (BDH Chemicals Ltd.). It was subsequently dialyzed against 0.05 M Tris-HCl pH 8.5, 1 mM EDTA. The hemoglobin solution was chromatographed on DEAE-A50 Sephadex using a linear pH gradient (0.05 M Tris-HCl pH 8.5 and 0.05 M Tris-HCl pH 7.2, 1 mM in EDTA). The major hemoglobin component, hemoglobin A_1, was collected and concentrated by ultrafiltration. Hemoglobin concentrations were determined spectrophotometrically as carboxyhemoglobin using a heme absorption coefficient of 14,000 $M^{-1}cm^{-1}$ at 537.5 nm.
Throughout this chapter we refer to hemoglobin A_1 as hemoglobin.

Preparation of the IHP Stock Solutions
A concentrated solution of IHP (sodium salt, BDH Chemicals Ltd.) was converted to the acid form by passage over Amberlite IR-120. IHP concentrations were determined by an automatic titration procedure (18,19).

Preparation of α-chain Carbamylated Hemoglobin ($\alpha_2^c \beta_2$)
Hemoglobin α- and β-chains were isolated according to the method of Bucci and Fronticelli (20) modified as described by Rollema et al. (21). Carbamylation of the α-chains was carried out with a five fold excess of KCNO in 0.1 M phosphate buffer, pH 6.0, for one hour at 20 ^{o}C. At this pH, KCNO reacts selectively with the

N-terminal NH_2 groups yielding neutral carbamylated groups. The reaction products were separated on CMC-50 Sephadex using a linear pH gradient (0.05 M phosphate pH 6.6 and 0.05 M phosphate pH 7.6). The blocked α-chains were dialyzed against deionized water, concentrated by ultrafiltration and stoichiometrically recombined with native β-chains.

Preparation of NMR Samples

Carboxyhemoglobin.

A solution of HbCO, 0.1 M in KCl and approximately $5x10^{-4}$ M in tetramer was adjusted to the required pH value with diluted HCl containing 0.1 M KCl. The solution was then concentrated by ultrafiltration up to a concentration of approximately $4x10^{-3}$ M in tetramer. Subsequently a solution of ^2H_2O (99.75% ^2H_2O (Merck), 0.1 M KCl, 1 mM EDTA) was added up to a concentration of 75% (v/v) ^2H_2O followed by ultrafiltration. Hereafter the pH (meter reading) and heme concentration were determined. Known aliquots were injected into 5 mm NMR tubes (Wilmad). The tubes were flushed with CO and sealed with a serumcap.

Deoxyhemoglobin.

Deoxyhemoglobin was prepared by first converting HbCO ($4x10^{-3}$ M HbCO in ^2H_2O, prepared as described above) in HbO_2 in a rotating tonometer by a stream of oxygen under constant illumination at 0 ^oC. The solution was then deoxygenated by a stream of pure nitrogen at 20 ^oC. After determining the pH, known aliquots of this solution were injected into sealed NMR tubes which were flushed with N_2 prior to use. The concentration of hemoglobin was determined as carboxyhemoglobin.

Addition of IHP to the hemoglobin NMR samples.

IHP stock solutions were diluted with ^2H_2O (0.1 M KCl, 1 mM EDTA) to 75% (v/v) ^2H_2O and adjusted to the pH of the protein solution with concentrated KOH. If necessary the solution was deoxygenated in a rotating tonometer by flushing with humidified N_2. Using microsyringes, known aliquots of this solution were injected into the sealed NMR tubes and thoroughly mixed with the protein solution. In those cases where IHP binding to hemoglobin is associated with proton uptake (see Chapter III) this was compensated for by adding a calculated amount of HCl to the IHP solution.

N	HbCO	IHP	K^+	Cl^-	EDTA	% ^2H_2O	pH
	mM	mM	M	M	mM		
.8	2.6	1.9	.11	.10	1.0	75	6.45
1.4	2.5	3.3	.12	.11	1.0	75	6.40
1.5	2.4	3.5	.13	.11	1.0	75	a)
2.2	.4	1.0	.11	.10	1.0	75	6.43
3.1	.4	1.3	.11	.10	1.0	75	6.40
6.0	.4	2.6	.12	.10	1.0	75	6.42

Table I. Concentration of the ions present in a typical series of experiments. In preparing the samples two different IHP solutions were used (see text). The pH (meter reading) was measured in the NMR sample tubes after the experiments.
N is defined as the molar ratio of IHP over HbCO.
a) pH not determined.

This solution was used to titrate the protein in the sample tubes up to a ratio of one mole of IHP per tetramer. With a second solution, not containing HCl, excess of IHP over hemoglobin was added. This rather complicated procedure had to be followed for the following reasons. Control experiments revealed that the ^{31}P NMR spectra of IHP bound to hemoglobin are dependent on the kind of buffer used and the percentage of ^2H_2O in the samples. Furthermore it is known that phosphate resonance positions are sensitive to the identity and concentration of cations in solution (22). Moreover the association constants of the Hb.IHP and HbCO.IHP complexes are strongly dependent on the ionic strength (unpublished results). Taking these observations into account no buffer was added to the solutions and care was taken to keep the percentage of ^2H_2O and the ionic strength constant for all experiments. As a consequence the protein concentration could not be kept constant throughout one series of experiments. The concentrations of ions present in a typical series are listed in Table I.

Data Collection

The ^{31}P NMR spectra were recorded on a Varian XL-100 NMR spectrometer operating at 40.5 MHz in the Fourier Transform mode. The spectra, having a digital resolution of 1Hz/point consist of 1000 to 50,000 scans accumulated in a Varian 620 L computer. The number of accumulations depended on the concentration of IHP. The spectra were recorded in the proton-decoupled mode. A pulse angle of 45° was used throughout all experiments. Field stabilization was achieved by pulse-locking to the ^{2}H signal of $^{2}H_2O$ present in the samples. The temperature of the samples was kept at 25 ± 2°C. Immediately after data accumulation a one pulse spectrum of 20% H_3PO_4 in $^{2}H_2O$ was recorded. The resulting signal which served as a reference was plotted on the same chart as the accumulated spectrum. Chemical shifts (δ) are reported in parts per million (ppm) from this external reference signal, downfield shifts being defined positive.

Miscellanious

Most model calculations were performed on a programmable pocket calculator (Texas Instruments TI-59) while the simulation of three site exchange spectra was carried out on an IBM 370/158 computer.

All reagents used in the preparation procedures were of analytical grade.

RESULTS

The ^{31}P NMR Spectra

In Table II the values for the association constants are listed characterizing the IHP binding to Hb and HbCO as derived from pH-stat experiments (see Chapter III). Below pH 7.0 it is seen that the constant for IHP binding to the central cavity of deoxyhemoglobin is larger than 10^8 M^{-1}. This means that under these conditions the ^{31}P NMR spectrum of IHP in the presence of excess Hb should not depent on the ratio IHP/Hb. This is illustrated by an example presented in Fig. 1. The spectra which correspond with different IHP/Hb ratios, N, of 0.75 and 0.33 are virtually identical, implying that the association constant for IHP binding

pH	K_{CO}	K_D
	M^{-1}	M^{-1}
5.5	$2x10^7$	$>1.6x10^9$
6.0	$5x10^6$	$1.6x10^9$
6.5	$4x10^5$	$4.0x10^8$
7.0	$2x10^4$	$5.0x10^7$
7.3	$4x10^3$	$1.6x10^7$

Table II. The association constants of the high affinity binding site in HbCO (K_{CO}) and Hb (K_D) at 25°C, 0.1 M KCl.
K_{CO} was determined by direct titration at pH 6.5, using the number of protons taken up upon IHP binding as a monitor of the fraction bound IHP. The values for K_{CO} at other pH values were obtained by graphical integration of a $^{CO}\Delta Z^{max}$ vs. pH plot where ΔZ^{max} is the number of protons taken up at full saturation.
K_D was determined by direct titration at pH 8; the values listed were obtained as described above.
See also Chapter III.

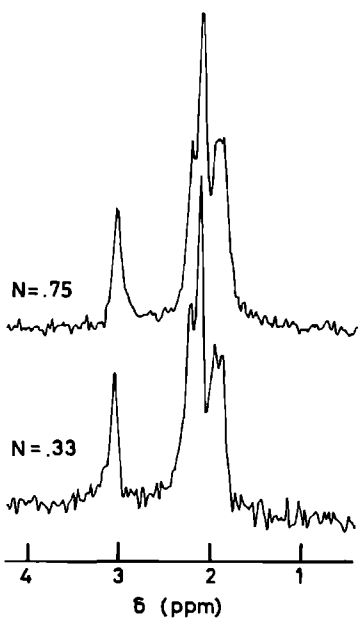

Fig. 1. Proton decoupled ^{31}P NMR spectra of IHP bound to deoxyhemoglobin, pH 6.7. Further conditions: 0.1 M KCl, 1 mM EDTA, 75% (v/v) ^2H_2O, 25°C, Hb concentration, 4 mM in tetramer.
N is the molar ratio of IHP over Hb.

to Hb must be larger than 10^4 M^{-1}. This is consistent with the value mentioned above. This result demonstrates that the spectra in Fig. 1 correspond with the spectrum of IHP bound to the central cavity of Hb. Spectra of IHP recorded in the presence of excess Hb and HbCO at pH values below 6.8 lead to the same conclusion. The resonance positions turn out to be different due to a difference in protonation of IHP (see Figs. 2 and 3 and see Chapter III). The linewidths of the resonances of the spectra of IHP bound can be quantitatively accounted for by the dipolar interaction between the phosphorous nuclei and the decoupled vicinal protons of IHP modulated by a correlation time, τ, of 4×10^{-8} s. This value for τ is equal to the value for the rotational correlation time calculated from the Stokes-Einstein relation for the Hb molecule at 298 K.

The spectra shown in Fig. 2 show an 1 : 1 : 2 : 1 : 1 intensity distribution, in contrast to the characteristic 1 : 2 : 2 : 1 distribution observed in the spectra of IHP free in solution (Chapter II; see also Fig. 2, top spectrum which provides an example of IHP free in solution). This reflects a breakdown of IHP symmetry when bound to hemoglobin, consistent with the mode of binding of IHP to the central cavity as derived from X-ray crystallographic studies (6).

Fig. 2 shows the spectrum of the Hb.IHP system at pH 5.6 as a function of the IHP/Hb molar ratio N. In the presence of excess IHP the resonances vary monotonously with N, i.e. a shift of 1.4 ppm is observed for the high field resonance of IHP when proceeding from the free to the bound state. This monotonous shifting is taken to represent fast exchange between the central cavity site and the solution. The linewidths of the resonances can be accounted for by the weighted average of the widths of the resonances of IHP free and IHP bound. This means that line broadening due to exchange is not observed for this system.

Fig. 2. (opposite page) ^{31}P NMR spectra of IHP as a function of the IHP/Hb molar ratio, pH 5.6, 0.1 M KCl.
The deoxyhemoglobin concentration varies from 1.3 to 4 mM in tetramer. Other conditions as in Fig. 1.

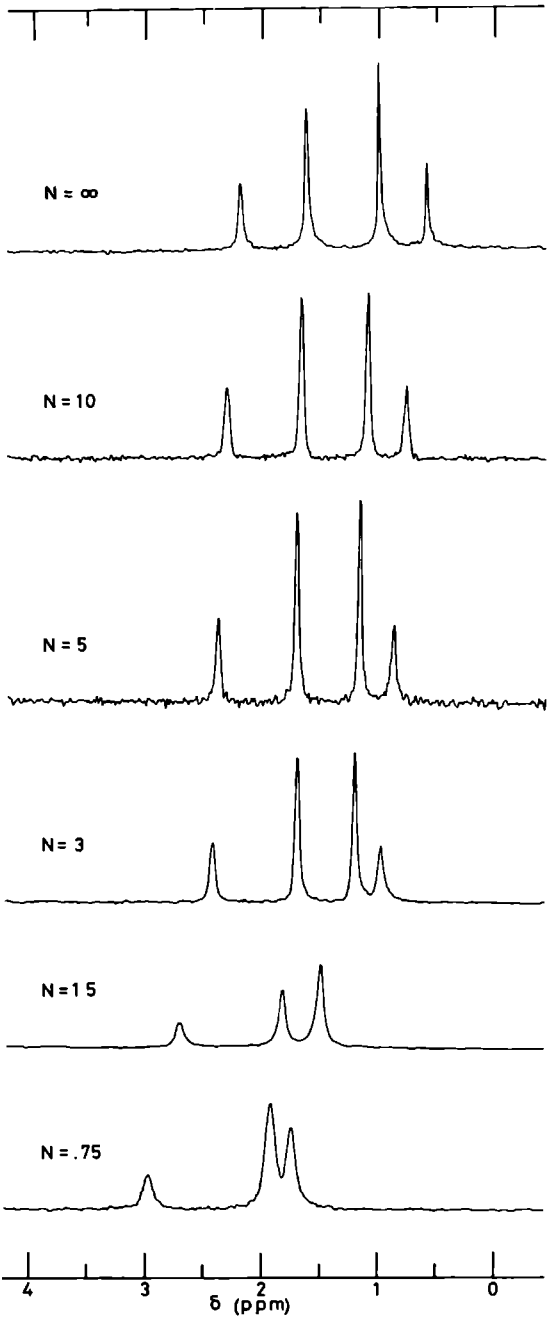
N = ∞
N = 10
N = 5
N = 3
N = 1.5
N = .75
4
3
2
1
0
δ (ppm)

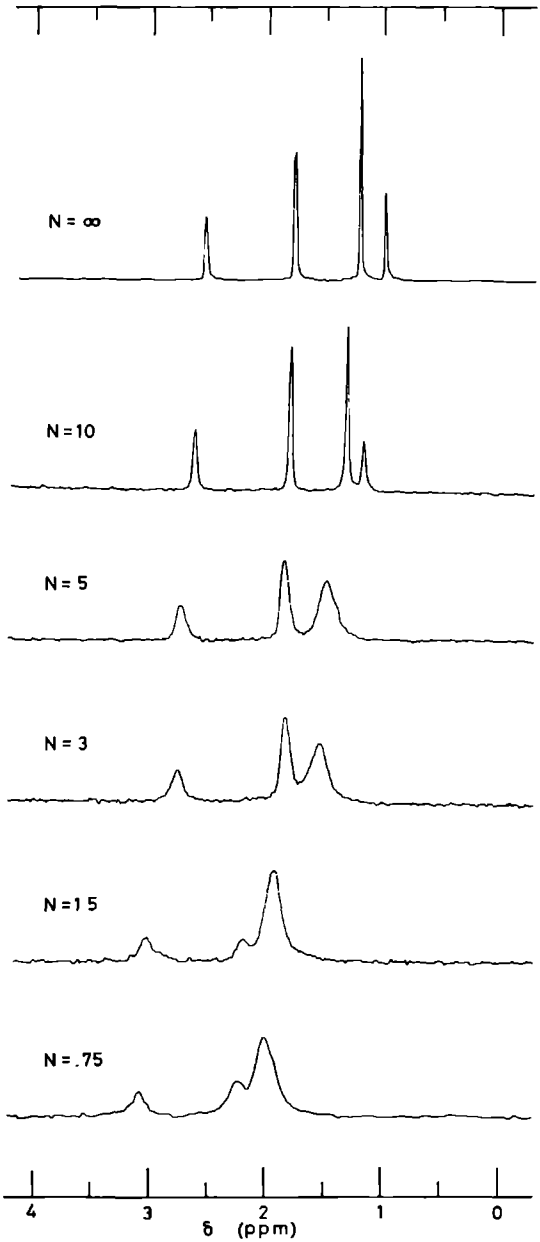
N = ∞
N=10
N=5
N=3
N=1.5
N=.75
4
3
2
1
0
δ (ppm)

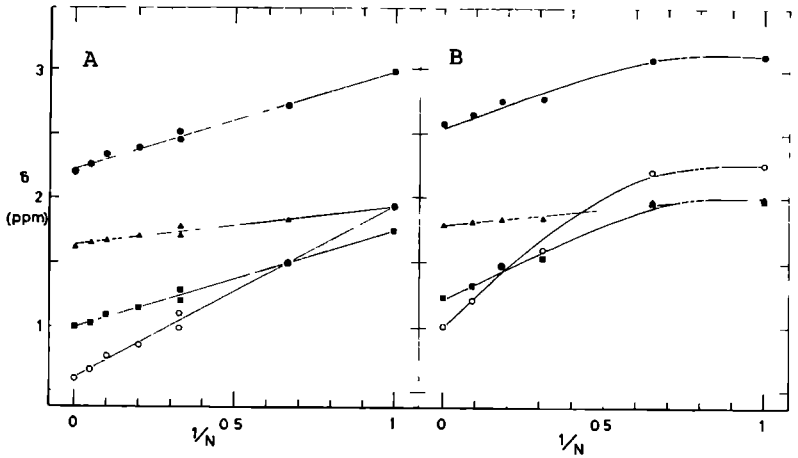

Fig. 4. (A) the chemical shift, δ, of the resonances shown in Fig.2 plotted as a function of 1/N. (Hb.IHP pH 5.6)
(B) δ vs 1/N plot of the resonance positions shown in Fig.3. (Hb.IHP pH 6.35)

Spectra of the Hb.IHP system recorded at pH 6.35 are presented in Fig. 3. Again the resonances shift to higher field with increasing N values showing fast exchange between IHP bound and IHP free in solution. However the shifting process is somewhat delayed with respect to that in Fig. 2.

This is illustrated in Fig. 4 where the resonance positions δ have been plotted versus 1/N. At pH 5.6 the resonances shift linearly as a function of 1/N (Fig. 4A), while at pH 6.35 the positions hardly change when proceeding from 1/N = 1 to 1/N = 0.6 (Fig. 4B). The resonances in the spectra recorded at pH 6.35 have approximately the same linewidth at N = 0.75 and N = 5. Obviously additional broadening is observed. This broadening is due to chemical exchange. Spectra recorded at pH 6.5 and pH 6.8 show similar fast exchange and linebroadening effects as observed at pH 6.35.

Fig. 5 presents the spectra obtained for the HbCO.IHP system at pH 5.6 as a function of N. Shifts similar to those for the Hb.IHP system at pH 6.35 are observed. This is particularly apparent when

Fig. 3. (opposite page) ^{31}P NMR spectra of IHP as a function of the IHP/Hb molar ratio, pH 6.35, 0.1 M KCl.
The deoxyhemoglobin concentration varies from 0.8 to 4.5 mM in tetramer. Other conditions as in Fig. 1.

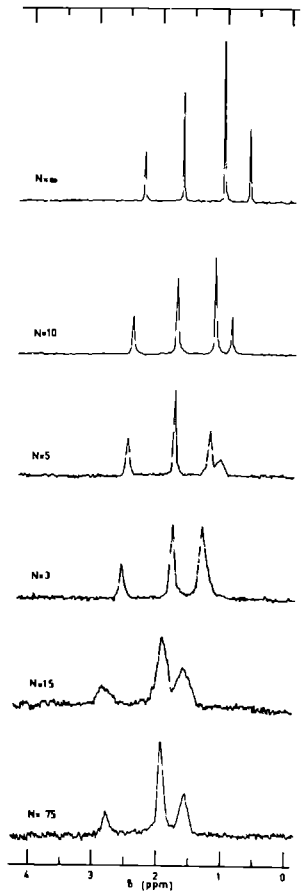

Fig. 5. ^{31}P *NMR spectra of IHP as a function of the IHP/HbCO molar ratio, pH 5.6, 0.1 M KCl. The carboxyhemoglobin concentration varies from 1.2 to 3.4 mM in tetramer.*
Other conditions as in Fig.1.

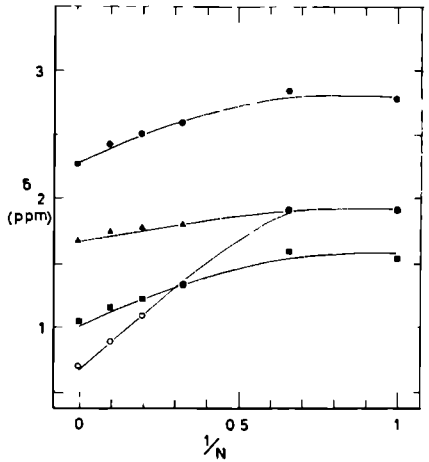

Fig. 6. The chemical shift, δ, of the resonances shown in Fig. 5 plotted as a function of 1/N. (HbCO.IHP pH 5.6).

comparing Fig. 4B and Fig. 6. In the latter the resonance positions of the HbCO.IHP system at pH 5.6 have been plotted as a function of 1/N.

It is noted that in Fig. 5 the resonances in the spectra with N = 0.75 and N = 1.5 differ in linewidth. Comparison of these spectra with those of the Hb.IHP system at the same pH value reveals that broadening effects are observed in the system with the lesser affinity only (i.e. HbCO.IHP). The reverse of the effect is usually encountered for systems in fast exchange.

Also experiments carried out at higher pH values for the HbCO.IHP system show a delay in the shifting of the resonance positions concomitant with exchange broadening effects (results not shown).

The Observation of Fast Exchange

The diffusion-controlled association-rate constant determines the upper limit of the rate constant for the binding of IHP to hemoglobin. The former constant can be estimated from the Smoluchskowski equation (23) corrected for the surface fraction of the protein being effective in the reaction with IHP (24). Using values of .5 nm and 3 nm for the radii of IHP and Hb respectively (18,25) and assuming that the effective protein reaction surface is equal to the area of a circle with a radius of .8 nm, we obtain

a value of 2×10^7 $M^{-1}s^{-1}$ for the diffusion-controlled association-rate constant at 25°C. This value is in accordance with the observed association-rate constants of 10^7 to 10^8 $M^{-1}s^{-1}$ for the binding of molecules of intermediate size to proteins (26,27). It is also consistent with the observations of Gibson and Gray (28) and Olson (29) that IHP binding to hemoglobin occurs within the dead-time of their stopped-flow experiments.

From an association-binding constant of of 2×10^9 M^{-1} for the Hb.IHP system at pH 5.6 (Table II) and a diffusion-controlled association-rate constant of 2×10^7 $M^{-1}s^{-1}$ we obtain a dissociation-rate constant of 10^{-2} s^{-1} for this complex. In case of a single step binding process (i.e. two site exchange) this figure is equal to P_{B-F}, the probability of the transition from IHP bound to IHP free. When the fraction bound and free IHP are approximately equal, the probability P_{F-B} for the transition from IHP free to IHP bound has the same magnitude, i.e. $P_{F-B} \simeq 10^{-2}$ s^{-1}.

Proceeding from the bound to the free state the resonances may shift about 1.4 ppm corresponding to a shift difference, $\Delta\omega$, of about 300 $rad.s^{-1}$ at 40.5 MHz.

Comparison of P_{B-F}, P_{F-B} and $\Delta\omega$ shows that the fast exchange condition $P_{B-F} + P_{F-B} \gg \Delta\omega$ is in no way fullfilled for this high affinity system. This means that a two site exchange mechanism cannot account for our data and that at least one intermediate step is involved in the binding of IHP to hemoglobin.

Briefly anticipating the Discussion where it is demonstrated that it is necessary to introduce an additional binding site for IHP on hemoglobin, we will consider the results in terms of a three site exchang mechanism. It is assumed that IHP exchanges between the solution (I), an additional catalytic site S (when occupied, IS) and the central cavity binding site C (when occupied, IC). In the fast exchange limit the observed position, δ, for a particular resonance is given by

$$\delta = F_I\delta_I + F_{IS}\delta_{IS} + F_{IC}\delta_{IC} \qquad (1)$$

where the symbols F_I, F_{IS} and F_{IC} refer to the fractions of the sites populated by IHP while δ_I, δ_{IS}, δ_{IC} denote the frequencies of that resonance of IHP when the molecule is present in these sites.

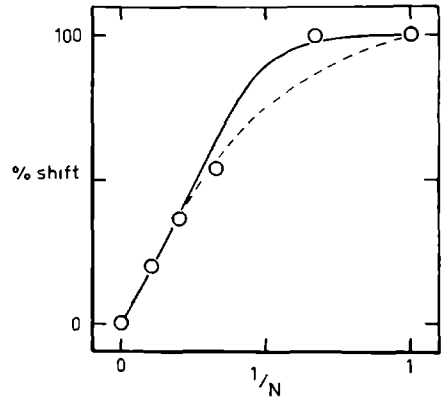

Fig. 7. The effect of an additional binding site on the chemical shift. The resonance frequencies of IHP in the additional and central cavity binding sites were taken to be equal (100%). The constant for IHP binding to the central cavity site was taken to be 10^6 M^{-1}. The curves were calculated according to equation (1) of Results. Protein concentration, 2 mM. Solid line, the effect of a single additional binding site (S) with an association constant of 10^4 M^{-1}; dashed line, the effect due to a single additional site (S) with an association constant of 10^3 M^{-1}. Data points were taken from Fig. 6 and refer to the resonance labeled by open circles.

When the fraction of IHP bound to the catalytic site is small ($F_{IS} \simeq 0$), eqn. (1) can be written as

$$\delta = \delta_I + F_{IC}(\delta_{IC} - \delta_I) \qquad (2)$$

Since the affinity of the central cavity for IHP is very large, F_{IC} can be replaced by 1/N. Hence under these conditions δ varies linearly with 1/N.

This behaviour is observed in Fig. 4A, indicating a low affinity of IHP for the catalytic site S. The data of the spectra with $N < 1$ are represented at $1/N = 1$ since they reflect the bound state ($F_{IC} = 1$).

The curves in Fig. 4B and Fig. 6 are clearly non-linear demonstrating the presence of additional binding at the catalytic site in both Hb and HbCO. The data shown in Fig. 6 can be quantitatively described by eqn. (1) using a value of 10^4 M^{-1} for the association

constant for the binding of IHP to the S site and a constant of 10^6 M^{-1} for the C site. In this calculation δ_{IC} is assumed to be equal to δ_{IS}. The result of this calculation is shown in Fig. 7 where the percentage of total chemical shift, defined as the shift difference $\delta_I - \delta_{IC}$, is plotted versus 1/N. The figure shows that when using a binding constant of 10^3 M^{-1} for the additional site, the agreement with the experimental data is less well.

Location of the Additional Binding Site on HbCO

In an attempt to identify the additional IHP binding site on HbCO, specific chemical modification of the N-termini of the α-chains was carried out by blocking the α-amino groups of the α-chains with KCNO (see Materials and Methods). The resulting hemoglobin derivative, $\alpha_2^C\beta_2$, is known to possess normal oxygen-binding properties (30) while recent X-ray diffraction studies show that no major structural changes are introduced by this modification (31). IHP binding to CO-ligated $\alpha_2^C\beta_2$ was studied by ^{31}P NMR at pH 5.4 and pH 6.25. Fig. 8 shows the data obtained at pH 6.25; the resonance positions vary monotonously with N while exchange broadening is small. A δ vs 1/N plot (not shown here) of these data yields straight lines showing that the affinity of the catalytic site is strongly reduced upon carbamylation of the α-chains. Fig. 9A presents a δ vs 1/N plot of the data obtained at pH 5.4. Comparison of this figure with the δ vs 1/N plot obtained for the HbCO.IHP system at nearly the same pH (Fig. 6) also indicates that upon carbamylation the affinity of the catalytic site is reduced. These observations suggest very strongly that the catalytic IHP binding site is located at the α-chain termini where a cluster of four positively charged groups is present in unmodified hemoglobin. These groups are Val 1α and the guanidino residue of Arg 141α of both α-chains.

The effect of high ionic strength on the resonance positions of the HbCO.IHP system at pH 5.8 was also studied. The affinity of

Fig. 8. (opposite page) ^{31}P NMR spectra of IHP as a function of the ratio IHP/$\alpha_2^C\beta_2$CO, pH 6.25, 0.1 M KCl. The $\alpha_2^C\beta_2$CO concentration varies from 1.1 to 1.4 mM in tetramer. Other conditions as in Fig. 1.

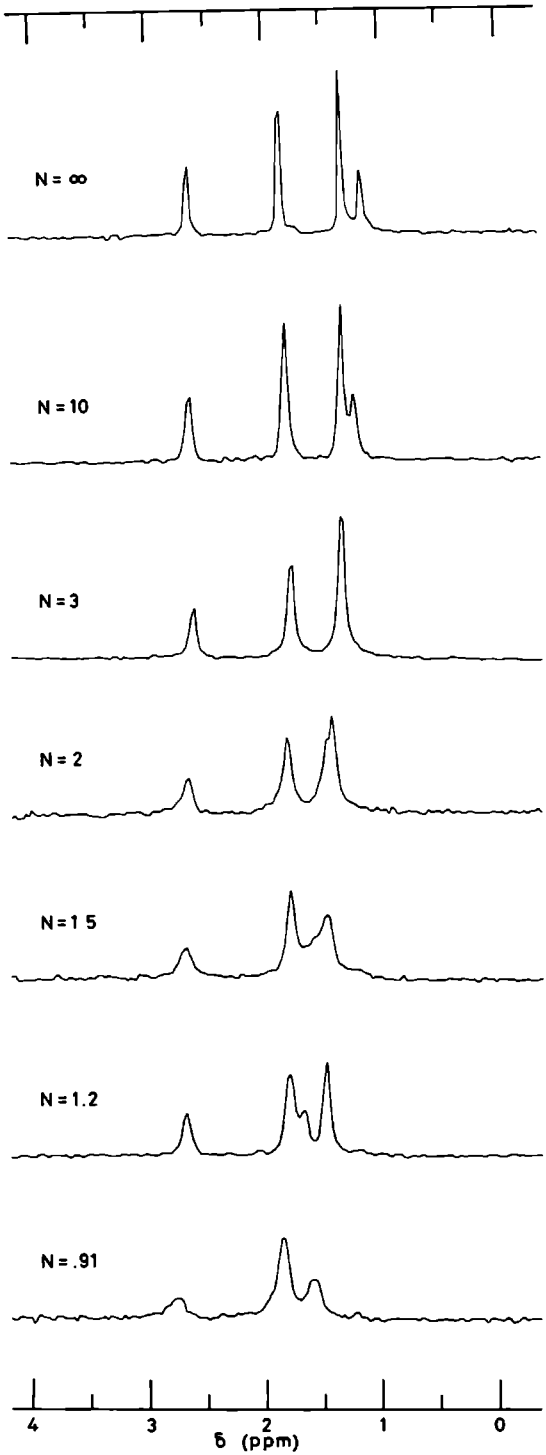
N = ∞
N = 10
N = 3
N = 2
N = 1 5
N = 1.2
N = .91
4
3
2
1
0
δ (ppm)

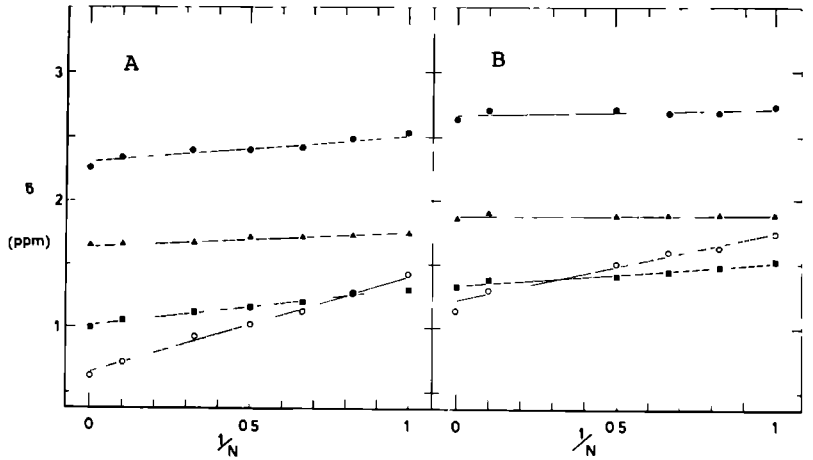

Fig. 9. (A) The chemical shift, δ, of the resonances of IHP in the presence of α-chain carbamylated hemoglobin, $\alpha^{CO}_{2}\beta_{2}$, plotted as a function of 1/N.
Conditions: pH 5.4, 0.1 M KCl. The protein concentration varies from 2 to 3 mM in tetramer. Other conditions as in Fig. 1.
(B) δ vs 1/N plot of the resonance positions of IHP in the presence of HbCO, pH 5.9, 0.5 M KCl. The HbCO concentration varies from 1.6 to 2.4 mM in tetramer. Other conditions as in Fig. 1.

the catalytic site for IHP is reduced as compared with the situation encountered for 0.1 M KCl. This follows from the comparison of Fig. 6 and Fig. 9B. Furthermore fast exchange is conserved at high ionic strength. The ionic-strength dependence is interpreted to reflect competitive binding of chloride and IHP ions to the catalytic site.

Furthermore it should be mentioned that comparison of the resonance positions of free and bound IHP in 0.5 M KCl with those in 0.1 M KCl at the same pH reveals that the free spectrum at high ionic strength is shifted approximately 0.3 ppm downfield with respect to the spectrum in 0.1 M KCl (see Chapter II) while the bound spectrum is unaffected (see Chapter III). The latter observation suggests that the characteristics of IHP binding to the central cavity remain unchanged upon an increase in ionic strength. The ionic-strength dependence of the free spectrum is probably due to a direct influence of potassium ions on the hydratation of the phosphate groups (22).

myo- Inositol hexakisphosphate exhibits high affinity for deoxy as well for carboxyhemoglobin at pH values below 6.3 (see Table II). Despite this high affinity the exchange between bound and free IHP is fast on NMR time scale. As discussed in the preceding section, this observation cannot be reconciled with a single-step binding mechanism.
The first paragraph of this Discussion will deal with a kinetic model for the binding of IHP to hemoglobin. Subsequent paragraphs focus on the observation of an additional IHP site on the hemoglobin molecule and on the dependence of the affinity of this site on chemical modification and ionic strength.

Catalysis by Site-Site Migration, a model which accounts for fast exchange kinetics in systems with high affinity

First let us consider the most simple extension of the single-step two site exchange mechanism to a multisite mechanism by introducing a transient intermediate in the binding process. This type of mechanism is represented by the following scheme:

$$I + C \underset{k_{-a}}{\overset{k_a}{\rightleftarrows}} IC^t \underset{k_{-b}}{\overset{k_b}{\rightleftarrows}} IC \qquad (1)$$

where I and C denote IHP free in solution and free cavity binding site respectively; IC^t represents a transient complex which is in equilibrium with the bound state IC.
Hence the magnetization of the phosphorous nuclei of IHP switches between three sites according to

$$I \underset{P_{-1}}{\overset{P_1}{\rightleftarrows}} IC^t \underset{P_{-2}}{\overset{P_2}{\rightleftarrows}} IC \qquad (2)$$

where the $P_{i's}$ ($i = -2, \ldots, 2$) are the transition probabilities between the three sites. By comparison with eqn.(1) we obtain

$$P_1 = k_a(C),\ P_{-1} = k_{-a},\ P_2 = k_b,\ P_{-2} = k_{-b} \qquad (3)$$

At least two sets of resonances will be observed when one out of these four parameters is smaller than the chemical shift difference. Indead, P_1 is equal to the transition probability P_{F-B} of the two site exchange problem described in the Results; this probability was shown to be much smaller than the shift difference. As indicated above this will result in two sets of resonances, one for free and one for bound IHP. Since this is not observed for any value of N the transient model can be rejected.
So we are led to a model in which the lifetime of IHP in solution is not determined by the concentration of free cavity site. The model, referred to as Catalysis by Site-Site Migration, abbreviated as CSSM, involves the postulation of a catalytic binding site denoted by the symbol S. This site is referred to as catalytic site because it is able to enhance the on- and off - rates of IHP by a factor of 10^5 as is shown in Appendix II.
The catalytic site and the central cavity site C can independently bind IHP and by hypothesis, the polyphosphate molecule can migrate between both sites on the same hemoglobin molecule. Accordingly we can write

$$I + S \underset{k_{-1}}{\overset{k_1}{\rightleftarrows}} IS \qquad (4)$$

$$IS + C \underset{k_{-2}}{\overset{k_2}{\rightleftarrows}} IC + S \qquad \text{(Site-Site Migration)} \qquad (5)$$

$$I + C \underset{k_{-3}}{\overset{k_3}{\rightleftarrows}} IC \qquad (6)$$

with the equilibrium constants

$$K_1 = \frac{k_1}{k_{-1}},\ K_2 = \frac{k_2}{k_{-2}},\ K_3 = \frac{k_3}{k_{-3}} \text{ and } K_1K_2 = K_3$$

Once the concentration of IHP exceeds the hemoglobin concentration the direct exchange of IHP between the central cavity and the solution as expressed in eqn. (6) is very slow. It is therefore not expected to influence the NMR spectrum and will be omitted from the considerations below.
The exchange of magnetization between the three sites is then represented by

$$I \underset{P_{-1}}{\overset{P_1}{\rightleftarrows}} IS \underset{P_{-2}}{\overset{P_2}{\rightleftarrows}} IC \qquad (7)$$

Analogously to the procedure applied for the transient state model, we obtain by inspection of eqns. (4) and (5)

$$P_1 = k_1(S),\ P_{-1} = k_{-1},\ P_2 = k_2(C),\ P_{-2} = k_{-2}(S) \qquad (8)$$

Note the important difference between eqns. (3) and (8); in eqn. (3), P_1, the probability of the transition from IHP free to IHP bound to the protein is dependent on the concentration of free cavity site. This concentration becomes vanishingly small in case of excess of IHP over hemoglobin. In eqn. (8) however, P_1, defined as above, is dependent on the concentration of free catalytic site S. When the affinity of this site is taken to be small (see below), the S-site serves as an entry site for IHP binding to the protein.
Adopting a notation that stresses the physical meaning of eqn. (8) we arrive at

$$P_1 = k_1(S),\ P_{-1} = k_{-1},\ P_2 = k_2' f_C,\ P_{-2} = k_{-2}' f_S \qquad (8a)$$

where k_2' and k_{-2}' are the migration rates from the S to the C-site and from the C to the S-site respectively and where f_C and f_S denote the fraction of time that the cavity and catalytic site on one molecule are unoccupied.

1/N	F_I	F_{IS}	F_{IC}	$k_1(S)$	k_{-1}	$k'_2 f_C$	$k'_{-2} f_S$
.75	.243	7.2×10^{-3}	.75	5.9×10^4	2×10^6	1.0×10^6	9.9×10^3
.50	.485	1.42×10^{-2}	.50	5.8×10^4	2×10^6	3.4×10^5	9.7×10^3
.25	.725	2.5×10^{-2}	.25	5.5×10^4	2×10^6	1.2×10^5	9.2×10^3

Table III. Typical model calculation of the fractions IHP in the solution (F_I), in the catalytic site (F_{IS}), in the central cavity (F_{IC}) and of the exchange kinetics between these sites. Parameters used (see text):
$K_1 = 10\ M^{-1}$, $K_2 = 2 \times 10^8$, (Hb) $3 \times 10^{-3}\ M$
$k_1 = 2 \times 10^7\ M^{-1} s^{-1}$, $k_{-1} = 2 \times 10^6\ s^{-1}$, $k'_2 = 2 \times 10^{12}\ s^{-1}$, $k'_{-2} = 10^4\ s^{-1}$.
Note that all kinetic parameters exceed $\Delta\omega = 3 \times 10^2$ rad.s^{-1} and that fast exchange is achieved while the fraction of IHP in the catalytic site (F_{IS}) is negligable.

Table III presents the results of a calculation of the transition probabilities occurring in eqn. (8a) for a system with $K_1 K_2 = 2 \times 10^9\ M^{-1}$, $k_1 = 2 \times 10^7\ M^{-1} s^{-1}$ and $k'_2 = 2 \times 10^{12}\ s^{-1}$, which is representative of the Hb.IHP system at pH 5.6 ($K > 1.6 \times 10^9\ M^{-1}$, see table II). With this set of parameters the value for all transition probabilities exceeds the value of 300 rad.s^{-1} observed for $\Delta\omega$ between the bound and free state of IHP at any value for N. Consequently fast exchange results for this high affinity system and the spectrum will consist of only one resonance per phosphate group at any value for N with a position, δ, determined by

$$\delta = F_I \delta_I + F_{IS} \delta_{IS} + F_{IC} \delta_{IC}$$

in which the symbols are defined as in eqn. (1) in Results.
In order to estimate the values of the exchange parameters, the chemical shift and exchange line broadening for one resonance were calculated as a function of N and compared with the experimental values. To this end a computer program was written based on the Bloch-McConnel relations (32). For reasons of simplicity the natural linewidths of the resonances of IHP in the three sites was assumed to be zero. As a result the calculations provide

1/N	P_1	P_{-1}	P_2	P_{-2}	$f_{\Delta\omega}$	$\Delta\nu_{\frac{1}{2}}$
	(s^{-1})	(s^{-1})	(s^{-1})	(s^{-1})		(Hz)
.75	5.9×10^4	2×10^6	1.0×10^6	9.9×10^3	.76	.2
.50	5.8×10^4	2×10^6	3.4×10^5	9.7×10^3	.51	.3
.25	5.5×10^4	2×10^6	1.2×10^5	9.2×10^3	.27	.5

Table IV. CSSM model calculation based on the Bloch-McConnel equations (32) showing the dependence of exchange line broadening ($\Delta\nu_{\frac{1}{2}}$) and resonance position ($f_{\Delta\omega}$) on the molar ratio of IHP over hemoglobin (1/N). P_1, P_{-1}, P_2, P_{-2} are defined in the text. $\delta_{IC} = \delta_{IS}$, $\delta_I - \delta_{IC} = 300$ rad.s^{-1}. Other parameters are chosen as in Table III. For further details see text.

the resonance positions and the linewidth due to exchange broadening only (see Appendix I).

Table IV presents the results of such a calculation in which the parameters listed in table III were used as input values. Furthermore, δ_{IC} was chosen to be equal to δ_{IS} (see below) and $\delta_I - \delta_{IC}$ was taken equal to 300 rad.s^{-1}. The calculated resonance positions are expressed as fraction ($f_{\Delta\omega}$) of the total shift difference between the I and IC site. The table shows that the calculations are in good agreement with the experimental data obtained for the Hb.IHP system at pH 5.6 (Figs. 2 and 4A), i.e. $f_{\Delta\omega}$ is equal to 1/N within the limits of experimental accuracy and the exchange broadening is small.

Hence the CSSM model accounts for the experimental data obtained for the Hb.IHP system at pH 5.6 provided that the affinity of the catalytic site is low ($K_1 < 10^2$ M^{-1}) and that the migration rate of IHP from the catalytic to the high affinity central cavity site has a value of the order of 10^{12} s^{-1}.

Similar calculations using different parameter values showed that in case i) the association constant characterizing the binding to the catalytic site (K_1) exceeds the value of 10^2 M^{-1} non-linear plots of δ vs 1/N are obtained, ii) the migration rate k_2' is slower than 5×10^{11} s^{-1} significant line broadening results, iii) the

affinity of IHP for the catalytic site is high, the line broadening becomes determined by the diffusion-controlled on-rate. Examples of these situations will be encountered for the HbCO.IHP systems and for the Hb.IHP system at higher pH. For the moment however, we proceed with the discussion of the Hb.IHP system at pH 5.6.

Information on the actual transfer of IHP from the solution to the central cavity site and vice versa can be obtained from the reciprocal lifetimes of IHP free and IHP bound to the central cavity. These lifetimes are related to the transition probabilities P_1 defined in eqns. (2) and (7) as is outlined in Appendix II. There equations are derived for the reciprocal lifetimes of IHP free and bound to the central cavity site according to the CSSM model and to the transient state model. Substituting the parameter values listed in Table III into these equations we obtain for $N = 2\ \tau_I^{-1} = \tau_{IC}^{-1} = 10^{-2}\ s^{-1}$ for the transient state model and $\tau_I^{-1} = \tau_{IC}^{-1} = 8.2 \times 10^3\ s^{-1}$ for the CSSM model. This result very clearly shows that the mere presence of a low affinity entry or leaving site enhances the actual transfer of IHP by a factor of 10^5 to 10^6. In other words, the reaction of IHP with Hb is catalysed by the catalytic site in the CSSM model.

We now turn to the discussion of the data obtained for the Hb.IHP system at pH 6.35 (Figs. 3 and 4B) and the HbCO.IHP system at pH 5.6 (Figs. 5 and 6). As was outlined in Results, these data can be described quantitatively by fast exchange between the sites I, IS and IC, with a value for the association constant for the IS site of about $10^4\ M^{-1}$ and with $\delta_{IC} = \delta_{IS}$.

Table V shows two CSSM model calculations for a system with $K_1K_2 = 5 \times 10^8\ M^{-1}$ (i.e. Hb.IHP pH 6.35); the results demonstrate clearly that the exchange broadening is dependent on the value for the diffusion controlled on-rate (k_1) due to the high degree of saturation of the IS site in this system. Comparison of the calculated and experimental broadening ($\pm$ 4 Hz, see Figs. 3 and 5) shows that the CSSM model does in principle account for the spectral data obtained for the systems considered, when a value of $10^7\ M^{-1}s^{-1}$ is chosen for k_1. This value for k_1 is consistent with that calculated from the modified Smoluchskowski equations (see Results).

	1/N	P_1	P_{-1}	P_2	P_{-2}	$f_{\Delta\omega}$	$\Delta\nu_{\frac{1}{2}}$
		(s^{-1})	(s^{-1})	(s^{-1})	(s^{-1})		(Hz)
	.75	$4.1x10^4$	$2x10^3$	$8.6x10^6$	$2.7x10^6$	.99	.3
A	.50	$1.0x10^4$	$2x10^3$	$8.0x10^5$	$6.7x10^5$	.92	.5
	.25	$1.0x10^3$	$2x10^3$	$6.8x10^4$	$6.8x10^4$	.50	3.8
	.75	$1.0x10^4$	$5x10^2$	$8.6x10^6$	$2.7x10^6$	.99	.3
B	.50	$2.5x10^3$	$5x10^2$	$8.0x10^5$	$6.7x10^5$	.92	.8
	.25	$2.5x10^2$	$5x10^2$	$6.8x10^4$	$6.8x10^4$	.50	16.0

Table V. CSSM model calculation based on the Bloch-McConnel equations (32) showing the dependence of exchange line broadening ($\Delta\nu_{\frac{1}{2}}$) and resonance position ($f_{\Delta\omega}$) on 1/N. P_1, P_{-1}, P_2 and P_{-2} are defined in the text.
Parameters used for A: $K_1 = 10^4\ M^{-1}$, $K_2 = 5x10^4$, $k_1 = 2x10^7\ M^{-1}s^{-1}$, $k_{-1} = 2x10^3\ s^{-1}$, $k_2' = 2x10^{11}\ s^{-1}$, $k_{-2}' = 4x10^6\ s^{-1}$, $\delta_{IC} = \delta_{IS}$, $\delta_{IC} - \delta_I = 300\ rad.s^{-1}$, protein concentration $2x10^{-3}$ M.
Parameters used for B: see A except $k_1 = 5x10^6\ M^{-1}s^{-1}$ and $k_{-1} = 5x10^2\ s^{-1}$.

Summarizing we can say that the CSSM model allows for fast exchange kinetics in high affinity systems. The model may therefore be considered of importance for biochemical reactions requiring both a high specifity and a fast recovery of the reaction partners. A further point that has to be stressed is that our results prove that the determination of association and rate constants by NMR techniques only may lead to errors. To illustrate this, we note that a straight-foreward analysis of the binding of IHP to Hb at pH 5.6 in terms of a two site exchange mechanism would yield on the basis of a value for the on-rate constant of about $10^8\ M^{-1}s^{-1}$ a value for the association constant of about 10^4 - $10^5\ M^{-1}$ whereas the actual value for the latter constant is larger by 4 orders of magnitude.

Identification of the Catalytic Site

Explanation of the NMR exchange data necessitate the introduction of an additional IHP binding site. The existence of this site is apparent from the curved δ vs 1/N plots (Figs. 4B and 6).

The carbamylation of the α-NH_2 groups of the α-chains provide us with a clue as to the identity of this site. In the carbamylated hemoglobin ($\alpha_2^c\beta_2$) two out of a cluster of four ionizable groups present at the α-chain side of the central cavity are neutralized. IHP binding to CO-ligated $\alpha_2^c\beta_2$ was studied at pH 6.25 (Fig. 8) and at pH 5.4 (Fig. 9A). Comparison of Fig. 9A with the data obtained for IHP binding to native HbCO at pH 5.6 (Fig. 6) reveals first, that the affinity of the catalytic site is suppressed, secondly, that fast exchange is conserved and thirdly, that the spectrum of the bound state remains unchanged (see also Results). The same conclusions can be reached from the δ vs 1/N plot of the data obtained for the $\alpha_2^c\beta_2$CO.IHP system at pH 6.25 (Fig. 8; the δ vs 1/N plot is not shown).

A low affinity for the catalytic site is associated with small exchange broadening effects as follows from calculations using the CSSM model (Table IV). A resolved high field resonance of unit intensity is observed for any value of N for the $\alpha_2^c\beta_2$CO.IHP system at pH 6.25 (Fig. 8). Since the chemical shift difference between the bound and free state for this resonance is rather large, this resolution is taken to represent the absence of exchange broadening.

These observations strongly suggest that the cluster of four ionizable groups present and the α-chain side of the central cavity in native hemoglobin constitutes the catalytic binding site for IHP. In this respect, it is interesting to note that Benesch et al. also observed binding of pyridoxal compounds to the α-chain termini in HbCO (6).

pH-stat experiments also reveal the existence of additional binding sites on both Hb and HbCO at low ionic strength. Representative results are shown in Fig. 10 where the proton uptake per hemoglobin molecule upon IHP binding is plotted versus N, the molar ratio of IHP over Hb or HbCO (for a description of the pH-stat technique, see Chapter III).

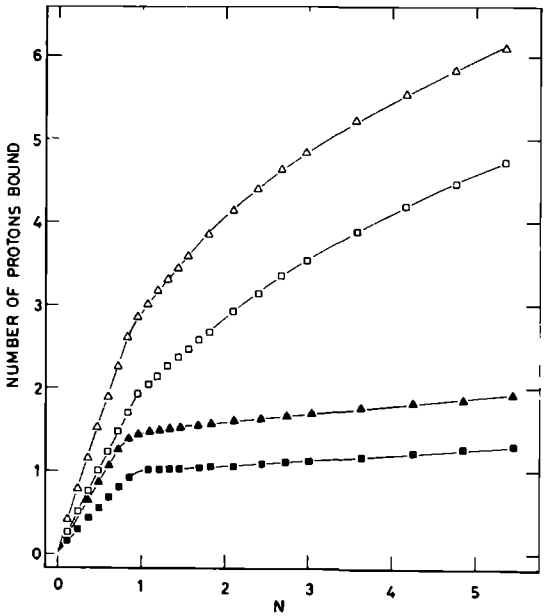

Fig. 10. Proton uptake per tetramer upon IHP binding to Hb and HbCO at pH 6.0, 25 °C. (■), binding to Hb, 0.1 M in KCl; (□), binding to Hb, 0.01 M in KCl; (▲), binding to HbCO, 0.1 M in KCl; (△), binding to HbCO, 0.01 M in KCl. Protein concentration, $2x10^{-4}$ M in tetramer. N is defined as in Fig. 1. The curves were not corrected for the dilution of IHP.

At a KCl concentration of 0.1 M, binding with a stoichiometry of unity is observed for both Hb and HbCO. At low ionic strength (0.01) however, additional binding is observed; in the region $0 < N < 1$ binding to the high-affinity β-chain side of the central cavity occurs while for values of N larger than unity additional proton uptake takes place. This latter effect is interpreted to reflect binding to one or more low affinity sites. Furthermore it is noted that the maximum number of protons absorbed upon IHP binding to the high affinity site ($N < 1$) inreases upon a decrease in chloride concentration.

This difference in proton binding as a function of the chloride concentration can be explained satisfactorily by assuming competitive binding of IHP and chloride ions to both the high- and low-affinity binding sites. However, an exact description of the effect is beyond the scope of this Chapter. We will restrict ourselves to the following remarks on this subject. First the affinity

of the additional site(s) is lowered upon an increase in chloride concentration, clearly a direct consequence of competition. Furthermore, chloride binding to hemoglobin was shown to be associated with proton uptake as well (33), consequently the proton uptake upon IHP binding is actually equal to the difference between the number of protons bound to hemoglobin partially saturated with chloride and to hemoglobin saturated with IHP. It is therefore expected that in addition to the lowering in affinity of the additional site(s) upon an increase in chloride concentration, the number of protons absorbed in the binding process also decreases upon an increase in chloride concentration.

In order to relate the additional binding site(s) observed by pH-stat techniques with that observed with ^{31}P NMR, IHP binding to HbCO at high ionic strength at pH 5.8 was studied with the latter technique. Fig. 9B shows a δ vs 1/N plot of the data obtained. The figure shows that straight lines are obtained from which it can be inferred that the affinity of IHP for the catalytic site is strongly reduced while fast exchange is conserved. This result demonstrates that the additional binding site observed in the pH-stat experiments can be identified with the catalytic site located at the α-chain termini.

An apparent discrepancy arises in that the additional site observed at 0.1 M KCl by ^{31}P NMR which displays an association constant in the order of 10^4 M^{-1} (Figs. 3 and 7) goes undetected in the pH-stat experiment carried out at the same ionic strength (Fig. 10). However is should be kept in mind that the NMR experiment is more sensitive to the presence of additional sites that the pH-stat experiments. This is due to three factors: first, the protein concentrations used in the NMR experiments are ten-fold those used in the pH-stat experiments; secondly, the pH-stat experiment detects binding correlated with proton release or uptake only; thirdly, the pH-stat experiments measure the change in protons bound upon replacing chloride ions by IHP ions as outlined above.

No experiments were carried out to identify the location of the catalytic site on deoxyhemoglobin, but some comments can be made. It is known that Val 1α residue of one α-chain in deoxyhemoglobin forms an ionic complex with chloride ions and the guanidino

residue of Arg 141α of the partner chain (31,33,34). This complex formation results in a rather high affinity for chloride ions ($K \simeq 10^3\ M^{-1}$ at pH 6 (33)). When IHP and chloride ions compete for the α-chain termini site in deoxyhemoglobin as well, this high affinity for chloride ions would result in chloride binding predominant to IHP binding at low pH. This effect might explain the low affinity of the catalytic site in the Hb.IHP system at pH 5.6 (Figs. 2 and 4A). Upon raising the pH, the negative charge of IHP increases. This in turn will increase the affinity of IHP for the catalytic site. As a result the binding of IHP will be stronger than the binding of chloride at higher pH values, as is observed (Figs. 3 and 4B).

Summarizing, we can say that an additional binding site with intermediate affinity for IHP is present on both Hb and HbCO at pH 6. In HbCO this site is located at the α-chain termini site of the central cavity while the pH dependence of the affinity of this site in Hb indicates the same location in deoxyhemoglobin. This α-termini binding site can be identified with the catalytic site. The ^{31}P NMR spectral data show that the resonance frequency of IHP bound to the α-chain termini site is approximately equal to the resonance frequency of IHP bound to the β-termini central cavity binding site. (see Figs. 4B and 6; between 1/N = 0.7 and 1/N = 1 the catalytic site becomes populated yet the resonance positions remain the same). This result suggests that the phosphorous chemical shift of IHP bound to the protein is not determined by the strength of the binding to a particular site nor by the geometry of that site. This conclusion is supported by experiments on the pH dependence of the resonance frequencies of IHP bound to excess Hb and HbCO (Chapter III).

Possible Migration Pathways between the two Binding Sites

The mechanism of Catalysis by Site-Site Migration in which the kinetics of population and depopulation of the high-affinity β-chain binding site is ruled by the low-affinity α-chain binding site, accounts for the observed fast exchange, line broadening and chemical shift patterns. The question arises in which way IHP migrates between the two sites. One possibility is that IHP jumps via the protein surface from one side of the hemoglobin

molecule to the other side (surface diffusion) over a distance of approximately 10 nm. Surface diffusion was suggested before for the *lac*-repressor DNA system to account for the high on-rates for binding of the protein to DNA (35).
Another possibility of site-site migration is worthwile considering; from X-ray studies it appears that the central cavity links the α-chain and β-chain termini (25). The dimensions of this cavity are such that IHP oscillation between both binding sites via the cavity - possibly facilitated by the molecular vibrations of hemoglobin - cannot be excluded.

APPENDIX I

The three site exchange problem of interest between the sites A, B and C is represented by

$$A \underset{P_{BA}}{\overset{P_{AB}}{\rightleftarrows}} B \underset{P_{CB}}{\overset{P_{BC}}{\rightleftarrows}} C$$

where P_{AB}, P_{BA}, P_{BC} and P_{CB} are the transition probabilities per unit time. The exchange is governed by the following Bloch-McConnel equations (32):

$$\frac{dG_A}{dt} + \alpha_A G_A + P_{AB} G_A - P_{BA} G_B = -i\gamma H_1 f_A M_0$$

$$\frac{dG_B}{dt} + \alpha_B G_B + (P_{BA} + P_{BC}) G_B - P_{AB} G_A - P_{CB} G_C = -i\gamma H_1 f_B M_0$$

$$\frac{dG_C}{dt} + \alpha_C G_C + P_{CB} G_C - P_{BC} G_B = -i\gamma H_1 f_C M_0$$

where M_0 is the total equilibrium Z magnitization, γ the gyromagnetic constant and H_1 the amplitude of the irradiating field; G_A is the complex magnetization the the A sites;
$\alpha_A = T_{2A}^{-1} - i(\omega_A - \omega)$ with T_{2A} the transverse relaxation time of site A, ω_A the resonance angular frequency of site A and ω the

angular frequency of the irradiating field; f_A is the time averaged fraction of nuclei in the A site. The definitions for G_B, G_C, α_B, α_C, f_B and f_C are analogous.
Applying the steady-state approximation,

$$\frac{dG_A}{dt} = \frac{dG_B}{dt} = \frac{dG_C}{dt} = 0$$

we obtain for the total complex magnitization $G = G_A + G_B + G_C$

$$G = \frac{-i\gamma H_1 M_0}{N} \times$$

$$\Big[f_A\{(\alpha_A + P_{BA} + P_{BC} + P_{AB})(\alpha_C + P_{CB}) + P_{BC}P_{AB} - P_{BC}P_{CB}\}$$

$$+ f_B\{(\alpha_C + P_{CB})P_{BA} + (\alpha_A + P_{AB})(\alpha_C + P_{CB}) + (\alpha_A + P_{AB})P_{BC}\}$$

$$+ f_C\{(\alpha_C + P_{BC} + P_{BA} + P_{CB})(\alpha_A + P_{AB}) + P_{BA}P_{CB} - P_{AB}P_{BA}\}\Big]$$

with

$$N = (\alpha_A + P_{AB})(\alpha_C + P_{CB})(\alpha_B + P_{BC} + P_{BA})$$

$$- (\alpha_A + P_{AB})P_{BC}P_{CB} - (\alpha_C + P_{CB})P_{BA}P_{AB}$$

The imaginary part of this expression is equal to the absorption mode NMR spectrum.
For reasons of simplicity, the natural linewidths of all sites were assumed to be zero, i.e. $T_2^{-1} = 0$. The absorption function Im G was programmed on an IBM 370/158 computer.
With chosen values for the transition probabilities, for the fractions and for the resonance frequencies, absorption spectra were calculated at intervals of 2 $rad.s^{-1}$. The results were plotted by hand and the line widths due to exchange broadening were estimated from the spectra obtained.

APPENDIX II

Direct comparison of the IHP Transfer Rates in the CSSM and Transient State Model

The CSSM model is represented by

$$I + S \underset{k_{-1}}{\overset{k_1}{\rightleftarrows}} IS \tag{1}$$

$$IS + C \underset{k_{-2}}{\overset{k_2}{\rightleftarrows}} IC + S \tag{2}$$

Since in equilibrium the equality $\frac{d(IS)}{dt} = 0$ applies, we obtain

$$(IS) = \frac{k_1(I)(S) + k_{-2}(IC)(S)}{k_{-1} + k_2(C)} \tag{3}$$

Substitution of this result in the equation

$$\frac{d(I)}{dt} = -k_1(I)(S) + k_{-1}(IS) \tag{4}$$

yields

$$\frac{d(I)}{dt} = -\frac{k_1k_2(S)(C)}{k_{-1} + k_2(C)}(I) + \frac{k_{-1}k_{-2}(S)}{k_{-1} + k_2(C)}(IC) \tag{5}$$

from which we obtain for the reciprocal lifetimes for IHP in solution (τ_I^{-1}) and IHP bound to the C site (τ_{IC}^{-1})

$$\tau_I^{-1} = \frac{k_1k_2(S)(C)}{k_{-1} + k_2(C)} = \frac{k_1k_2'(S)f_C}{k_{-1} + k_2'f_C} \quad \text{(see Discussion)} \tag{6}$$

$$\tau_{IC}^{-1} = \frac{k_{-1}k_{-2}(S)}{k_{-1} + k_2(C)} = \frac{k_{-1}k_{-2}'f_S}{k_{-1} + k_2'f_C} \tag{7}$$

For the transient state model,

$$I + C \underset{k_{-a}}{\overset{k_a}{\rightleftarrows}} IC^t \underset{k_{-b}}{\overset{k_b}{\rightleftarrows}} IC \tag{8}$$

we obtain in analogous way (i.e. $\frac{d(IC^t)}{dt} = 0$)

$$\tau_I^{-1} = \frac{k_a k_b (C)}{k_{-a} + k_b} \tag{9}$$

$$\tau_{IC}^{1} = \frac{k_{-a} k_{-b}}{k_{-a} + k_b} \tag{10}$$

We will compare the values of the reciprocal lifetimes given in eqns. (6), (7), (9) and (10) upon insertion of the rate parameters listed in Table III for N = 2[§]. For the concentration of free cavity site in eqn. (9) we use the approximation $N \simeq \frac{(I)}{(IC) + (I)}$ which yields with $K_1K_2 = \frac{(IC)}{(I)(C)} = 2x10^9\ M^{-1}$ and N = 2, $(C) \simeq 5x10^{-10}$ M.
We obtain $\tau_I^{-1} = \tau_{IC}^{-1} = 10^{-2}\ s^{-1}$ in the transient state model (eqns. (9) and (10)) and $\tau_I^{-1} = \tau_{IC}^{-1} = 8.2\ x10^3\ s^{-1}$ in the CSSM model (eqns. (6) and (7)).
From these results it is seen that IHP transfer from the solution to the cavity and vice versa as arising from the CSSM model is enhanced by a factor of 8.2×10^5 as compared to the IHP transfer calculated according to the transient state model.
Hence the S-site can be described as a catalyst for the reaction of IHP with the central cavity.

§ $k_1 = k_a = 2x10^7\ M^{-1}s^{-1}$, $k_{-1} = k_{-a} = 2x10^6\ s^{-1}$, $k_2' = k_b = 2x10^{12}\ s^{-1}$, $k_{-2}' = k_{-b} = 10^4\ s^{-1}$.

REFERENCES

1. Greenwald, I.J. (1925) J. Biol. Chem. 63, 339-349
2. Johnson, L.F. & Tate, M.E. (1969) Can. J. Chem. 47, 63-73
3. Benesch, R. & Benesch, R.E. (1967) Biochem. Biophys. Res. Commun. 26, 162-167
4. Chanutin, A. & Curnish, R.R. (1967) Arch. Biochem. Biophys. 121, 96-102
5. Benesch, R., Benesch, R.E. & Yu, C.I. (1968) Proc. Natl. Sci. U.S.A. 59, 526-532
6. Arnone, A. & Perutz, M.F. (1974) Nature (London) 249, 34-36
7. Benesch, R.E., Yung, S., Suzuki, T., Bauer, C. & Benesch, R. (1973) Proc. Natl. Acad. Sci. U.S.A. 70, 2595-2599
8. Bare, G.H., Alben, J.O., Bromberg, P.A., Jones, T.J., Brimhall, B. & Padilla, F. (1973) J. Biol. Chem. 249, 773-779
9. Bonaventura, J., Bonaventura, C., Sullivan, B. & Godette, G. (1975) J. Biol. Chem. 250, 9250-9255
10. Bonaventura, J., Bonaventura, C., Sullivan, B. & Ferruzi, G. (1976) J. Biol. Chem. 251, 7563-7571
11. Brygier, J., de Bruin, S.H., van Hoof, P.M.K.B. & Rollema, H.S. (1975) Eur. J. Biochem. 60, 379-383
12. Gupta, R.K., Benevic, J.L. & Rose, B.R. (1979) J. Biol. Chem. 254, 8250-8255
13. van Beek, G.G.M. & de Bruin, S.H. (1979) Eur. J. Biochem. 100, 497-502
14. Garby, L., Gerber, G. & de Verdier, C.H. (1969) Eur. J. Biochem. 10, 110-115
15. Gray, R.D. & Gibson, Q.H. (1971) J. Biol. Chem. 246, 7168-7174
16. Desbois, A. & Banerjee, R. (1975) J. Mol. Biol. 92, 479-493
17. Drabkin, D.L. (1946) J. Biol. Chem. 164, 703-723
18. Zuiderweg, E.R.P., van Beek, G.G.M. & de Bruin, S.H. (1979) Eur. J. Biochem. 94, 297-306
19. Janssen, L.H.M., de Bruin, S.H. & van Os, G.A.J. (1970) Biochem. Biophys. Acta 221, 214-227
20. Bucci, E. & Fronticelli, C. (1965) J. Biol. Chem. 240, PC 551-PC552
21. Rollema, H.S., de Bruin, S.H. & van Os, G.A.J. (1976) Biophys. Chem. 4, 223-228

22. Costello, A.J.R., Glonek, T. & van Wazer, J.R. (1976) Inorg. Chem. 15, 972-974
23. Smoluchskowski, M.W. (1917) Z. Phys. Chem. 92, 124-128
24. Nakatani, H. & Dunford, H.B. (1979) J. Phys. Chem. 83, 2662-2665
25. Perutz, M.F., Muirhead, H., Cox, J.M. & Goaman, L.C.G. (1968) Nature (London) 219, 131-139
26. Chelebowski, J.F., Armitage, I.M., Tusa, P.P. & Coleman, J.E. (1976) J. Biol. Chem. 251, 1207-1216
27. Gast, R. & Müller, F. (1978) Helv. Chim. Acta 61, 1353-1363
28. Gibson, Q.H. & Gray, R.D. (1970) Biochem. Biophys. Res. Commun. 41, 415-420
29. Olson, J.S. (1976) J. Biol. Chem. 251, 447-458
30. Kilmartin. J.V. & Rossi-Bernardi, L. (1971) Biochem. J. 124, 31-45
31. O'Donnel, S., Mandaro, R., Shuster, T.M. & Arnone, A. (1979) J. Biol. Chem. 254, 12204-12208
32. McConnel, H.M. (1958) J. Chem. Phys. 28, 430-431
33. van Beek, G.G.M., Zuiderweg, E.R.P. & de Bruin, S.H. (1979) Eur. J. Biochem. 99, 379-383
34. Arnone, A., Benesch, R.E. & Benesch, R.E. (1977) J. Mol. Biol. 115, 627-642
35. Richter, P.H. & Eigen, M. (1974) Biophys. Chem. 2, 255-263

This thesis describes the interaction of *myo*- inositol hexakisphosphate (IHP) with human hemoglobin. IHP is known to lower the oxygen affinity of human hemoglobin. This effect is due to a preferential binding of IHP to unligated hemoglobin as compared to ligated hemoglobin. To provide the better understanding of these phenomena, the binding of IHP to both ligated and unligated hemoglobin was investigated using phosphorous nuclear magnetic resonance spectroscopy (^{31}P NMR) and pH-stat methods.
In the introductory chapter the structure and function of hemoglobin are briefly reviewed. Furthermore some aspects of polyphosphate binding to hemoglobin are discussed.
In Chapter II a study of the proton-binding behaviour of IHP free in solution is described. The proton binding by IHP appears to be strongly anti-cooperative giving rise to an anomalous buffer capacity. These effects are explained by a model which takes into account the large electrostatic interaction between the phosphate groups of the IHP molecule. Furthermore evidence is provided that the line broadening observed in the ^{31}P NMR spectra at high pH is due to the influence of the electric charge of the IHP molecule on the exchange kinetics of hydrogen- and hydroxylic-ions.
Chapter III presents a study on IHP bound to deoxy- and carboxyhemoglobin. It appears that the proton binding curves of IHP bound retain virtually the same shape but are somewhat shifted with respect to those of IHP free. A modified version of the model presented in Chapter II appears to be capable to grossly account for the observed effects. The pH-stat results presented in this chapter show that the affinity of IHP towards deoxy- and carboxyhemoglobin is very different at neutral pH only. This large difference in affinity is attributed to an IHP induced conformational change in carboxyhemoglobin.
In Chapter IV a ^{31}P NMR study on the kinetics of IHP binding is described. It turns out that IHP rapidly exchanges between the

solution and the central cavity of hemoglobin. This observation is quite unexpected in view of the high affinity of IHP towards the protein. Evidence is provided for an additional binding site of low affinity on both deoxy- and carboxyhemoglobin. From experiments with chemically modified hemoglobin it is inferred that the N-termini of the α-chains are part of this site. A kinetic model is proposed which accounts for the observation of fast exchange in this high-affinity system. In the model the additional site serves as an entry or leaving site for IHP binding to the central cavity.

In dit proefschrift wordt de interactie van *myo*- inositol hexakisfosfaat (IHP) met menselijk hemoglobine beschreven. Van IHP is bekend, dat het de zuurstofaffiniteit van menselijk hemoglobine verlaagt. Dit effect is het gevolg van een verschil in bindingssterkte van IHP ten opzichte van ongeligandeerd en geligandeerd hemoglobine. Teneinde een beter inzicht te verkrijgen in deze effecten, werd de binding van IHP aan ongeligandeerd en geligandeerd hemoglobine bestudeerd met behulp van fosfor kernspin resonantie (^{31}P NMR) en pH-stat methodes.

In het inleidende hoofdstuk worden de structuur en de functie van hemoglobine kort besproken. Tevens wordt hier een kort overzicht gegeven van de tot dusver bekende aspecten van poly-fosfaat binding aan hemoglobine.

Een studie van het proton bindingsgedrag van IHP vrij in oplossing wordt beschreven in het tweede hoofdstuk. De protonbinding blijkt sterk anticooperatief te zijn hetgeen aanleiding geeft tot een anomale buffercapaciteit in het IHP molecuul. Tevens wordt in dit hoofdstuk de pH-afhankelijke lijnverbreding van de fosfor resonanties besproken. Het blijkt, dat deze verbredingen veroorzaakt worden door de electrostatische invloed van het IHP molecuul op de uitwisselings kinetiek van waterstof- en hydroxyl-ionen.

In het derde hoofdstuk wordt een studie van IHP gebonden aan deoxy- en carboxy-hemoglobine beschreven. Het blijkt, dat de proton bindingscurven van IHP gebonden aan het eiwit, zoals bepaald met behulp van ^{31}P NMR, dezelfde vorm hebben als die van IHP vrij, doch slechts een weinig verschoven zijn. Een gemodificeerde versie van het in hoofdstuk II beschreven model, blijkt in staat te zijn de waargenomen effecten te verklaren. De tevens in dit hoofdstuk beschreven pH-stat resultaten tonen aan, dat er slechts bij neutrale pH een groot verschil in affiniteit van IHP voor deoxy- en carboxy-hemoglobine bestaat. Dit verschil in affiniteit wordt toegeschreven aan een door IHP geïnduceerde conformatieovergang in carboxy-hemoglobine.

In het vierde hoofdstuk wordt een ^{31}P NMR studie betreffende de kinetiek van de binding van IHP aan deoxy- en carboxy-hemoglobine beschreven. Het blijkt, dat IHP snel uitwisselt tussen de oplossing en de bindingsplaats op hemoglobine. Dit is zeer onverwacht gezien de hoge affiniteit van IHP voor het eiwit. Tevens wordt de aanwezigheid van een additionele bindingsplaats met lage affiniteit op zowel deoxy- als carboxy-hemoglobine aangetoond. Door middel van chemische modificatietechnieken werd gevonden, dat de N-termini van de α-ketens deel uit maken van deze additionele bindingsplaats. In dit hoofdstuk wordt een model ontwikkeld, dat in staat blijkt te zijn de snelle uitwisseling in dit systeem van hoge affiniteit te verklaren. In het model fungeert de additionele bindingsplaats als "entry" en/of "leaving-site" voor de binding van IHP aan de central cavity van hemoglobine.

CURRICULUM VITAE

Erik Zuiderweg werd op 28 maart 1950 geboren te Amsterdam. Na het behalen van het diploma H.B.S.-B. aan het Willem de Zwijger Lyceum te Bussum in 1967, ging hij in dat zelfde jaar Chemische Technologie studeren aan de Technische Hogeschool Twente. Het algemeen propaedeutisch examen werd in 1968 afgelegd. In 1970 zette hij zijn studie scheikunde voort aan de Universiteit van Amsterdam. Het kandidaatsexamen S_3 volgde in 1973. Het doctoraal examen legde hij af in 1975 met als hoofdvak Fysische Chemie (Magnetische Resonantie onder begeleiding van Dr. M. Glasbeek en Prof. J.D.W. van Voorst), het bijvak Chemische Fysica (Groepentheorie en Kwantummechanika), de speciale richting Wiskunde en een scriptie getiteld: "De Phonon-Bottleneck".
Van 1 december 1975 tot 1 april 1980 was hij als wetenschappelijk ambtenaar in dienst van Z.W.O., werkzaam op de afdeling Biofysische Chemie van de Katholieke Universiteit te Nijmegen.
Hij is gehuwd en heeft een dochter en een zoon.

STELLINGEN

I

De door Yuan et al. waargenomen smeltovergang bij ± 20 °C in het colicine fragment van het E. Coli 16S rRNA rechtvaardigt niet de door hen voorgestelde revisie van de zgn. bulge-loop parameters.

R.C.Yuan, J.A.Steitz, P.B.Moore en D.M.Crothers (1979)
Nuc. Acids Res. 7, 2399-2418

II

De bepaling van associatie constanten voor de binding van liganden aan biomacromoleculen met behulp van NMR technieken alleen kan tot substantiele fouten leiden.

Dit proefschrift

III

De door van der Eijk et al. voorgestelde procedure voor de verwijdering van de beschermgroep p-tolueensulfonyl (tosyl) in N^{im}-tosylhistidine derivaten biedt geen reëel alternatief voor de reeds hiertoe ter beschikking staande methodieken.

J.M. van der Eijk, R.J.M.Nolte en J.W.Zwikker (1980)
J. Org. Chem. 45, 547-548

IV

In toonaangevende studies aan cyano-met valentiehybrides van hemoglobine worden deze moleculen representatief geacht voor half geliganderd natief hemoglobine. Deze aanname moet echter herzien worden.

S.Ogawa en R.G.Shulman (1972) J. Mol. Biol. 70, 315-336
R.Cassoly en Q.H.Gibson (1972) J. Biol. Chem. 247, 7332-7341

De door Möller et al. bepaalde constante voor de binding van het codon AAA aan E. Coli $tRNA^{Lys}$ in aanwezigheid van CGA is onbetrouwbaar.

A.Möller, U.Wild, D.Riesner en H.G.Gassen (1979)
Proc. Natl. Acad. Sci. U.S.A. 76, 3266-3270

VI

Dwek geeft in de sectie "Basic Resonance Theory" van zijn monografie over NMR een volstrekt foutieve benadering van het gedrag van een kernspin in een magnetisch veld.

R.A.Dwek (1973) Nuclear Magnetic Resonance in Biochemistry: Applications to Enzyme Systems, 1st edn., reprinted with corrections (1975), Clarendon Press, Oxford

VII

Valdes en Ackers geven een vergelijking voor de zuurstof saturatiegraad van β-ketens van hemoglobine waarin keten tetramerisatie is verdisconteerd. In deze vergelijking zijn de concentraties van partieel geligandeerde tetrameren ten onrechte verwaarloosd.

R.Valdes Jr en G.K.Ackers (1978)
Proc. Natl. Acad. Sci. U.S.A. 75, 311-314

VIII

Zwart geeft een oplossing voor de paradoxen van Zeno, waarvan de tweede bekend staat als Achilles en de Schildpad, in termen van het gequantiseerd zijn van ruimte en tijd. Deze door hemzelf aangemerkte "ware oplossing" gaat echter voorbij aan de essentie van deze paradoxen en is onnodig.

P.J.Zwart (1971) Het Mysterie Tijd, Een Filosofische Analyse, van Gorckum & Comp. N.V., Assen

E.R.P. Zuiderweg

Nijmegen, 25 juni 1980